Quality assessment and enhancement of soil-bentonite cutoff wall

Yan Tian

Abstract

The vertical barrier is one of the most effective countermeasures for contamination migration and seepage control. Soil-bentonite (SB) is widely used to construct cutoff walls as barrier material due to its extremely low hydraulic conductivity and deformability. While backfill is mixed in place during the construction of SB cutoff walls, it is hard to ensure the homogeneity of SB mixtures.

SB cutoff walls require proper quality control in order to ensure hydraulic performance, particularly in geo-environmental applications. However, the post-construction quality of SB wall has yet to be assessed using undisturbed samples obtained from the actual cutoff wall due to SB's unique material components as well as the softness of the SB wall even following construction. In this present work, laboratory tests were conducted to examine the physical properties, consolidation behaviour and hydraulic conductivity of core samples obtained from two sites in Japan in which SB walls have been installed using trench cutting with an equal thickness. One wall is a 10-m deep wall that was installed in Tochigi, 15 years ago, while the other is a 40-m deep wall installed in Kanagawa, 14 days prior to sampling. The results show that SB has a more unified fines content (<75 μm in particle size) ranging from 20% to 50%, although the fines content in native soil is much scattered (8–80%). From one-dimensional consolidation tests done on the core samples, the consolidation yield stress is approximately 30% of overburdened pressure without considering the arching effect. Moreover, hydraulic conductivity of SB ranged between 1.0×10^{-12} m/s and 1.0×10^{-9} m/s and was determined by consolidation tests and hydraulic conductivity tests using flexible-wall permeameters. Overall, the results demonstrate that the quality of SB wall is satisfactory and homogenous at any depth. Cement amendment to enhance the mechanical properties of SB cutoff walls for geoenvironmental containment is assessed in this study since a certain level of strength is required in some cases. The influence of adding cement on strength and barrier performance was evaluated through a series of laboratory experiments. The contents of cement powder, C_{CP}, considered were 50, 75 and 100 kg/m^3. Unconfined compression tests were conducted to evaluate the strength and stiffness of amended SB. Hydraulic conductivity, k, of basic and

amended SB was studied by using flexible-wall permeameters with the falling head system and distilled water as permeant. Batch tests were used to discuss the attenuation performance of basic and amended SB against arsenic, which is a major contaminant of geogenic and artificial contamination in Japan. By using the results of the hydraulic conductivity and batch tests, one-dimensional advection-dispersion analysis by the finite element method was conducted to simulate arsenic transport through a 0.5-m thick amended SB wall. The results show that C_{CP} =100 kg/m^3 and 90-day curing resulted in the strength of 200 kPa and stiffness of 180 kPa, while the strength of basic SB could not be assessed by the UCS test. The k of amended SB varies between 1.0×10^{-9} m/s and 3.0×10^{-10} m/s. Amended SB with C_{CP} = 100 kg/m3 and cured for 28 days has the highest arsenic attenuation performance, which is 8 times higher than basic SB. Suppose with the typical barrier configuration, and the influent arsenic concentration is 10 mg/L, the outflux from basic and amended SB with C_{CP} = 100 kg/m^3 is 0.11 and 0.65 mg/m^2/year after 100 years, based on the advection-dispersion analyses. On the other hand, if strength requirements are not critical, it is suggested to employ $C_{CP} \leqslant 75$ kg/m^3. However, a relatively low barrier performance is expected in this case but could be improved by increasing bentonite content.

Table of contents

Chapter 1. Introduction

1.1 General remarks

Modern industry and urban life have incurred numerous serious environmental problems worldwide. Particularly, pollution due to toxic chemicals, waster material, and other hazardous materials have become one of the most critical environmental problems, especially in regard to the contamination present in the subsurface and/or groundwater. However, nature-resourced contamination has also gained increasing attention due to the large amount from construction excavation such as tunnel engineering in recent years. Compared to other types of pollutions (e.g., air and noise pollution), studies pertaining to countermeasures for contamination in soil and/or groundwater are relatively limited since the occurrence of subsurface and groundwater contamination is less visible. The soil contamination draws not only great attention in Japan but also in many other countries such as India (Govil et al., 2008), China (Wang et al., 2011) and Australia (Jafari et al., 2020).

Recently, the significance of contamination has become recognized, and additional efforts were devoted to researching measures against soil contaminations. The Japanese government enacted the first Soil Contamination Countermeasures Law (SCCL) in 2003. However, SCCL in 2003 has relatively immature regulations for the conditions which need to be investigated for site characterization, and many contaminated sites are not included based on the law. Moreover, the excavation and disposal method is applied as the main countermeasure regardless of the types and distribution of the contaminants. While in case of wide contamination area excavation method may cost too much and has the possibility of secondary contamination during transportation. Therefore, in 2010 the Japanese law was amended so as to extend the conditions needed to investigate and develop more proper and effective countermeasures. As shown in Figure 1.1, after 2010, due to the amendment of Japanese law, the number of investigations significantly increased from approximately 1300 to over 2000. Therefore, developing countermeasures for soil contamination remains challenging.

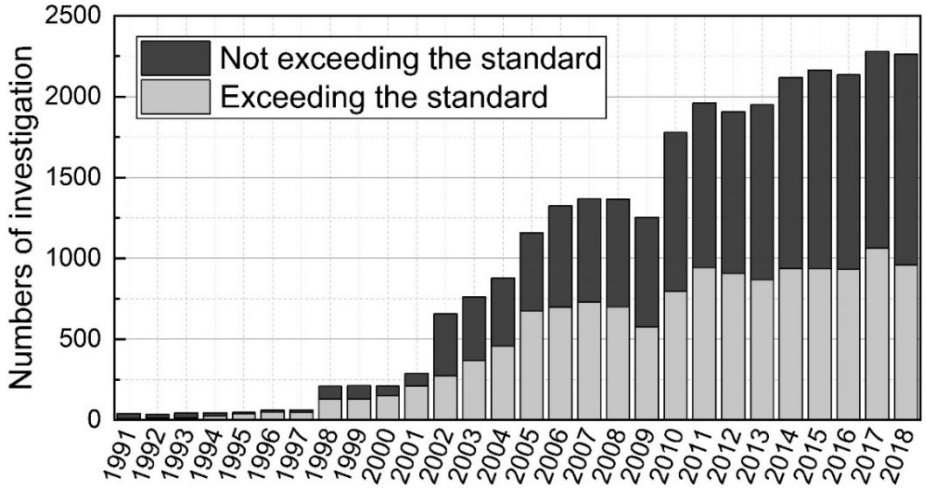

Figure 1.1. Numbers of investigations by the Ministry of the Environment (MOE) focusing on soil contaminations in Japan (MOE, 2021).

1.2 Countermeasures to soil and/or groundwater contamination

The countermeasures to soil and/or groundwater contamination can be mainly divided into two types, the ex-situ treatment method and the in-situ treatment method. As mentioned in the previous section, excavation of the contaminated soil and subsequent disposal to landfills is one method that directly removes the contamination. However, the excavation method is just simply the process of transferring the contamination to another place instead of solving the underlying issue. This excavation method also may cause secondary contamination during transportation. Regarding cost-effectiveness, the excavation method is usually more expensive than other methods when the contaminated area is relatively large. Thermal treatments, washing techniques, decomposition, etc., are widely applied to clean excavated contaminated soil. Through the cleaning treatments, the contaminated soil can be reused as construction materials or geo-materials after proper quality verification.

In terms of the in-situ technicals, multiple kinds and types of this method have been developed. The widely used in-situ treatment method includes decomposition, melting, extraction. These technicals are focusing on clean the contaminated soil without excavation by biological or chemical reactions. The containment technique is another typical kind of in-situ technicals to prevent contamination from migrating to the aquifer. Solidification and

immobilization are often applied to fixed the contamination by employing chemical additives to contaminated soil, which could adsorb target contamination. Using an impermeable layer or vertical cutoff is another kind of containment technique to isolate the contaminants from the surrounding environment without excavations.

The vertical cutoff wall system is effective when the contaminants are located in areas where existing structures are present. In this case, it is technically and economically difficult to actively remove or degrade the contaminants. Here, the vertical cutoff wall is able to reduce migration contamination, especially through advection. Additionally, compared to the excavation method, the budget needed for the vertical cutoff wall method is much less due to the large reduction of excavation amount.

Multiple kinds of materials already have been applied in cutoff walls, such as steel, concrete, geomembrane, cement-bentonite and soil-bentonite (SB). Since cutoff walls are used to directly contain a contaminant by sealing it from the outside environment or manipulating the flow of groundwater to avoid contaminant transport through advection, it requires the material for cutoff has a very low hydraulic conductivity. Cutoff walls are usually installed from the ground surface to the low permeable layer underground so that they can create a complete containment structure to avoid contaminant migration by groundwater flow.

1.3 Application of soil-bentonite in contamination migration control

The prevalent use of SB relative to other materials and methods used in vertical cutoff walls is attributed to the following merits of SB. First, montmorillonite in sodium bentonite can swell when it comes into contact with a polar fluid such as water (Figure 1.2). The swollen bentonite can fill pores between soil particles, which leads to an extremely low hydraulic conductivity (k) of SB (e.g., Takai et al., 2013). The typical k of an adequately mixed SB can be as low as 1.0×10^{-9} m/s (or even lower), decreasing seepage velocity and containing the contamination in situ. Second, high deformability can be achieved for the SB wall, unlike rigid vertical cutoff walls such as soil-cement walls (Grube, 1992). Due to the deformability, the SB

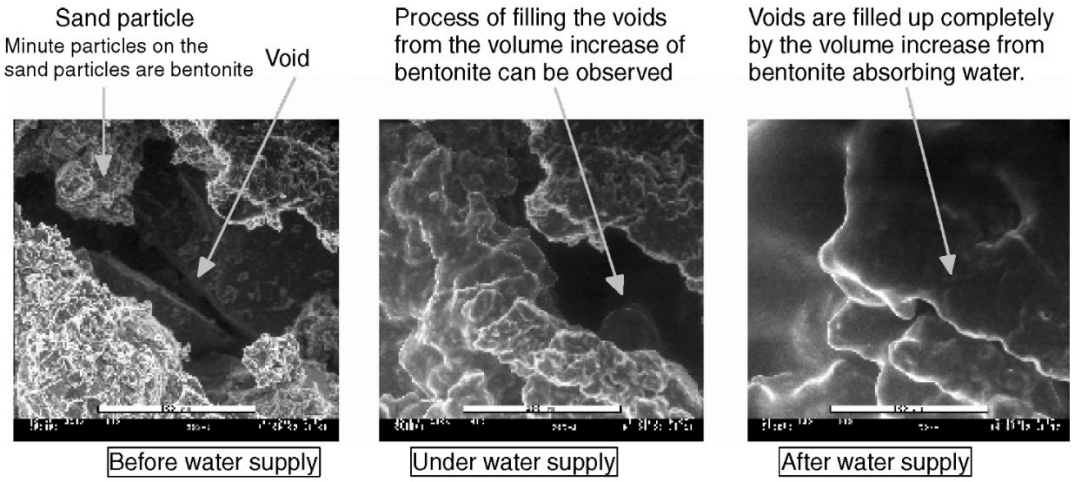

Figure 1.2. Swelling behaviour of bentonite in sand-bentonite (Komine and Ogata, 2003).

wall can keep continuity with large deformations and maintain its soundness even after experiencing large loads. Third, SB also has a high attenuation/sorption capacity against contamination, including arsenic (Minja et al., 2002), lead (Daniels et al., 2004), and caesium (Inui et al., 2016). Lastly, there are benefits to its installation. For example, it can immediately become useable, while a concrete wall needs several days (e.g., 28 days) before reaching its design hydraulic conductivity.

SB walls constructed by slurry trench methods have been employed for over 60 years (D'Appolonia, 1980). SB slurry walls are constructed by excavating a continuous narrow trench. During and after excavation, bentonite slurry was used to stabilize the excavated trench. The mixture of sieved native soil and bentonite mixture was injected into the trench, thereby displacing the bentonite slurry which used for stabling. The SB slurry walls were widely applied in the world due to their extremely low hydraulic conductivity, deformability and cost-effectiveness.

SB cutoff wall is installed using trench cutting with an equal thickness, with which SB cutoff wall is expected to achieve high homogeneity (Katsumi et al., 2008). SB cutoff walls are constructed by excavating and mixing the native soil and bentonite inside the trench, Unlike the slurry walls created by mixing a base soil (i.e., sieved trench-excavated soil or a suitable replacement soil) with viscous bentonite slurry (Malusis et al., 2009). Mixing in place can significantly increase the stability of the trench compared to the slurry wall. However, it also

leads to the mixing quality of SB cutoff wall being challenging to be controlled. It is necessary to do further studies for the quality analysis of SB cutoff wall.

The basic and engineering properties of in situ cutoff walls have been studied in order to establish the proper quality control method. However, there have been few studies that utilized real samples obtained from the actual cutoff wall. In situ field and laboratory testing of existing cutoff walls, particularly SB slurry cutoff walls, have been conducted to provide technical information about the walls in-service (e.g., Filz et al., 2001; Evans and Ray, 2005; Marcial et al*.,* 2006; Fan et al., 2014; Ruffing et al., 2015; Carreto et al., 2016; Malusis et al., 2020). However, for SB cutoff walls, in situ quality assessment methods are required. Takai et al. (2016) used the piezocone penetration test (CPTU) to evaluate hydraulic conductivity and strength characteristics, etc., on a laboratory scale; however, this has not been applied this technique in a full-scale project. The biggest issue complicating the SB wall quality assessment is the technical difficulty that exists in obtaining undisturbed samples due to the softness of SB cutoff walls even following construction and the inclusion of large gravels that originating from the in-situ ground. Therefore, conducting a post-construction quality assessment of SB walls is still challenging in gaining a deeper understanding of on-site behaviour for SB walls and long-term reliability.

Therefore, the motivation of the present study is to confirm the post-construction quality of SB cutoff wall installed using an equal-thickness trench cutting machine, especially for hydraulic conductivity of undisturbed SB samples. The homogeneity of SB also plays a vital role in achieving the design hydraulic performance, since large variability of hydraulic conductivity, k, may cause much more outflux than a homogenous system with the same average k (Britton et al. 2005). Geotechnical properties are also discussed in order to evaluate whether the mixing effect could ensure the homogeneity of SB.

Since the main material of SB is native soil and bentonite additive, the strength of SB is highly dependent on its consolidation state. In terms of the SB wall, the previous consolidation state of the native soil is broken during the SB wall construction. During the consolidation of SB, it is more compressible than rigid walls, which leads to lower consolidation stress (Evans

et al., 2019). A particular study (Malusis et al., 2017) has shown that, after SB wall construction, both total stress and pore stress will decrease with time, while effective stress increases slightly. Malusis et al. (2016) and Ruffing et al. (2011) reports that the total pressure and pore pressure in the SB wall reaches a peak when backfilling is completed, after which total stress and pore stress will decrease with time, while effective stress is slightly increasing. The reason for the reduction in total stress is that the load is transferred through shear to the sidewalls of the trench. The dissipation of excess pore water pressure may lead to a decrease in pore stress. Hence, these factors impact the consolidation pressure of SB is much lower compared to that of the surrounding ground. This phenomenon is called the arching effect, which is caused by friction between the SB and trench interface of the adjacent ground. Therefore, the strength and stiffness of SB are relatively low.

The low strength and stiffness may limit the application of SB cutoff wall. In areas where previous structures have strict requirements for ground deformation, SB cutoff walls may not be applied due to their low stiffness. Therefore, it is necessary to develop a suitable additive in order to improve the mechanical performance of SB mixture, thereby helping extend the use of SB cutoff wall.

Cement has been widely used as a ground improvement additive for a long time. Compared to other additives, cement not only has a significant advantage in cost-effectiveness as well as in material supply. Cement additives may increase the strength of ground soil by cation adsorption between soil particles with an alkaline condition along with mechanisms in hydration mechanisms of cementitious material (Anagnostopoulos, 2015; Daraei et al., 2018; Goodarzi et al., 2016; Kamon et al., 1996). However, the cementitious material may also introduce cations such as Ca^{2+} or Mg^{2+}, thus increasing the EC of the effluent and restricting the swelling of bentonite. Calcium-silicate-hydrate (C-S-H) and Calcium-aluminum-silicate-hydrate (C-A-S-H) are generated in hydration reactions, which may bind soil particles that not only change the consolidation behaviour while restricting the swelling capacity of bentonite. These factors may have a negative influence on the hydraulic performance of cement amended SB.

Meanwhile, cement additives may introduce cations such as Ca^{2+} or Mg^{2+}, which may coprecipitate with contaminations. C-S-H generated in hydration reaction may benefit the adsorption. Therefore, cement additives may increase the attenuation capacity of SB. Barrier performance of cutoff wall consists of hydraulic and attenuation performance. Hence, it is necessary to discuss the influence of cement additives on both hydraulic and attenuation hydraulic and attenuation performance.

According to these soil contaminations investigations, it is found that in cases of investigation exceeding the environmental standard, the contaminations exceeding standard caused by Class II Specified Chemical Substances according to Japanese law mainly includes heavy metal, fluorine and arsenic. In light of the investigation data, the contaminations caused by lead, fluorine and arsenic took up over 60% among all the investigated contamination cases, including recently (Figure 1.3) as well as in historical accumulation (Figure 1.4) (MOE, 2021). Based on previous studies, lead is relatively easy to adsorbed, even only by clay material the remove ratio can be over 90% with 100 mg/L Pb concentration, liquid/solid (*L*/*S*) ratio = 10. Therefore, compared to lead, arsenic may need to be discussed in this study.

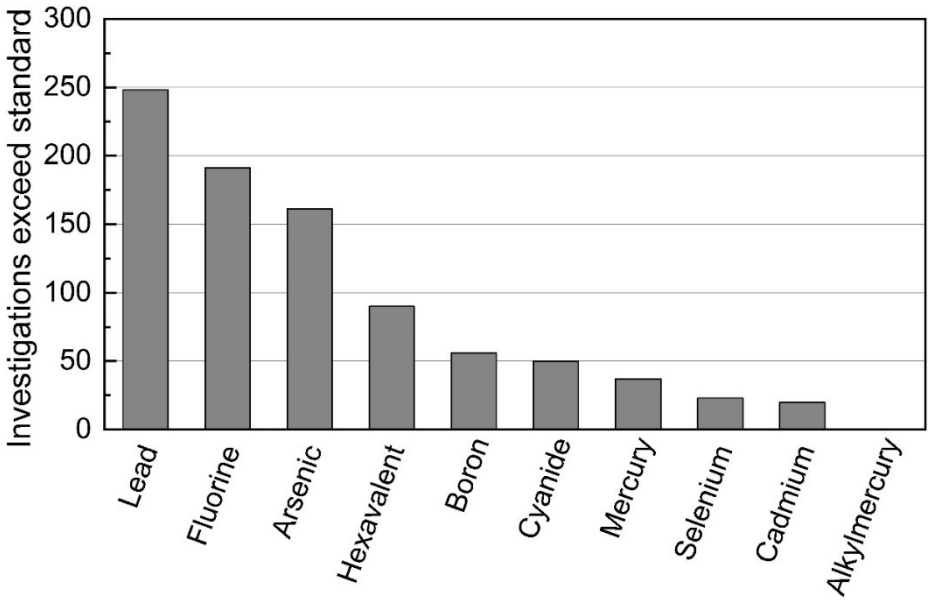

Figure 1.3. Contaminations caused by Class II specified chemical substances in 2019 (MOE, 2021).

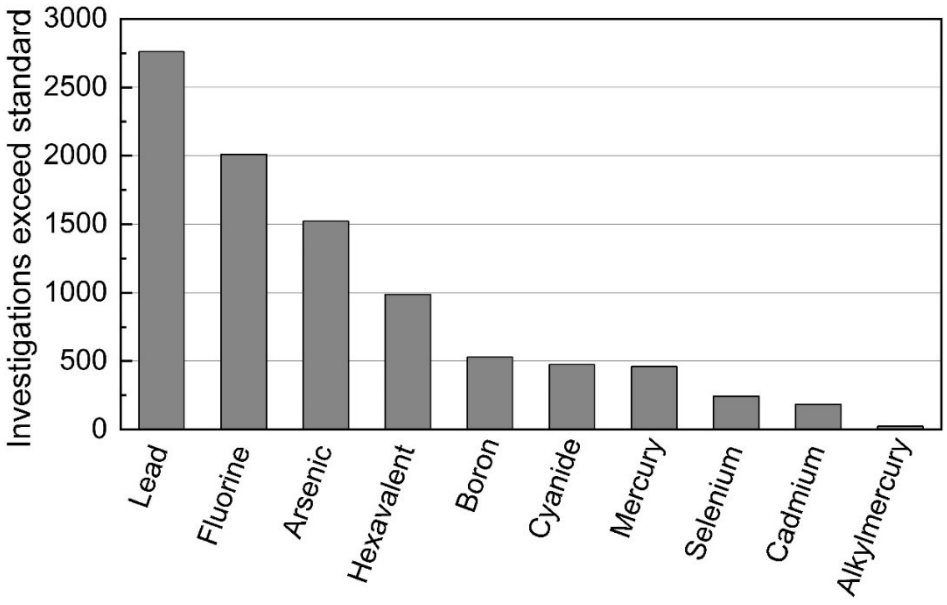

Figure 1.4. Contaminations caused by Class II specified chemical substances in historical accumulation from 2003 to 2019 (MOE, 2021).

1.4 Research objectives of the thesis

The main objective of this study is to confirm the post-construction quality of SB cutoff wall installed via an equal-thickness trench cutting machine, especially in regard to its hydraulic performance and vertical variation. According to the test results of in-situ core samples obtained from the actual cutoff wall, the quality and homogeneity of SB can be evaluated in order to provide a further reference for the future application of SB cutoff wall installed using the equal-thickness trench cutting machine. The other issue is to improve the mechanical performance of SB using cement addition. The influence of cement addition on hydraulic and attenuation performance must be evaluated in order to ensure that the barrier performance of amended SB is still suitable for contamination migration control. Experimental methodologies applied in this study is shown in Figure 1.5. The research can be mainly divided into two parts, basic SB and amended SB. The post-construction quality of SB was evaluated based on geotechnical properties, consolidation and hydraulic conductivity tests by in-situ samples. Unconfined compression, hydraulic conductivity and batch tests were done to assess the mechanical and barrier performance of amended SB, and the main content of each chapter is shown as follow:

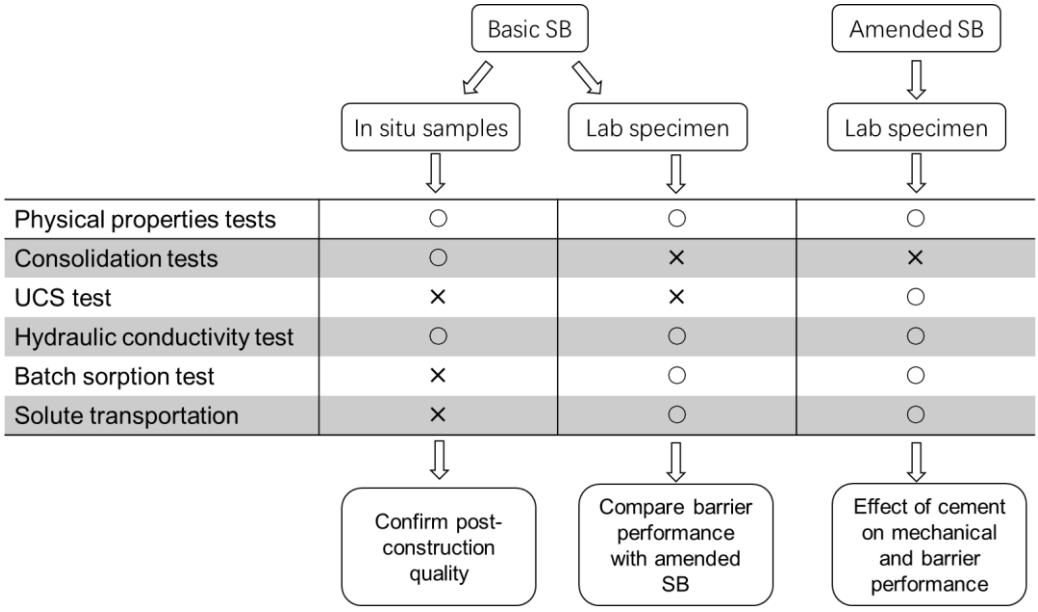

Figure 1.5. Experiments were conducted in this study.

In Chapter 3, laboratory tests are conducted to evaluate the physical properties, consolidation behaviour and hydraulic conductivity of undisturbed samples obtained from two sites in Japan in which SB vertical cutoff walls were installed. The SB walls were installed using an equal thickness trench cutting machine. Accordingly, this is the first study that attempts to assess the post-construction quality of SB installed via the equal thickness trench cutting machine using undisturbed samples. One of the SB walls is a 10-m deep wall that was installed in Site A (Tochigi prefecture, Japan) 15 years ago; this study is the first to assess the quality of the SB wall 15 years after its construction. The other SB wall is a 40-m deep wall installed in Site B (Kanagawa prefecture, Japan) 14 days before sampling. The cutoff wall is the deepest SB wall installed by the equal thickness trench cutting machine, making this study the first to evaluate the post-construction quality of such deep SB walls, particularly through laboratory tests.

In Chapter 4, the effect of cement addition on the mechanical and barrier performance of amended SB is evaluated through a series of laboratory experiments. The cement additive content, C_{CP}, is 50, 75 or 100 kg/m^3. The unconfined compression test was conducted to evaluates the mechanical performance of the amended SB. Hydraulic conductivity of amended SB was studied using a flexible-wall permeameter with the falling head system and distilled

water. Batch tests are then used to discuss the attenuation capacity of amended SB against arsenic. Arsenic contaminations are a big issue in many countries, including Japan (Jung et al., 2004) and China (Zhang et al., 2008). This is particularly true for groundwater, As contamination contributed to risks in drinking water in multiple countries such as Bangladesh (Khan et al., 2000), China (Rodríguez-Lado et al., 2013), Japan (Hossain et al., 2016), and Nepal (Mueller and Hug, 2018). Accordingly, an appropriate countermeasure is essential in controlling the migration of As contamination and promoting groundwater use. Therefore, the attenuation capacity of amended SB against As requires discussion.

Chapter 5 discusses the possible practical implications according to the experiment results in each chapter regarding design consideration and long-term contamination migration. One-dimensional dispersion-advection analysis by finite element method (FEM) is then conducted in order to simulate the transport of arsenic in groundwater through a 0.5-m thick cement-amended SB wall.

Chapter 6 summarizes all of the results and includes the discussion of all chapters as the conclusion of this thesis, in which future directions are mentioned.

References for Chapter 1

Anagnostopoulos, C.A., 2015. Strength properties of an epoxy resin and cement-stabilized silty clay soil. Applied Clay Science, 114, 517–529. https://doi.org/10.1016/j.clay.2015.07.007

Britton, J.P., Filz, G.M., Little, J.C., 2005. The effect of variability in hydraulic conductivity on contaminant transport through soil–bentonite cutoff walls. Journal of geotechnical and geoenvironmental engineering 131 (8), 951–957. https://doi.org/10.1061/(ASCE)1090-0241(2005)131:8(951)

Carreto, J., Caldeira, L., Neves, E.M.D., 2016. Processes involved in the formation and performance of self-hardening slurry walls: santa clara-a-velha monastery cutoff wall. Journal of Geotechnical and Geoenvironmental Engineering, 142 (7), 04016019. https://doi.org/10.1061/(ASCE)GT.1943-5606.0001483

Daniels, J.L., Inyang, H.I., Chien, C.C., 2004. Verification of contaminant sorption by soil and

bentonite barrier materials using scanning electron microscopy/energy dispersive X-ray spectrometry. Journal of Environmental Engineering, 130 (8), 910–917. https://doi.org/10.1061/(ASCE)0733-9372(2004)130:8(910)

Daraei, A., Herki, B.M.A., Sherwani, A.F.H., Zare, S., 2018. Slope stability in swelling soils using cement grout: A case study. International Journal of Geosynthetics and Ground Engineering, 4 (1), 10. https://doi.org/10.1007/s40891-018-0127-9

D'Appolonia, D.J., 1980. Soil-bentonite slurry trench cutoffs. Journal of the Geotechnical Engineering Division, 106 (4), 399-417. https://doi.org/10.1061/AJGEB6.0000945

Evans, J. C., 1994. Hydraulic conductivity of vertical cutoff walls. In D. E. Daniel and S. J. Trautwein (Eds.), Hydraulic conductivity and waste contaminant transport in soils, ASTM. Philadelphia: ASTM. pp. 79–94

Filz, G.M., Henry, L.B., Heslin, G.M., Davidson, R.R., 2001. Determining hydraulic conductivity of soil-bentonite using the API filter press. Geotechnical Testing Journal 24 (1), 61–71. https://doi.org/10.1520/GTJ11282J

Geo-Environment protection center of Japan, 2021, Survey Results on “Soil Contamination Assessment and Countermeasures” in 2019, http://www.env.go.jp/water/report/r1-01/index.html.（In Japanese）

Goodarzi, A.R., Akbari, H.R., Salimi, M., 2016. Enhanced stabilization of highly expansive clays by mixing cement and silica fume. Applied Clay Science, 132-133, 675–684. https://doi.org/10.1016/j.clay.2016.08.023

Govil, P. K., Sorlie, J. E., Murthy, N. N., Sujatha, D., Reddy, G. L. N., et al., 2008. Soil contamination of heavy metals in the Katedan industrial development area, Environmental Monitoring and Assessment, 140(1), 313–323. https://doi.org/10.1007/s10661-007-9869-x

Grube, W., 1992. Slurry trench cutoff walls for environmental pollution control. In: Paul, D., Davidson, R, Cavalli, N. (Eds.), Slurry Walls: Design, Construction, and Quality Control. ASTM International, West Conshohocken, US, pp. 69–77. https://doi.org/10.1520/STP19723S

Hossain, S., Hosono, T., Ide, K., Matsunaga, M., Shimada, J., 2016. Redox processes and

occurrence of arsenic in a volcanic aquifer system of kumamoto area, Japan. Environmental Earth Sciences, 75 (9), 740. https://doi.org/10.1007/s12665-016-5557-x

Inui, T., Katsumi, T., Takai, A., 2016. Cesium sorption/desorption characteristics of sodium bentonite affected by major cations in leachate from MSW incinerator ash. Japanese Geotechnical Society Special Publication, 2 (53), 1841–1844. https://doi.org/10.3208/jgssp.JPN-071

Ismail, M.A., Joer, H.A., Sim, W.H., Randolph, M.F., 2002. Effect of cement type on shear behavior of cemented calcareous soil. Journal of Geotechnical and Geoenvironmental Engineering, 128 (6), 520–529. https://doi.org/10.1061/(ASCE)1090-0241(2002)128:6(520)

Jafari, Y., Jones, B.G., Pacheco, J.C., Umoru, S., 2020. Trace element soil contamination from smelters in the Illawarra region, New South Wales, Australia. Environmental Earth Sciences, 79 (15), 372.

Jung, C., Matsuto, T., Tanaka, N., Okada, T., 2004. Metal distribution in incineration residues of municipal solid waste (MSW) in Japan. Waste Management, 24 (4), 381–391. https://doi.org/10.1016/S0956-053X(03)00137-5

Kameshima, H., Nakamura, S., Suzuki, H., Okamoto, H., 2012. Effect of cement admixture on characteristics of concrete. Cement Science and Concrete Technology, 66 (1), 346–352. https://doi.org/10.14250/cement.66.346

Kamon, M., Ying, C., Katsumi, T., 1996. Effect of acid rain on lime and cement stabilized soils. Soils and Foundations, 36 (4), 91–99. https://doi.org/10.3208/sandf.36.4_91

Kaniraj, S.R., Havanagi, V.G., 1999. Compressive strength of cement stabilized fly ash-soil mixtures. Cement and Concrete Research, 29 (5), 673–677. https://doi.org/10.1016/S0008-8846(99)00018-6

Katsumi, T., Kamon, M., Inui, T., Araki, S., 2008. Hydraulic barrier performance of SBM cutoff wall constructed by the trench cutting and re-mixing deep wall method. In: Krishna, R.R., Milind V.K., Akram, N.A. (Eds.), GeoCongress 2008: Geotechnics of Waste Management and Remediation, ASCE. New Orleans, US, pp. 628–635. https://doi.org/10.1061/40970(309)79

Khan, A.H., Rasul, S.B., Munir, A.K.M., Habibuddowla, M., Alauddin, M., Newaz, S.S., Hussam, A., 2000. Appraisal of a simple arsenic removal method for ground water of Bangladesh. Journal of Environmental Science and Health, Part A, 35 (7), 1021–1041. https://doi.org/10.1080/10934520009377018

Komine, H., Ogata, N., 1999. Experimental study on swelling characteristics of sand-bentonite mixture for nuclear waste disposal. Soils and Foundations, 39 (2), 83–97. https://doi.org/10.3208/sandf.39.2_83

Komine, H., Ogata, N. 2003. New equations for swelling characteristics of bentonite-based buffer materials. Canadian Geotechnical Journal, 40(2), 460-475. https://doi.org/10.1139/t02-115

LaGrega, M.D., Buckingham, P.L., Evans, J.C. 1994. Hazardous Waste Management: McGraw Hill, New York. US.

Li, C., Ren. R., Jia. Y., Jiang. S.et al., 2009. Study on Removing Fluorine Experiment Used the Bentonite and Its Products. China Non-Metallic Minerals Industry Herald, 6.

Malusis, M.A., Barben, E.J., Evans, J.C., 2009. Hydraulic conductivity and compressibility of soil-bentonite backfill amended with activated carbon. Journal of Geotechnical and Geoenvironmental Engineering 135 (5), 664–672. https://doi.org/10.1061/(ASCE)GT.1943-5606.0000041

Marcial, D., Delage, P., Cui, Y., 2006. A laboratory study of the self-sealing behaviour of a compacted sand–bentonite mixture. Geomechanics and Geoengineering: An International Journal 1 (1), 73–85. https://doi.org/10.1080/17486020600585470

Minja, RJ, Ebina, T., 2002. Arsenic adsorption capabilities of soil-bentonite mixtures as buffer aterials for landfills. Clay Science, 12 (1), 41-47. https://doi.org/10.11362/jcssjclayscience1960.12.41

Mueller, B., Hug, S.J., 2018. Climatic variations and de-coupling between arsenic and iron in arsenic contaminated ground water in the lowlands of nepal. Chemosphere, 210, 347–358. https://doi.org/10.1016/j.chemosphere.2018.07.024

Opdyke, S.M., Evans, J.C., 2005. Slag-cement-bentonite slurry walls. Journal of Geotechnical and Geoenvironmental Engineering, 131 (6), 673–681.

https://doi.org/10.1061/(ASCE)1090-0241(2005)131:6(673)

Rodríguez-Lado, L., Sun, G., Berg, M., Zhang, Q., Xue, H., Zheng, Q., Johnson, C.A., 2013. Groundwater arsenic contamination throughout China. Science, 341 (6148), 866−868. https//doi.org/10.1126/science.1237484

Ryan, C.R. 1985. Slurry cutoff walls: Applications in the control of hazardous wastes. In: Hydraulic barriers in soil and rock: ASTM International, West Conshohocken, US, pp. 9−23. https://doi.org/10.1520/STP34562S

Ryan, C.R., Day, S.R., 2002. Soil-cement-bentonite slurry walls. In: Deep Foundations 2002: An International Perspective on Theory, Design, Construction, and Performance. ASCE, Orlando, US, pp. 713−727.

Shevade, S., Ford, R.G., 2004. Use of synthetic zeolites for arsenate removal from pollutant water. Water research, 38 (14-15), 3197−3204. https//doi.org/10.1016/j.watres.2004.04.026

Takai, A., Inui, T., Katsumi, T., Kamon, M., Araki, S., 2012. Factors affecting the hydraulic barrier performance of soil-bentonite mixture cutoff wall. Journal of Japan Society of Civil Engineers, Ser. C (Geosphere Engineering), 68 (1), 1-14. https://doi.org/10.2208/jscejge.68.1

Takai, A., Inui, T., Katsumi, T., Kamon, M., Araki, S., 2013. Hydraulic barrier performance of soil bentonite mixture cutoff wall. In: Manassero, M., Dominijanni, A., Foti, S., Musso, G. (Eds.), Coupled Phenomena in Environmental Geotechnics. Taylor and Francis, Politecnico di Torino, Italy, pp. 707–714. https://doi.org/10.1201/b15004-96

Tremblay, H., Duchesne, J., Locat, J., Leroueil, S., 2002. Influence of the nature of organic compounds on fine soil stabilization with cement. Canadian geotechnical journal, 39 (3), 535−546. https://doi.org/10.1139/t02-002

Wang, X., Cao, J., Chen, X., 2011. Synthesis of composite bentonite and its adsorption to fluorine ion. Environmental Science and Technology (China), 34 (1), 65−69.

Wijayawardhana, H.M.J.T., Silva, L. I. N. De., 2017. Strength, deformation and permeability characteristics of soil-cement-bentonite slurry cut off materials. In:19th International Conference on Soil Mechanics and Geotechnical Engineering, Seoul, Korea, pp.341–344.

Zhang, H., He, P.J., Shao, L.M., Lee, D.J., 2008. Source analysis of heavy metals and arsenic in organic fractions of municipal solid waste in a mega-city (Shanghai). Environ Sci Technol, 42 (5), 1586−1593. https://doi.org/10.1021/es702303x

Chapter 2. Background

2.1 General remarks

In this chapter, studies about the swelling mechanism of bentonite were introduced, including osmotic swelling and diffuse electrical double layer. Bentonite could effectively reduce the void between soil particles after contacting water, enforce permeant to pass through the two montmorillonite layers. The narrow distance between montmorillonite layers may greatly reduce the velocity of flow which explains how bentonite contributes to the decrease of k for SB. It also illustrates why effective stress may play an important role in the hydraulic performance of SB. Chemical properties of permeant may affect the swelling performance of SB, therefore in the previous studies, the influence of permeant on hydraulic performance is discussed, e.g. (Malusis et al., 2013). Besides the mechanism of SB, the construction procedure of SB wall with an equal thickness trench cutting machine was also introduced.

2.2 Influence factors for bentonite in the enhancement of hydraulic performance

Hydraulic performance is an essential characteristic in governing the barrier performance of SB cutoff wall. The hydraulic performance of SB is mainly determined by the hydraulic conductivity value, k. The k values of SB are affected by both chemical and physical factors. Chemical factors mainly consist of the chemical property of bentonite composition, groundwater and original ground. Physical factors include effective stress, consolidation state, bentonite additive amount, and the physical property of native soil. The effects of these factors would be introduced in the following sub sections.

2.2.1 Chemical factors

The enhancement of hydraulic performance for SB material mainly relies on the swelling of the montmorillonite in bentonite (Komine, 2004). The schematic of the swelling process of SB mixture is shown in Figure 2.1. After contact with water, the montmorillonite in bentonite will swell to fill up the void between soil particles.

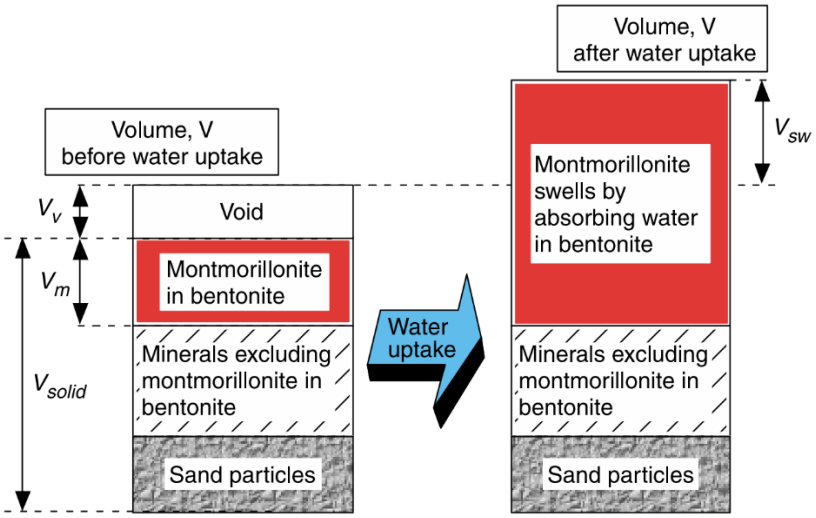

Figure 2.1. Composition of SB mixture before and after contacting water (Komine, 1999).

where V_m is the volume of montmorillonite, V_v is the volume of voids, V_{solid} is the volume of soil and bentonite particles, V_{sw} is the maximum swelling deformation of the buffer material at constant consolidation pressure.

The amount of swelling volume is designed to be even larger than the void volume with constant consolidation pressure. Therefore, the swelling montmorillonite is able to fill up all the void between soil particles, and the liquid is enforced to pass through the montmorillonite mineral layers, as shown in Figure 2.2. In this condition, the flow velocity of liquid in SB mixture may be determined by flow velocity through montmorillonite layers (Komine, 2008). The distance between the parallel montmorillonite layers may decide the hydraulic conductivity of two montmorillonite parallel-plate layers as poiseuille flow estimated by the model (Mitchell, 1993). The equation is shown as followed:

$$k_{montmorillonite} = \frac{\rho_{aw}}{12\mu_{aw}}(2d)^2 \tag{2.1}$$

Where $k_{montmorillonite}$ = hydraulic conductivity between two montmorillonite layers (m/s); d = half distance between two montmorillonite layers.

The enhance of bentonite powder for the barrier performance of SB mainly depends on the swelling characteristics of bentonite. The main mechanism of the swelling of bentonite

when contacting with water can be attributed to “Osmotic swelling” and “Diffuse double layer”.

Figure 2.3 illustrates the main mechanism of osmotic swelling for bentonite. The surface of bentonite clay is mostly negatively charged because of the isomorphous substitution in-plane crystals of montmorillonite (Katsumi et al., 2008). The cations such as potassium, sodium, or calcium exist between the plates as exchangeable cations. When contacting with water, the negatively charged side of molecules will be attracted to exchangeable cations to balance the charge. In this situation, cations will be hydrated by attracted water molecules. It leads to the layers of water molecules are electrically intercalated between the montmorillonite plane layers, and the distance between crystal sheets increases. This process causes the bentonite to expand, knowing as osmotic swelling. However, when the exchangeable cations are attracted not only

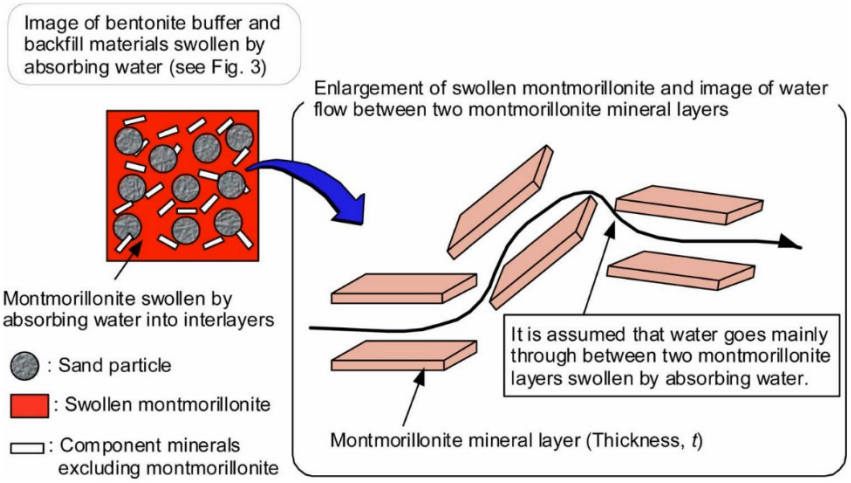

Figure 2.2. Liquid flow in SB mixture after contacting with water (Komine, 2008).

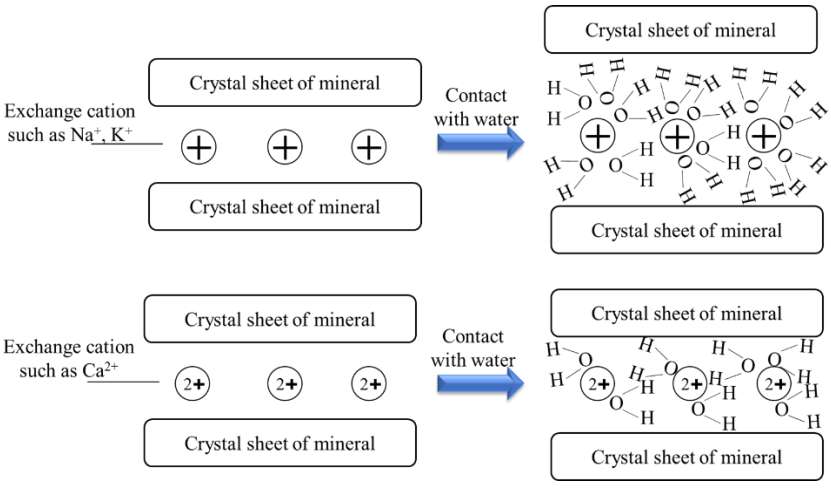

Figure 2.3. Schematic diagram of osmotic swelling (Komine, 2009).

to the fluid molecules but also with clay minerals. In these conditions, there are multiple exchangeable cations, the bond between the exchangeable cations and clay minerals is relatively stronger. Therefore, the swelling capacity of bentonite would be reduced, as shown in Figure 2.3, which is why the swelling performance of calcium-bentonite is poor compared to sodium-bentonite.

The diffuse electrical double layer is known as that the cation in solution would be tightly absorbed by clay surface. The concentrated cation near the clay surface may diffuse away to equalize concentrations throughout the pore fluid. The charged surface and the distributed charge in the adjacent phase are together termed the diffuse electrical double layer. In distilled water, there is no cation in solution; only positively-charged sides of water molecules are adsorbed on the surface of clay particles. These adsorbed water molecules cannot contribute to water permeation through the soil because the water molecules are tightly held. Therefore, the thicker diffuse electrical double layer reduces effective porosity. On the other hand, in the case of high cation concentration, those cations are preferentially adsorbed on the clay particles, and the diffuse double layer becomes thin. Therefore, the thickness of the diffuse electrical double layer plays an important role in the hydraulic barrier performance of SB.

2.2.2 Physical factors

Physical factors also may have an influence on the hydraulic performance of SB, such as particle size and void ratio (Sivapullaiah et al., 2000). Usually, over 70% of bentonite can be classified as clay contents (<2 μm in diameter), which may contribute to lower hydraulic conductivity due to a change in particle size distribution. Generally, fine-grained soil has lower k than coarse-grained soil. Moreover, compared to soil with a uniform particle size distribution, well-graded soil may have a lower hydraulic conductivity. Considering an area with high hydraulic conductivity in a practical engineering project, it usually lacks clay material. Construction of SB cutoff wall not only increase the clay particle amount but also change the coefficient of uniformity and coefficient of curvature. It also helps with a lower void ratio, which contributes to better hydraulic performance. Evans et al. (2016) discuss the influence of fine particle contents, dry bentonite mass and effective stress. The results suggest that low fine

contents SB may have high hydraulic conductivity with the same dry bentonite mass and consolidation stress compared to medium or high fine contents SB. The hydraulic conductivity of SB may decrease with an increase of dry bentonite mass and consolidation stress, as shown in Figure 2.4. A rise in dry bentonite mass may increase the swelling volume of montmorillonite, as discussed in the previous subchapter. The higher consolidation may lead to a lower void ratio, which means the smaller void space between the soil particles and narrower seepage path. These factors all contribute to lower hydraulic conductivity.

2.3 Chemical compatibility of soil-bentonite

2.3.1 First exposure effect

As mentioned in the previous sub-chapter, the mechanism of bentonite in the enhancement of SB mainly relies on the swelling capacity of bentonite. Permeant liquids were reported to have a strong influence on the hydraulic performance of SB according to previous studies, which was referred to as the "first exposure effect". The application of pre-hydration for bentonite may be an effective countermeasure to improve the chemical compatibility of SB. Figure 2.5 is the schematic diagram of the effect of pre-hydration and non-pre hydration on *k*. Without pre-hydration, the hydraulic conductivity of SB will significantly increase if the liquid has a large amount of cation. While, if the SB mixture is hydrated with distilled water, even after the pre-hydration process, the permanent liquid changes to a chemical solution, the change of the hydraulic conductivity is not very significant.

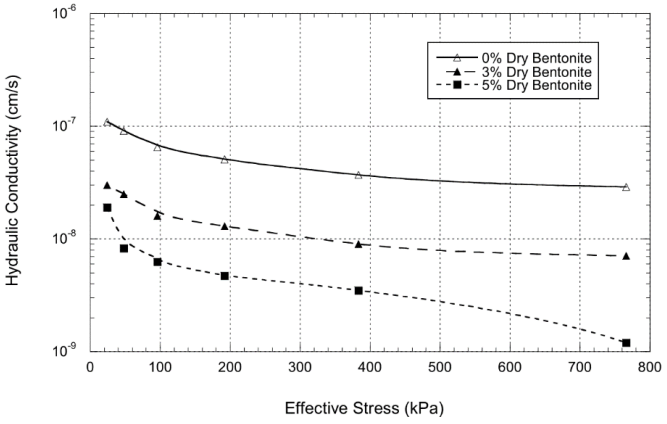

Figure 2.4. Influence of stress and fry bentonite content on SB (Evans and Huang, 2016).

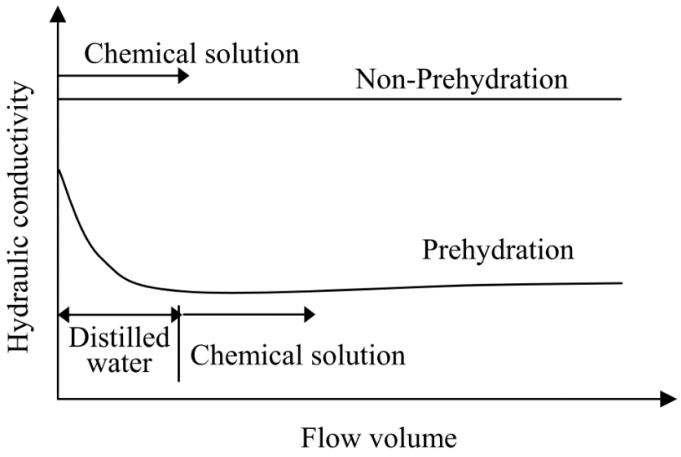

Figure 2.5. Effect of pre-hydration and none pre-hydration on k (Katsumi et al., 2004).

Malusis et al. (2013) evaluated the first exposure effect by using tap water and calcium chloride as permeant liquid ($CaCl_2$) in the hydraulic conductivity test of SB with a flexible-wall system. The test results suggested that since the SB specimens were hydrated with tap water, the first exposure ratio (FER) is relatively low, while the GCL materials have a significant breakthrough when the concentration of $CaCl_2$ in permeant liquid is over 80 mM. As barrier material in the contaminated site, SB has a high possibility to contact with high cation concentration solution with a relatively high EC value. In contrast to SB slurry wall, which mixing the SB backfill out of the trench, SB wall is installed using an equal thickness trench cutting machine to mix the native soil, bentonite slurry and powder in place. There is no pre-hydration process for SB cutoff walls installed by an equal thickness trench cutting machine. The influence of the environment on hydraulic performance may be more significant. Therefore, it is necessary to do research about the chemical compatibility of SB cutoff wall.

2.3.2 Attenuation capacity of SB against contaminants

Previous studies have discussed the attenuation capacity of SB against multiple contaminants, including arsenic (Minja et al., 2002), caesium (Inui et al., 2016) and lead. The previous studies showed the attenuation capacity of SB is related to multiple factors. Minja et al. (2002) tested the attenuation capacity of SB for different host soil, including Masado and Murram, against both As(III) and As(V). The results show the attenuation performance of SB

is highly dependent on the host soil. With the same mass ratio of bentonite addition, the attenuation capacity of Masado mixtures is almost two times that of Murram mixtures. On the other side, the pH value of the solution also played an important role in the attenuation performance of SB against arsenic. The absorbed As(V) amount decreased when pH was over 7, while for As(III), the maximum sorption peaked at a pH value around 8. An increase or decrease in pH may lead to a decrease in attenuation performance.

Inui et al. (2016) studied the sorption capacity of Na-bentonite against caesium and the influence of co-existence cation on sorption capacity. The results suggested Na-bentonite has a sorption capacity against caesium, and the existence of Ca^{2+}, K^{+} and Na^{+} will reduce the sorption capacity of Na-bentonite. Therefore, it may be better to increase the stability of attenuation capacity of SB to extend the application of SB cutoff wall.

2.4 Quality assessment of SB wall

2.4.1 In-situ methods

As described in Chapter 1, since SB wall was an underground structure with a relatively large depth, it is hard to judge the construction quality from the ground. Therefore, it is important to develop a suitable method to ensure the post-construction quality of SB wall. Especially, different from SB slurry wall, SB cutoff wall is mixed in-place without excavation and sieving of the native soil (Katsumi et al., 2008). It means that it is more difficult to make the mixture in SB cutoff wall homogeneous compared to the mixture in SB cutoff wall. It requires more attention not only to hydraulic conductivity but also a homogeneity of SB cutoff wall because the variability of hydraulic conductivity may have a strong influence on the barrier performance of the cutoff wall system (Britton et al., 2015).

In-field quality analysis during and after construction is one of the key issues to enhance the reliability of SB wall. Since laboratory measurement is limited due to the size of the testing devices and the amount of samples, an in-situ test for quality assessment of SB wall has drawn great attention. Compared to laboratory measurement, in-situ tests are able to provide the opportunity to test larger, more representative volumes of material and to include flow through

secondary features, e.g., macropores, fissures, and slickensides, in a manner that often cannot be simulated properly in small laboratory test specimens (Daniel, 1989).

In terms of quality control for bentonite slurry used in construction, Abu-Hassanein et al. (1996) developed a method using electrical conductivity to estimate the bentonite content ratio in the bentonite slurry. The electrical conductivity will have a linear relationship with the bentonite mass ratio in slurry. Through this method, the SB slurry used in cutoff walls or slurry walls can be monitored.

Ruffing et al. (2010) developed a method by Marchetti Dilatometer Test (MDT) to evaluate the lateral stress distribution of SB wall. The DMT protocol and data analysis are mainly referred to ASTM D6635-01(2007). Figure 2.6 shows the main parts of the test device, which are the dilatometer control panel and blade. The lateral stress was measured by using compressed air to expand the steel membrane on the dilatometer blade. The reading of air pressure was used to calculate the lateral earth pressure at the test depth. The DMT results were found to have a reasonable agreement between lateral stresses from the DMT and the prediction from a modified lateral squeezing model.

Ruffing et al. (2015) do studies about using cone Penetration test (CPT) to evaluate the strength and stiffness of SB wall. CPT was widely used for assigning soil properties to the subsurface since it is robust and could quickly collect continuous data at targeted depth. A limitation of this method (and many others) is its dependence on the choice of the cone factor.

Although there have been several studies about the quality of SB wall, there still were no researches done before about the laboratory tests of the SB wall constructed using an equal-thickness type trench cutting machine. Takai et al. (2016) applied piezocone penetration test, CPTU method, as an on-site test method to evaluate several indices, including hydraulic conductivity, water head and strength characteristics. During the test, sleeve friction, cone resistance and pore pressure was measure by the sensor installed in the probe. The schematic diagram of the cone probe is shown in Figure 2.7. The method is verified by a large scale soil tank test. The test results that hydraulic conductivity from pore pressure dissipation tests showed a good correlation with those measured by the laboratory falling head test. The

difference between the *k* from of CPTU method and the falling head test is less than 10 times. Thus, the CPTU method may be a suitable method to be applied in the quality assessment of the barrier performance of SB cutoff walls.

2.4.2 Laboratory test method

While these in-field tests provide basic information on the SB wall, laboratory tests are required for clarifying the quality of the SB wall. Considering the hydraulic conductivity of SB, the falling head test with a flexible wall system is often used to evaluate the hydraulic conductivity of SB. For example, Takai et al. (2013) used a falling head test with a flexible wall

Figure 2.6. Dilatometer control panel and blade in DMT test (Ruffing et al., 2015).

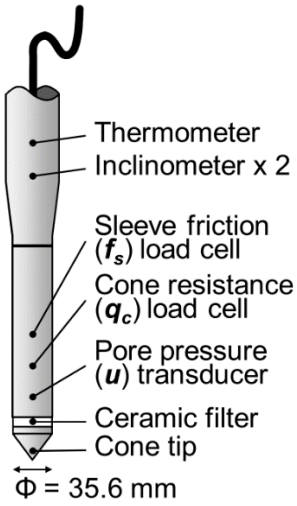

Figure 2.7. The schematic diagram of cone probe in CPTU test (Takai et al., 2016).

system to discuss the factors that may have an influence on the hydraulic conductivity of SB. It found that the EC of the permeant solution may have a strong influence on the swelling performance of bentonite, which leads to the change in the hydraulic conductivity of SB.

Besides hydraulic performance, the diffusion coefficient was also well discussed by many previous studies (e.g. Khandelwal et al. 1998 and Krol et al. 2004). Modified column tests and the Dialysis leaching test (DLT) method are the main methods applied to evaluate the diffusion coefficient of SB. Takai et al. (2017) tested the diffusion coefficient of SB against Cl^- based on modified column tests. While, Sample-Lord et al. (2021) applied a dialysis leaching test for clay-bentonite and sand-bentonite to evaluate the diffusion coefficient against NaCl. Results show that although, through different methods, the diffusion coefficients are similar, which proves both these two methods could evaluate the diffusion coefficient effectively.

In terms of consolidation behaviour, Evans and Ray (2005) used a consolidation test to evaluate the time rate of consolidation based on grab samples from field-mixed SB backfill, which was immediately prior to backfill placement in the trench. Ma et al. (2001) carried out triaxial tests of the soil–bentonite with different stress paths to examine mechanical properties of the SB. A nonlinear model (Baxter 2000) used to predict the stress-strain behaviours meets well with the results from triaxial tests.

Nevertheless, laboratory tests were seldom conducted using core samples because of technical difficulty in obtaining undisturbed core samples. Since during construction of SB cutoff wall, gravel still remains in the SB wall. Therefore, the device needs to both consider the soft clay and tough gravels at the same time during sampling. Therefore, there was no laboratory test has been done based on in-situ core samples from a real SB cutoff wall. It is necessary to provide more detailed information to verify the reliability of SB wall installed by an equal thickness trench cutting machine.

2.5 Construction process of SB wall installed by equal thickness trench cutting machine

In order to achieve high homogeneity of SB wall and generate less construction waste, an

equal-thickness trench cutting machine which used to be used in Trench cutting and Re-mixing Deep wall (TRD) method is considered at the construction of SB wall. The construction process of SB wall installed by an equal thickness trench cutting machine is shown in Figure 2.8. The construction processes are mainly 3 steps as follow:

(1) Cutting chain is installed in a base machine to rotate and cut the trench with bentonite slurry supply, as shown in Fig. 2.8. The slurry supply is injected through the piles in the chain and contacted with soil at the bottom of the trench. The bentonite slurry is supplied at the same time as trench cutting. Bentonite slurry is used as cutting fluid to increase the workability of the excavated soil.

(2) Assemble the cutting chain parts to extend the chain to design depth, cutting from the starting position in horizontal.

(3) After cutting the whole cutoff wall in a horizontal direction, bentonite powder is added and remixing when the chain removes to the initial position.

Compared to previous methods such as SB slurry, which mainly needs slurry to maintain the stability of the trench after excavation and blender the backfill outside, an equal-thickness trench cutting method could cutting and mixing the soil with bentonite slurry at the same time. Mixing soil and bentonite slurry in place also benefit the workability of the trench. Therefore, few slurry wastes would be generated during construction. Since the additive is added by injecting through the pipe of chains, this construction method can be suitable for multiple kinds of additives such as cement slurry or powder.

2.6 Application of cement amendment in SB mixture

Cement has been widely used as a ground improvement additive for a long time. Compared to other additives, cement has a significant advantage in not only cost-effectiveness but also in material supply. Cement additives may increase the strength of ground soil by cation adsorption between soil particles with an alkaline condition and the hydration mechanisms of cementitious material (Kamon et al., 1996). There already have some applications of using cementitious materials as the main material to improve strength performance in bentonite cutoff walls, such

as slag-cement-bentonite (slag-CB), Cement-bentonite (CB) and soil-cement-bentonite (SCB) slurry wall. slag-CB and CB walls

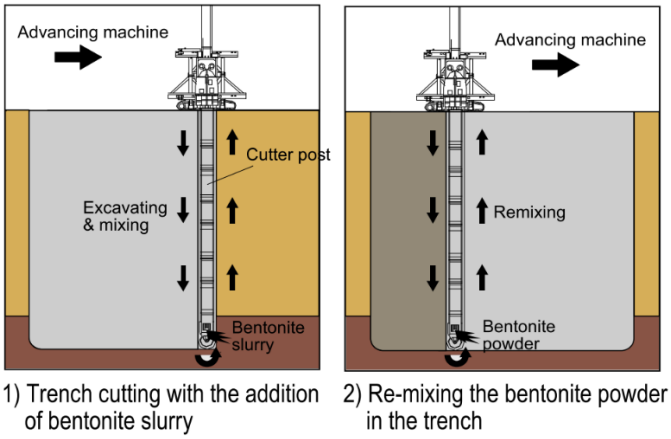

Figure 2.8. Schematic diagram of SB wall installed by trench cutting machine with an equal thickness (Katsumi et al., 2008).

2.6.1 Cement-bentonite wall

Slag-CB and CB walls are already frequently used in the United Kingdom. The compression stress of slag-CB material can be up to over 1000 kPa with approximately 150 kg/m^3 cement material which already becomes plastic concrete instead of soil. However, the disadvantage of slag-CB material is also ignorable. The hydraulic conductivity of slag-CB is very sensitive to soil gradation and needs around 90 days of curing to achieve design value (Opdyke and Evans, 2005). Before curing finishes, especially in the first 60 days, the hydraulic conductivity would be much higher than the designed value. The construction process of the slag-CB wall also brings wasted excavated soil and slurry (LaGrega et al., 2010).

Considering cement materials are the main additive in CB or slag-CB wall, the volume change of the backfill materials also needs considering. As shown in Fig. 2.9, the backfill of CB/slag-CB mixture may go through 5 different stages after construction is finished. The volume of the backfill may shrinkage significantly during pre-set and hardening stages. Compared to concrete, this issue is even more critical since there are much fewer gravels and no steels in the CB mixture to restrict the shrinkage.

Cement material also may have some reaction with bentonite, since in practical Na-

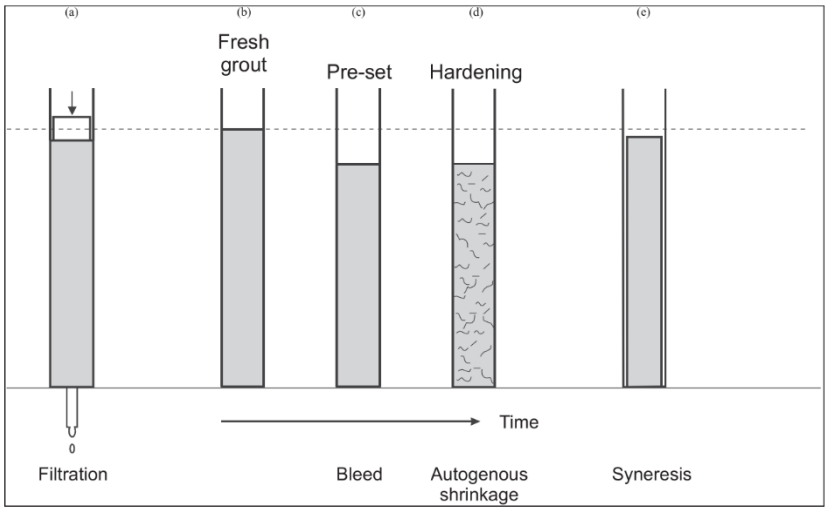

Figure 2.9. Schematic of volume changes prior to and post set (Jefferis, 2012).

bentonite is more wildly applied in the construction site. Cement addition will create a strong alkaline condition and high calcium concentration due to the hydration reaction of CaO. Na-bentonite may have a reaction with calcium cation in this situation which forms Ca-bentonite (BSW, 1992). Considering the activity and swelling performance of Ca-bentonite is relatively poor compared to Na-bentonite, the hydraulic performance of CB-bentonite is not as good as SB (Koch, 2002).

2.6.2 Soil-cement-bentonite wall

SCB slurry wall was applied with increasing frequency as a hydraulic barrier to the lateral underground seepage when the strength of the basic SB wall was not inadequate to carry the ground stress. While comparing with CB slurry wall, the construction process of SCB slurry wall is close to conventional SB slurry wall (Ryan, 1985). A narrow trench is excavated by the machine under bentonite slurry to avoid the trench from collapsing, as shown in Figure 2.10. Then, backfill material is a blended mixture of soil, bentonite slurry, dry bentonite and cement. When the excavation machine finishes the construction of the trench, the backfill is injected back to the trench.

Figure 2.10. Trench of SCB wall under bentonite slurry (Ryan and Day, 2002).

With the amendment in mechanic performance, the backfill slope of SCB is usually in the range of 3:1 to 6:1 (horizontal to vertical), which is much steeper than SB backfill slopes. However, there are still several disadvantages of SCB wall. First of all, SCB needs more complicated equipment that is used for the trench mixing and placing the backfill. Secondly, the hydraulic conductivity of SCB material immediately finished construction increases to 1×10^{-8} m/s (Ryan and Day, 2002). SCB may not be suitable for those projects which have strict requirements for barrier performance. Therefore, it is necessary to research how to improve to moderate strength with acceptable hydraulic conductivity (lower than 10^{-9} m/s).

References for Chapter 2

ASTM D6635-01, 2007. Standard Test Method for Performing the Flat Plate Dilatometer, ASTM International, West Conshohocken, US.

Baxter, D.Y., 2000. Mechanical behavior of soil–bentonite cutoff walls. Ph.D. thesis, Virginia Tech., Blacksburg, USA.

Britton, J.P., Filz, G.M., Little, J.C., 2005. The effect of variability in hydraulic conductivity on contaminant transport through soil–bentonite cutoff walls. Journal of Geotechnical and Geoenvironmental Engineering 131 (8), 951–957. https://doi.org/10.1061/(ASCE)1090-0241(2005)131:8(951)

Daniel, D. E., 1989. In situ hydraulic conductivity tests for compacted clay. Journal of Geotechnical Engineering, 115(9), 1205-1226.

Dietrich, K., 2002. Bentonites as a basic material for technical base liners and site encapsulation cut-off walls. Applied Clay Science, 21 (1), 1-11. https://doi.org/10.1016/S0169-1317(01)00087-4

Evans, J., Ryan, C., 2005. Time-dependent strength behavior of soil-bentonite slurry wall backfill. In Waste Containment and Remediation, pp. 1–9.

Hamidpour, M., Kalbasi, M., Afyuni, M., Shariatmadari, H., Furrer, G., 2011. Sorption of lead on Iranian bentonite and zeolite: kinetics and isotherms. Environmental Earth Sciences, 62 (3), 559-568.

Inui, T., Katsumi, T., Takai, A., 2016. Cesium sorption/desorption characteristics of sodium bentonite affected by major cations in leachate from MSW incinerator ash. Japanese Geotechnical Society Special Publication 2 (153), 1841–1844. https://doi.org/10.3208/jgssp.JPN-071

Jefferis, S., 2012. Cement-bentonite slurry systems. In: Grouting and Deep Mixing 2012, ASCE , New Orleans, Louisiana, US , pp. 1–24. https://doi.org/10.1061/9780784412350.0001

Katsumi, T., Ogawa, A., and Fukagawa, R., 2004. Effect of prehydration on hydraulic performance of geosynthetic clay liners permeated with inorganic chemical solutions, GeoAsia2004 (Proceedings of the 3rd Asian Regional Conference on Geosynthetics -Now and Future of Geosynthetics in Civil Engineering), J.B. Shim, C. Yoo, and H.-Y. Jeon (eds.), pp.937–944.

Katsumi, T., Kamon, M., Inui, T., Araki, S., 2008. Hydraulic barrier performance of SBM cutoff wall constructed by the trench cutting and re-mixing deep wall method. In: Krishna, R.R., Milind V.K., Akram, N.A. (Eds.), GeoCongress 2008: Geotechnics of Waste Management and Remediation, ASCE. New Orleans, US, pp. 628–635. https://doi.org/10.1061/40970(309)79

Khandelwal, A., Rabideau, A. J., and Shen, P., 1998. Analysis of diffusion and sorption of organic solutes in soil-bentonite barrier materials. Environmental science & technology,

32(9), 1333–1339.

Komine, H., 1999. Theoretical equations for evaluating hydraulic conductivities of bentonite based buffer and backfill 2289–2292. https://doi.org/10.1061/(ASCE)1090-0241(2008)134:4(497)

Komine, H., Ogata, N., 2004. Predicting swelling characteristics of bentonites, Journal of Geotechnical and Geoenvironmental Engineering, 130(8), 818–829. https://doi.org/10.1061/(ASCE)1090-0241(2004)130:8(818)

Komine, H., 2004. Simplified evaluation for swelling characteristics of bentonites, Engineering Geology 71, 265–279.

Komine, H., 2008. Theoretical equations on hydraulic conductivities of bentonite-based buffer and backfill for underground disposal of radioactive wastes. Journal of Geotechnical and Geoenvironmental Engineering, 134(4), 497–508. https://doi.org/10.1061/(ASCE)1090-0241(2008)134:4(497)

Krol, M.M., Rowe, R.K., 2004. Diffusion of TCE through soil-bentonite slurry walls. Soil & Sediment Contamination, 13(1), 81–101.

LaGrega, M.D., Buckingham, P.L., Evans, J.C. 1994. Hazardous Waste Management: McGraw Hill, New York. US.

Ma, P., Ke, H., Tong, X., and Chen, Y., 2021. Nonlinear constitutive model of soil–bentonite based on triaxial tests along different stress paths.Canadian Geotechnical Journal,58(5), 682–694.

Malusis, M., McKeehan, M. 2013. Chemical compatibility of model soil-bentonite backfill containing multiswellable bentonite, Journal of Geotechnical and Geoenvironmental Engineering, ASCE, 139(2).189–198.

Minja, R.J., Ebina, T., 2002. Arsenic adsorption capabilities of soil-bentonite mixtures as buffer materials for landfills. Clay Science 12 (1), 41–47. https://doi.org/10.11362/jcssjclayscience1960.12.41

Mitchell, J.K., and Soga, K. (2005): Fundamentals of soil behavior, John Wiley & Sons, pp.153−156.

Opdyke, S.M., Evans, J.C., 2005. Slag-cement-bentonite slurry walls. Journal of Geotechnical

and Geoenvironmental Engineering, 131 (6), 673−681. https://doi.org/10.1061/(ASCE)1090-0241(2005)131:6(673)

Ruffing, D. G., Evans, J. C., and Malusis, M. A., 2011. Evaluations of lateral earth pressure in a soil-bentonite slurry trench cutoff wall. In:2011 Joint Pan American and Canadian Geotechnical Society Conference.

Ryan, C.R., Day, S.R., 2002. Soil-cement-bentonite slurry walls. In: Deep Foundations 2002: An International Perspective on Theory, Design, Construction, and Performance. ASCE, Orlando, US, pp. 713−727.

Sample-Lord, K. M., Ahmed, M., and Malusis, M. A.,2021. Diffusion through soil-bentonite backfill from a constructed vertical cutoff wall. Soils and Foundations, 61(2), 429–443.

Sivapullaiah, P.V., Sridharan, A., Stalin, V.K. 2000. Hydraulic conductivity of bentonite-sand mixtures, Canadian Geotechnical Journal 37(2), 406–413.

Takai, A., Inui, T., Katsumi, T., Kamon, M., Araki, S., 2012. Factors affecting the hydraulic barrier performance of soil-bentonite mixture cutoff wall. Journal of Japan Society of Civil Engineers, Ser. C (Geosphere Engineering), 68 (1), 1−14. https://doi.org/10.2208/jscejge.68.1

Takai, A., Inui, T., Katsumi, T., Kamon, M., Araki, S., 2013. Hydraulic barrier performance of soil bentonite mixture cutoff wall. In: Manassero, M., Dominijanni, A., Foti, S., Musso, G. (Eds.), Coupled Phenomena in Environmental Geotechnics. Taylor and Francis, Politecnico di Torino, Italy, pp. 707–714. https://doi.org/10.1201/b15004-96

Takai, A., Inui, T., Katsumi, T., 2016. Evaluating the hydraulic barrier performance of soil-bentonite cutoff walls using the piezocone penetration test. Soils and Foundations 56 (2), 277–290. https://doi.org/10.1016/j.sandf.2016.02.010

Chapter 3. Laboratory testing of soil-bentonite cutoff walls using core samples

3.1 General remarks

As introduced in Chapter 1, compared to the previous construction method for SB walls such as SB slurry wall, the mix of native soil and bentonite slurry of SB cutoff wall is in place to provide better stability for the excavated trench and reduce waste of slurry. While backfill mixing in the trench instead of mixing outside makes the homogeneity of the backfill harder to guarantee. Therefore, it is necessary to do the post-construction quality assessment of the SB cutoff wall using in-situ core samples. In this Chapter, the physical properties and hydraulic conductivity of SB from two sites were tested to discuss the quality and homogeneity of the SB cutoff wall. One SB wall was built 15 years ago in Tochigi Prefecture to study the long-term performance of the SB cutoff wall, and the other SB wall was built up to 40m depth in Kanagawa Prefecture to verify whether the quality of such deep SB cutoff wall could be ensured.

3.2 Sites and materials

3.2.1 Site A—A fifteen-years-old SB wall

In 2003, a 10-m deep, 14-m long, 0.7-m wide SB wall was constructed in Site A (i.e., in Tochigi Prefecture, Japan) as a pilot-scale test. The groundwater level in this site is G.L.−5.0 m. During trench cutting, native soil was mixed with bentonite slurry (5% bentonite by weight). Approximately 300 kg/m^3 of bentonite slurry was injected to maintain the workability of the soil inside the trench. During re-mixing, ~100 kg/m^3 bentonite powder was added. The bentonite is sodium bentonite with >65% montmorillonite as per the product standard. Because the dry density of the native soil is ~1.50 g/cm^3, the mass ratio of dry bentonite to native soil is ~7.1%.

Fifteen years after the SB wall construction (i.e., in 2018), core samples of the SB wall and native soil were collected using a boring method described in Section 3.2.3. Figure 3.1

shows the boring profile of native soil in this site, while Fig. 3.2 shows the appearance of the core samples. The native soil has clearly defined layers, while slight colour differences exist among the SB wall layers. Therefore, the SB wall was relatively homogeneous in the vertical direction.

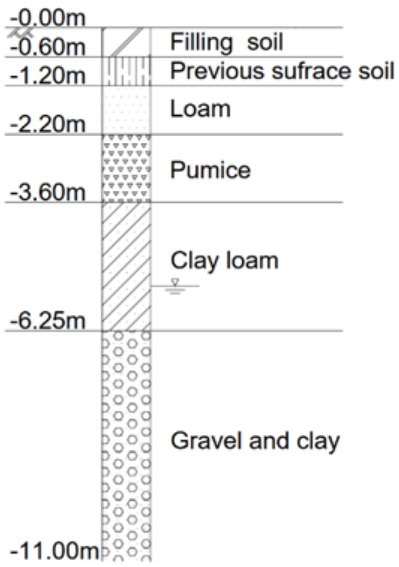

Figure 3.1. Boring log of native soil from Site A.

(a) Native soil (b) SB wall

Figure 3.2. The appearance of the core samples from the Site A.

3.2.2 Site B—A 40m depth SB wall

In 2019, a 40-m deep, 0.55 m wide SB wall was constructed in Site B (i.e., in Kanagawa Prefecture, Japan). This SB wall is constructed for seepage control at a river embankment. The groundwater level in this site is G.L.−2.7 m. During trench cutting, native soil was mixed with bentonite water slurry (5% bentonite by weight). Approximately 65 kg/m^3 of bentonite slurry was injected to maintain the workability of the soil inside the trench. During re-mixing, ~125 kg/m^3 bentonite powder was added. This bentonite is the same type of bentonite used in Site A. The native soil is composed mainly of sand and silt. Because the dry density of the native soil is ~1.59 g/cm^3, the mass ratio of dry bentonite to native soil is ~7.5%.

Fourteen days after construction of the SB wall was completed, core samples of the wall and native soil were collected using the boring method described in Section 3.2.3. Figure 3.3 shows the appearance of the core samples. Compared to native soil, SB samples almost has no difference in appearance. Figure 3.4 shows that native soil has a complex boring profile with various thin layers.

3.2.3 Sampling method

To collect core samples of the SB walls, after the surface ground with a thickness of 1.3 m was removed using a backhoe, a drilling machine was placed on a steel sheet, while the same machine was directly placed on the ground surface to sample native soil. A rotary drilling machine with a hydraulic feed control system was used in this study. Since the SB walls in this study were installed by mixing in situ soils and bentonite, and the mass ratios of dry bentonite to native soil are less than 10%, gravels contained in native soil largely remain in the SB walls. To collect core samples from such grounds with various sizes of particles, a diamond bit was attached to the tip of the drill, and water was jetted to cut the SB walls. The diamond bit is often used with the hydraulic feed control system to collect stiff samples such as rock. By feeding a plastic bag attached to the inner wall of the core tube, intact samples were collected. There were technical difficulties of sampling from the SB wall, for instance, the wall been soft and containing large gravels. Therefore some portions were loosened by the jetting and not

smoothly collected, especially at Site A. The core diameters of the native soil and the SB walls were 86 mm and 116 mm, respectively. Because careful attention was needed, two or three days were required to complete each sampling. The SB wall's boring hole is located at the centre of the wall, while the hole for the native ground is less than 10 m away from the SB wall.

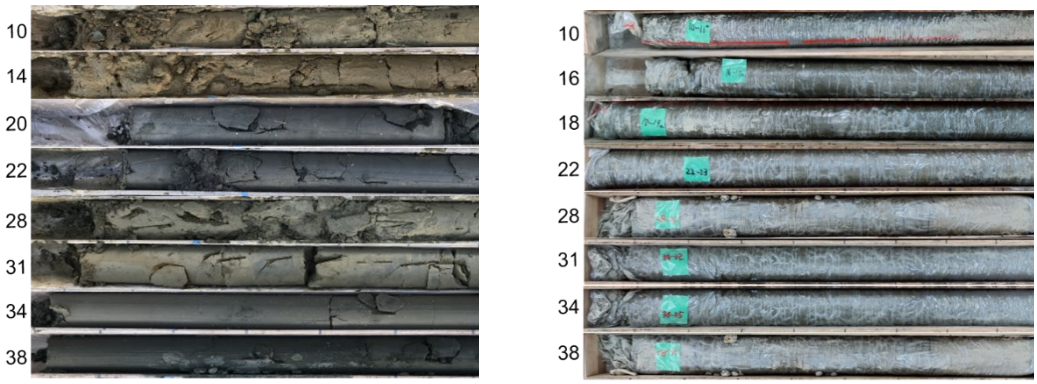

(a) Native soil (b) SB wall

Figure 3.3. The appearance of the core samples from Site B.

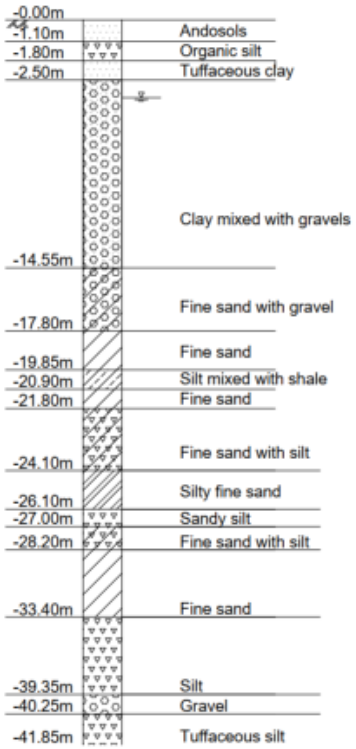

Figure 3.4. Boring log of native soil from Site B.

3.3 Methods

Several laboratory tests were carried out on the core samples to determine their physical properties. The physical properties investigated include particle density, particle size distribution, Atterberg limits and void ratio. To discuss consolidation properties of SB with depth, consolidation tests using incremental loading were conducted for saturated samples using a conventional oedometer as per JIS A 1217 (2009). A flexible-wall permeameter with a falling head system was used to evaluate the k of SB. The test corresponds to ASTM D 5084-16a (2016). In addition, in situ k of SB was measured using the BAT permeameter in Site A.

3.3.1 Physical property tests

Physical properties of core samples were determined and used for discussing the homogeneity of the SB walls. Wet density, particle density and Atterberg limits tests were conducted as per JIS A 1225 (2009), JIS A 1202 (2009) and JIS A 1205 (2009), respectively. The wet density was determined by cutting a sample to a cylinder of 10 cm in height and measuring its weight and volume. Atterberg limits were obtained using a sample oven-dried at 40ºC for several days and with <0.425 mm in diameter. The particle density was determined using an oven-dried sample with <9.5 mm in diameter.

However, the maximum size of particles in the core samples was 53 mm. To minimise the errors in measurement, some tests required large amounts of samples. For instance, JIS A 1203 (2009), the standard for water content test, requires >5 kg, and JIS A 1204 (2009), the standard for particle size distribution test, requires >30 kg. Unfortunately, the amount of samples available was limited, particularly from Site A. Therefore, some guidelines were partially followed for Site A's samples. That is, 30–100 g was used for the water content tests, and 3 kg was used for the particle size distribution tests.

3.3.2 Consolidation tests

Consolidation tests were conducted for SB for various depths. From Site A, 5 depths were considered for SB, namely, 3.0–4.0, 5.3–5.5, 6.4–6.7, 7.5–7.6 and 8.3–8.4 m. From Site B, 4

depths were considered for SB, namely, 9.0–10.0, 19.0–20.0, 29.0–30.0 and 39.0–40.0 m. Core samples were about ϕ 12 cm, and therefore, the size was reduced to ϕ 6 cm × h 4 cm using a ring cutter to fit in the oedometer. The height of specimens was increased from the standard height of 2 cm by considering the gravels in the specimens. Although the maximum particle size of the SB wall in Site A was 53 mm, it was confirmed that gravels larger than 19 mm are not contained in specimens used for consolidation tests. The consolidation stress was determined by JIS A 1217 (2009). The loading increment ratio is recommended to be 1. In addition, two or three stages above consolidation yield stress (p_c) are required to determine the p_c. Since the p_c of specimens used in this study ranged from 40 to 100 kPa, the consolidation stress starts from 9.8 kPa and increases by two times until 628 kPa. The completion of consolidation was confirmed using the Taylor method, where the degree of consolidation (U) is more than 95%. The p_c was estimated from the e-log p curves by applying Mikasa's graphical method, which is a modified Casagrande's method and standardised in JIS A 1217 (2009). Because samples are under saturated conditions, consolidation results can be extended to determine the hydraulic conductivity of the samples. Hydraulic conductivity was estimated as $k = c_v \cdot m_v \cdot \gamma_w$, where c_v is the coefficient of consolidation, m_v is the coefficient of volume change, and γ_w is the unit weight of water. Using c_v to estimate k is based on Terzaghi's theory and includes several assumptions (Tavenas et al., 1983). Some of the assumptions may not be satisfied in this study, for instance, the strain needs to be small, and there should be a linear relationship between effective stress and strain. These unsatisfied assumptions may lead to some errors in the k measurement. Furthermore, estimating k by c_v is an indirect measurement, which does not consider the chemical effect induced by permeation (e.g., bentonite-water interactions). As a consequence, there might be some errors in the k measurement.

3.3.3 Hydraulic conductivity tests

A flexible-wall permeameter with a falling head system was used to evaluate the k of SB. This test is also widely used to measure hydraulic conductivity of barrier materials, including SB in previous studies, and conducted to discuss the compatibility of results with the ones obtained by the consolidation test. Five depths were considered for SB from Site A, namely,

2.3–2.4, 4.0–4.1, 5.0–5.1, 6.4–6.5 and 8.3–8.4 m. Seven depths were considered for SB from Site B, namely, 2.0–3.0, 8.0–9.0, 14.0–15.0, 20.0–21.0, 26.0–27.0, 32.0–33.0 and 36.0–37.0 m. SB samples from Sites A and B were cut to ϕ 10.0 cm × h 9.0 cm and ϕ 6.0 cm × h 7.0 cm, respectively. A relatively large specimen is chosen because the maximum particle size in SB is more than 19 mm. After cutting, the specimens were submerged in distilled water and saturated by vacuum deaeration for over 24 hours. Then, the saturated specimen was set on the flexible wall permeameter. The hydraulic gradient (i) was set to ~10 or 15 for Sites A or B. Distilled water was used as the permeant. Cell pressure of 50 kPa was applied as confining pressure.

3.3.4 In situ hydraulic conductivity measurement with the BAT permeameter

The BAT permeameter developed by Torstensson (1984) was used in this study for in situ measurements of horizontal hydraulic conductivity (k_h) of the SB wall in Site A. The BAT permeameter results can be considered the baseline measurements of k_h because it is directly measured (Bo et al., 2014). Several benefits exist for using BAT permeameter as an on-site hydraulic conductivity measurement tool, namely, ease of installation, short test time, applicability at large depths, etc. (Daniel, 1989). The BAT permeameter measures the pore pressure locally in the soil, with little water movement, resulting in a quick reaction time. Since this device measures the horizontal hydraulic conductivity, the applicability to walls with a small width (<1.0 m) needs clarification but remains to be discussed.

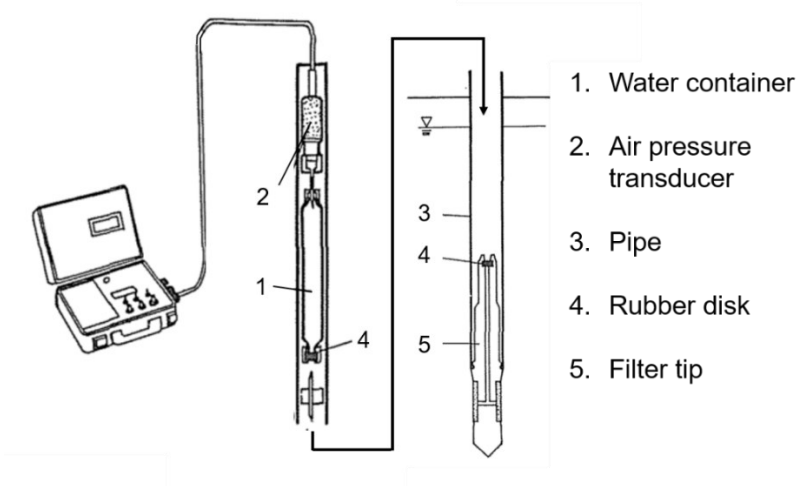

Figure 3.5. The schematic of the BAT permeameter.

The schematic of the BAT permeameter is shown in Fig. 3.5. The BAT system's key elements are the filter tip, pore pressure transducer, and a water container. The diameter of the filter tip was 30 mm, and the length was 40 mm. The pore pressure adaptor containing a pore pressure transducer is threaded to an extension pipe, lowered into a pre-bored borehole, and placed at the desired elevation. When the pore pressure transducer is lowered down the borehole, it is coupled to the nozzle in the filter tip, and gravity draws the hypodermic needle downward, penetrating the rubber disk mounted in the filter tip. The in situ measurement of k_h can be carried out as an inflow test. The container is completely gas-filled at the start of the test. An inflow test can be conducted simultaneously with the extraction of pore water samples. The air in the chamber is evacuated as water flows into the probe, resulting in a change in air pressure in the chamber. A pressure transducer monitors the pressure change. This rate is computed by the pressure change measured in the container using Boyle's Law, which can be translated into a volume change and analysis of the time-pressure record yields the horizontal hydraulic conductivity using the following equations:

$$k_h = \frac{P_0 V_0}{F \cdot t \cdot 10^3}\left[\frac{1}{U_0 P_0} - \frac{1}{U_0 P_t} + \frac{1}{U_0^{\,2}} \ln\left(\frac{P_0 - U_0}{P_0} \times \frac{P_t}{P_t - U_0}\right)\right] \tag{3.1}$$

$$F = \frac{2\pi L}{\ln\left[L/d + \sqrt{1 + \left(L/d\right)^2}\right]} \tag{3.2}$$

where k_h is the horizontal hydraulic conductivity (m/s) defined by the Eq. 3.1; P_0 is the absolute initial air pressure in the container (mH_2O); P_t is the absolute air pressure in the container at time t (mH_2O); V_0 is the initial air volume (mL); F is the shape factor defined by the Eq. 3.2; U_0 is the static pore water pressure (mH_2O); L is the length of filter in mm and d is the diameter of filter in mm.

The BAT permeameter was placed at G.L.−10.5 m, which corresponds to a layer of gravel mixed with clay in the native soil of Site A. Since the BAT permeameter test uses the same boring hole created for sampling, the BAT test could be carried at the bottom of the boring hole, G.L. -10.5 m. This depth was selected to ensure that the test was done below the groundwater level. The measurement was conducted at the centre of the length and the width direction of the SB wall.

3.4 Experimental results for Site A

3.4.1 Particle size distribution

Figure 3.6 shows particle size distribution curves of the core samples. The particle sizes of soils in native soil broadly vary at each depth. Contrasted to native soil, SB has a similar particle size at any depth. The guideline for classifying geomaterials standardised in JGS 0051 (2020) was used to classify the soils. The soils in native soil were classified as sandy gravel (GS), sand (S), sand with fine fraction (S-F), silt (M), clay (C), etc. The well-graded soil in SB was classified as sandy gravel of fine fraction nature (GFS).

Figure 3.7 shows the gravel (>2 mm in diameter), sand (2–0.075 mm in diameter), and fines (<0.075 mm in diameter) content in different depths of the core samples. Gravels are contained in all depths of SB, with contents ranging from 20 to 60%. However, gravels were concentrated in the upper layer at a depth of 1.3–2.3 m and near the depth where native soil contains ~60% gravel content (i.e., depth of 6.7–6.8 m). Considering the fines content, SB from all depth keep >20% fine contents, even if the content in native soil is scattered (8–80%). Results suggest that even 15 years after the SB wall construction, the SB wall keeps enough fines content.

3.4.2 Atterberg limits

Figure 3.8 shows the relationship between the samples' plastic index (I_p) and liquid limit (w_L). In the native soil, pumice and loam have a high w_L and a high plastic limit (w_p), while the gravel layer has a low $w_L \approx 25\%$ and a low $w_p \approx 20\%$. However, SB has a much narrow range

of w_L = 60–75% and w_p = 90–100%. Since clay with a high I_p has a low k value, the k of the SB wall should be low due to the high plastic index of the SB.

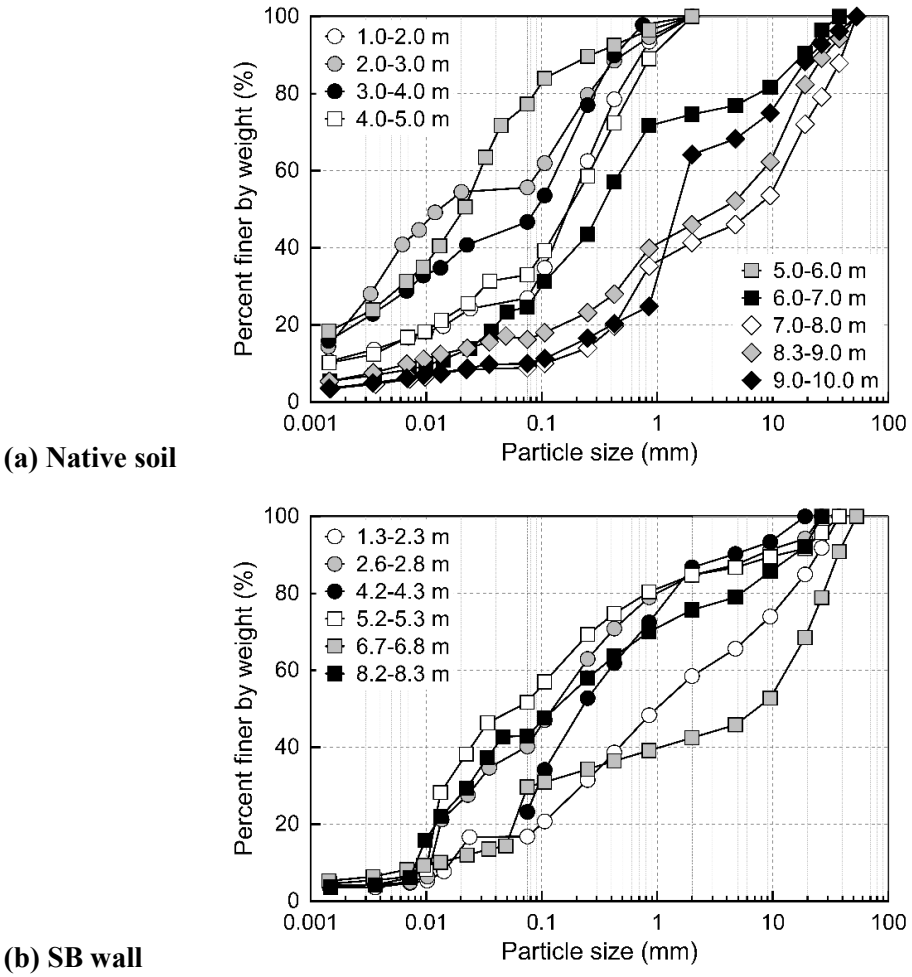

(a) Native soil

(b) SB wall

Figure 3.6. Particle size distribution curves of the core samples from Site A.

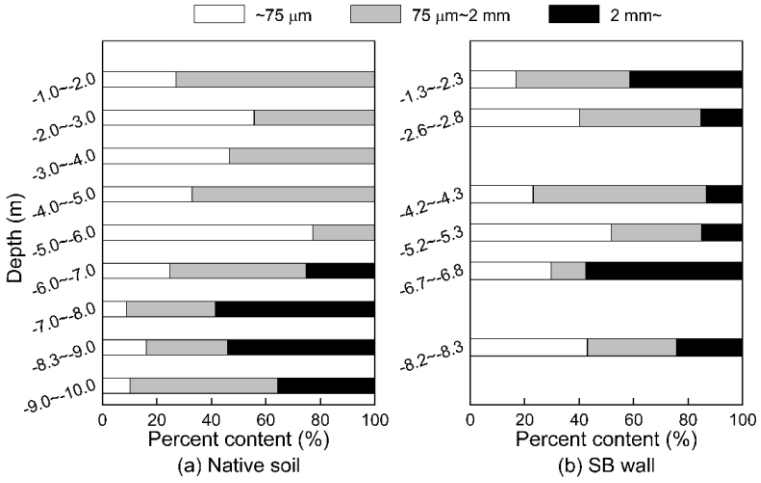

Figure 3.7. Percent of gravel, sand, and fines content in the core samples from Site A.

Activity is an index of physisorption and chemical affinity of clay. The equation for Activity is shown in Eq. 3.3. The activity of SB is 7.88, which is higher than that of native soil (1.28) as shown in Fig. 3.9. High activity suggests lower effective voids that contribute to permeation, limiting the movement of free water and decreasing the coefficient of consolidation (Ogawa et al., 2020). However, SB's activity value is higher than that of pure bentonite (Asad et al., 2013). Activity is determined using weight percent of clay content (< 2 μm) and I_P as shown in Eq.3.3:

$$Activity = \frac{I_p}{\text{mass ratio}(\leq 2\mu\text{m})} \tag{3.3}$$

Since clay content in SB is ~5%, while it is ~70% in pure bentonite, the bentonite's high clay content makes it have lower activity, given that the plastic index of both materials is close.

3.4.3 Consolidation behaviour

The consolidation yield stress (p_c) is determined from the *e*-log *p* curve, based on Mikasa's method (Fig. 3.10). The p_c is the maximum effective vertical overburden stress that a particular soil sample has sustained in the past (Solanki and Desai, 2008). Here, p_c is taken as the effective vertical stress of SB wall. The vertical distribution of consolidation pressure (p) and void ratio(e) of SB from Site A is shown in Fig. 3.11. The p_c is ~30 kPa constantly except in the

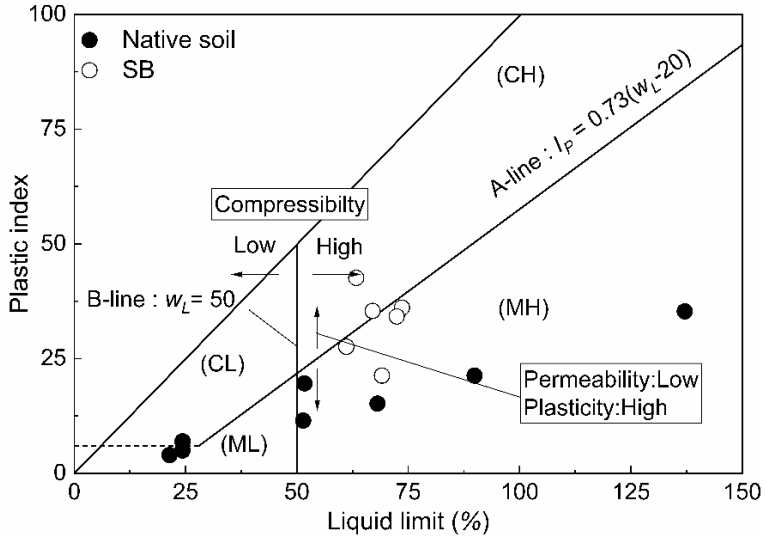

Figure 3.8. Plasticity chart of the core samples from Site A.

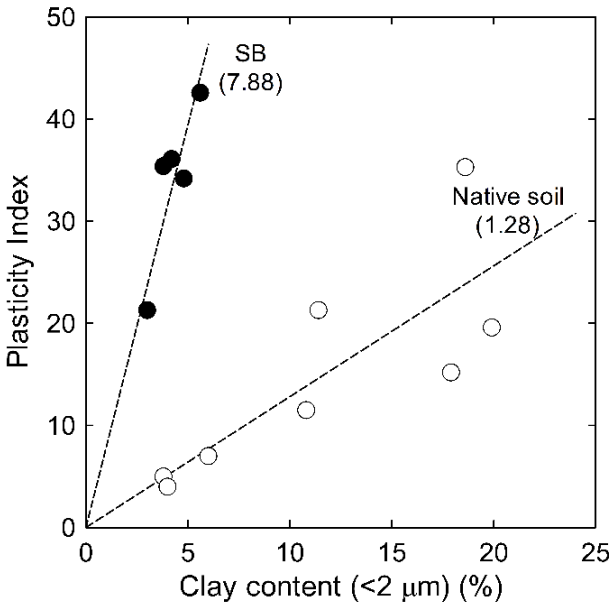

Figure 3.9. Relationship between plasticity index and clay content in the core samples from Site A. Figures in brackets are the 'activities' of the clays.

depth of 7.45–7.60 m, which is much smaller than overburden pressure approximated by the average wet density of the SB and the groundwater level at the site. Most samples have a heterogeneous settlement at the end of the test. It may be caused if the cover of settlement mould already touches the gravels, which cannot be compressed. The special point occurs in the depth of 7.45–7.60 m, where the void ratio, e = 1.0, is much lower than the other layers, e ≈ 2.0. The high gravel contents might cause the high p_c and low void ratio of SB at a depth of 7–8 m. The large gravels may decrease the void ratio due to their material property (Nakaya 2019). It is also much more difficult to compress due to the skeleton effect of large gravels. Once the gravel contacts with each other, the load may be mainly transferred by gravel only. The compression process changes to compressing gravel instead of compressing soil mixture.

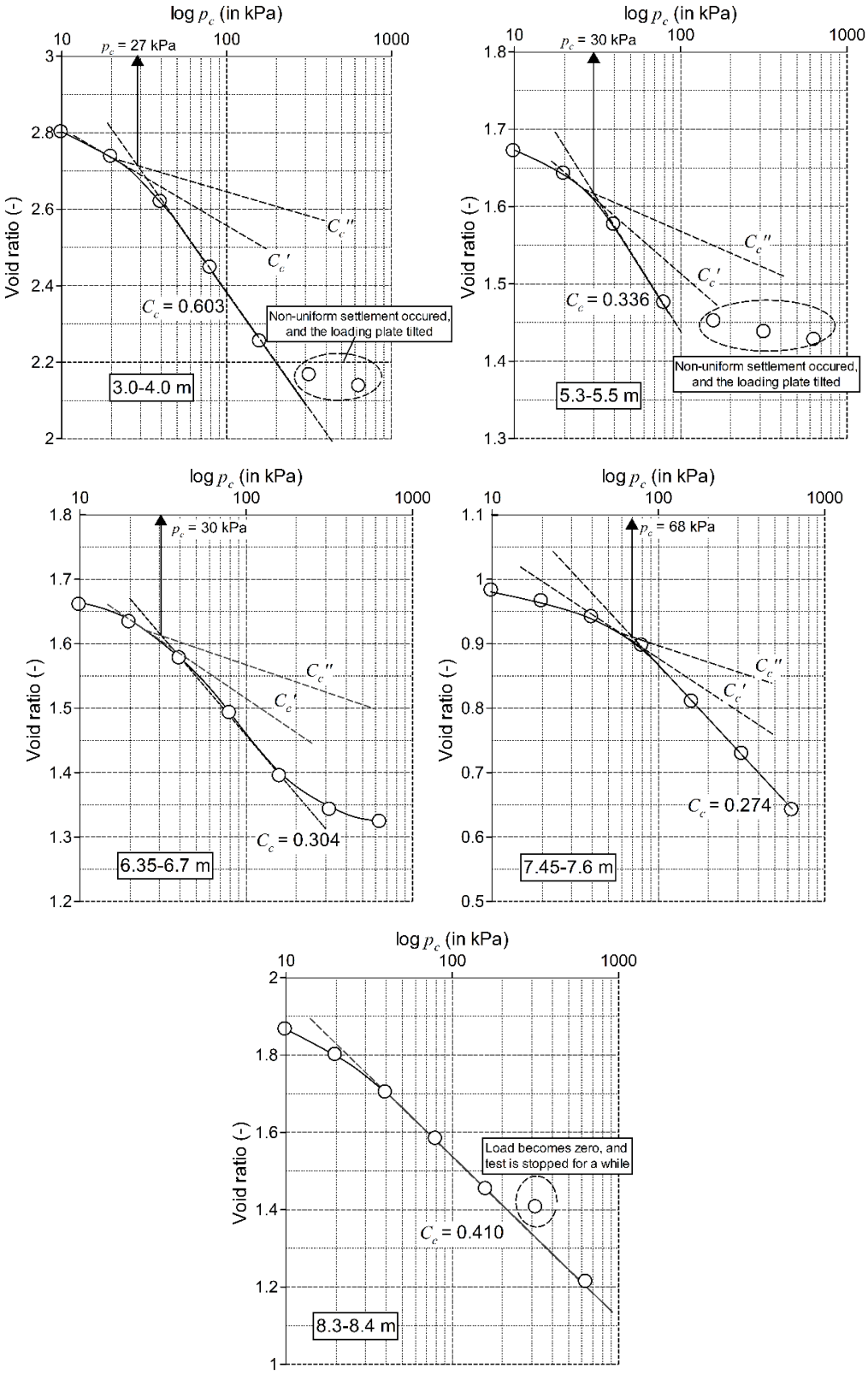

Figure 3.10. *e*-log p_c curves of the consolidation tests on the SB of Site A.

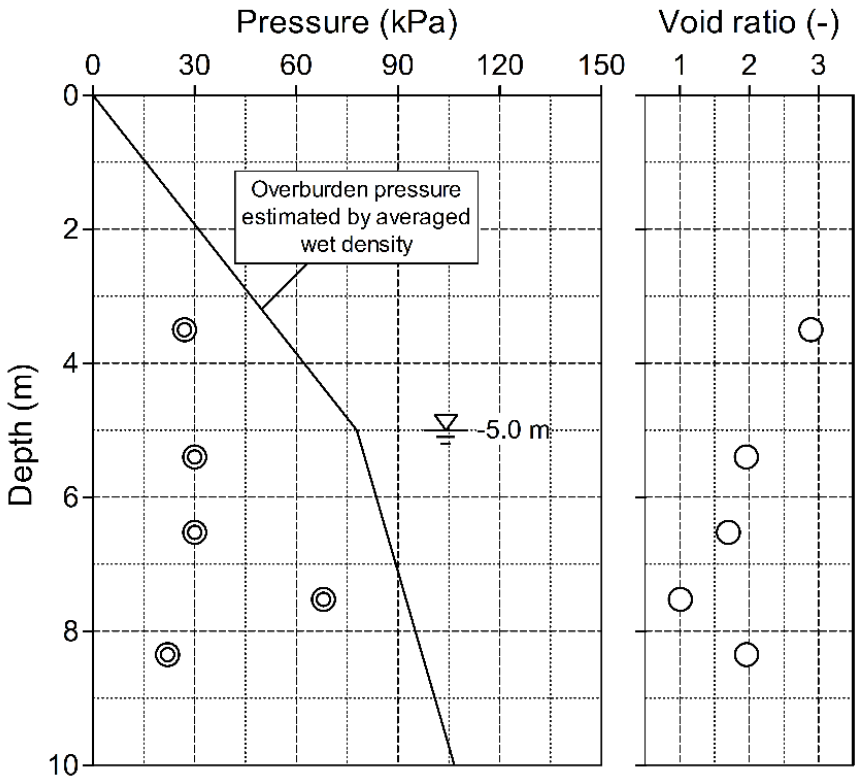

Figure 3.11. Stress and void ratio distribution in the SB wall of Site A.

3.4.4 Hydraulic conductivity

Figure 3.12(a) shows the k of SB determined from the consolidation tests. The k of the SB ranges from 1.0×10^{-9} m/s to 1.0×10^{-10} m/s under confining pressure of 55.5 kPa. Hydraulic conductivity tests were conducted for more than six months. However, as shown in Fig. 3.12(b), only a few data were obtained. As a result of using a large specimen size and extremely low k of SB, the k still decreased, which does not meet the termination criteria as per the ASTM D 5084-16a (2016), although the tests have been conducting for over six months. From the data, the highest k of the SB is ~3.0×10^{-10} m/s. Results suggest that even after 15 years, the k of the SB wall will still be lower than the design value (i.e., $k = 1.0 \times 10^{-9}$ m/s). The low k of the SB can ensure the SB wall functions to control seepage.

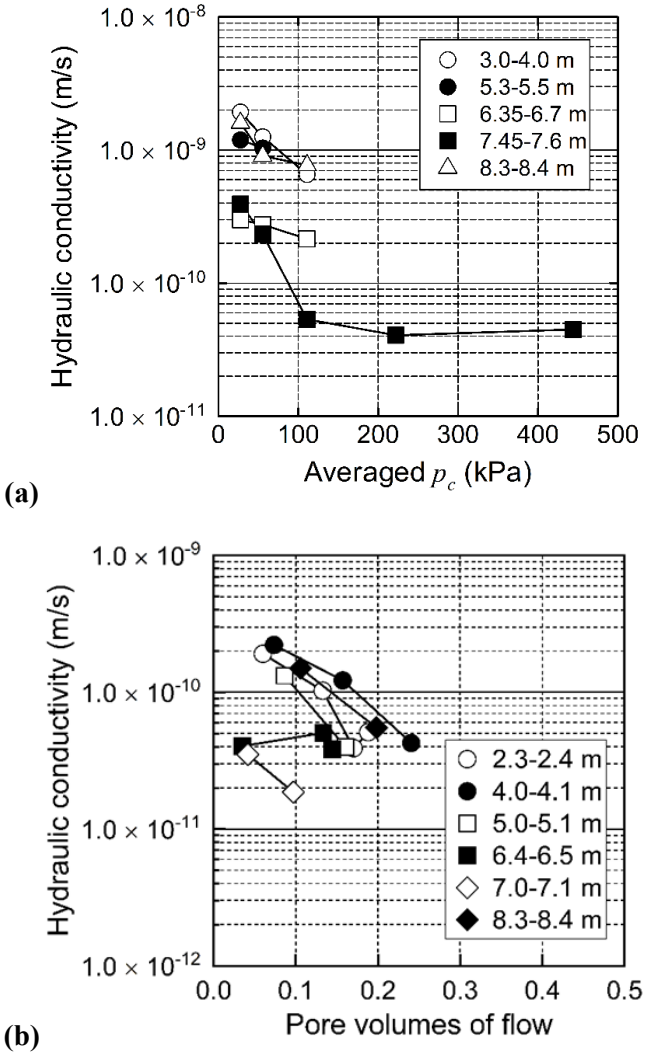

Figure 3.12. *k* values of SB from (a) consolidation tests and (b) flexible wall *k* tests. The results of flexible wall *k* tests might not necessarily meet the requirements of ASTM D5084-16a (2016).

Figure 3.13 shows the change in the air pressure in the container obtained by the BAT permeameter and the relationship between measurement time and k_h. After initial pore pressure in the container reached a steady state, air pressure in the container was measured for 2 hours at a 15-second interval. This result demonstrates that a sufficient time of more than 2 hours is recommended for in situ hydraulic conductivity measurement of SB walls using the BAT permeameter. Table 3.1 shows the result of hydraulic conductivity measurement using the BAT permeameter, which is needed in Eq. (3.2). By assigning these values, the k_h is determined as

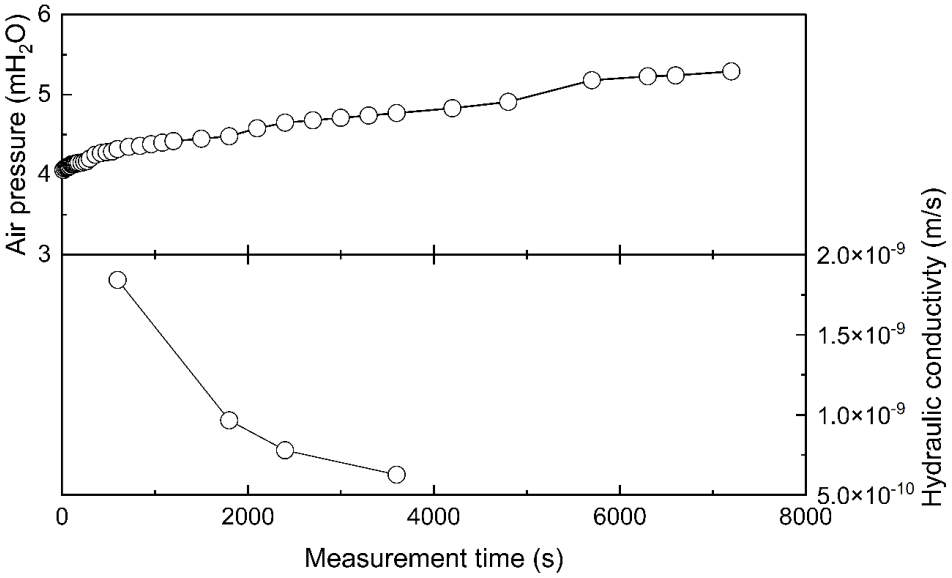

Figure 3.13. Relationship between air pressure, hydraulic conductivity and measurement time in BAT test.

Table 3.1. Results of *k* of SB at a depth of 10.5 m using the BAT permeameter.

t (min)	P_0 (mH_2O)	U_0 (mH_2O)	P_t (mH_2O)	V_0 (mL)	*F* (mm)	k_h (m/s)
10	4.06	12.5	4.32	35	230	1.8×10^{-9}
30			4.48			9.7×10^{-10}
60			4.77			7.8×10^{-10}
120			5.29			6.3×10^{-10}

~6.3×10^{-10} m/s with 120 minutes elapsed. While the tested depth of each experiment is not completely the same, this result is in good harmony with the *k* of SB at 8.3–8.4 m depth; the closest to the depth of the test by the BAT permeameter, measured by the consolidation test. Therefore, the *k* of the SB wall can be assessed on-site using the BAT permeameter.

Figure 3.14 shows the relationship between *k* from the consolidation tests and hydraulic conductivity tests. The *k* from the consolidation tests is based on the value under 55.5 kPa consolidation pressure, which is most close to the confining pressure used in the hydraulic conductivity tests. The difference between *k* of the two tests is approximately 10 times in this present work. The difference might occur due to a low hydraulic gradient, which may underestimate hydraulic conductivity.

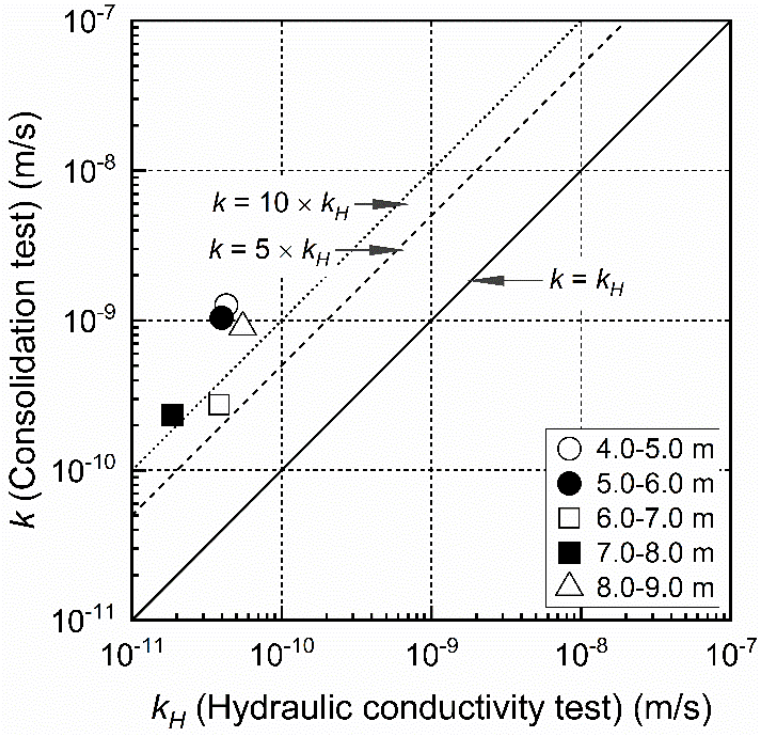

Figure 3.14. Comparison of the *k* values of SB from consolidation tests and flexible wall *k* tests.

3.5 Experimental results for Site B

3.5.1 Particle size distribution

Figure 3.15 shows the particle size distribution curves of the core samples. The distribution curves of SB and native soil differ from each other. While fines and gravel content are concentrated in different layers in the native soil, the particle sizes in SB are much more similar at each depth. That may be because, during the SB wall construction, the machine's chain brought gravels and fine particles to each layer. Therefore, less variability of particle sizes in the SB wall is expected when constructing the SB wall using an equal thickness cutting machine.

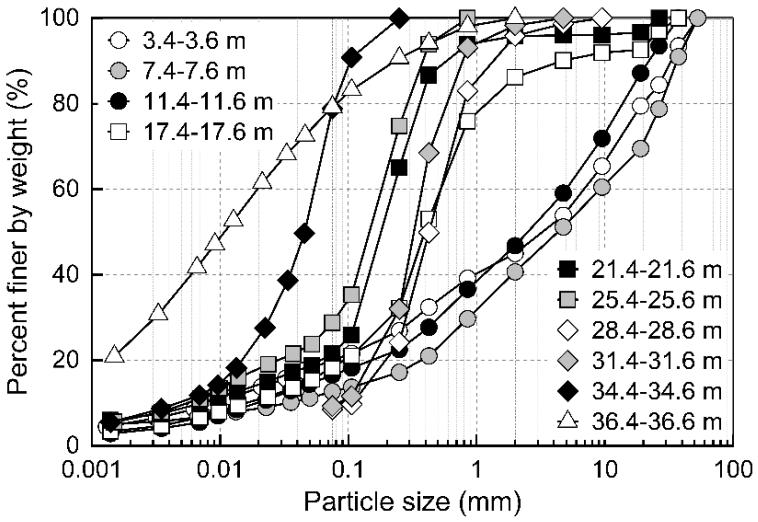

(a) Native soil

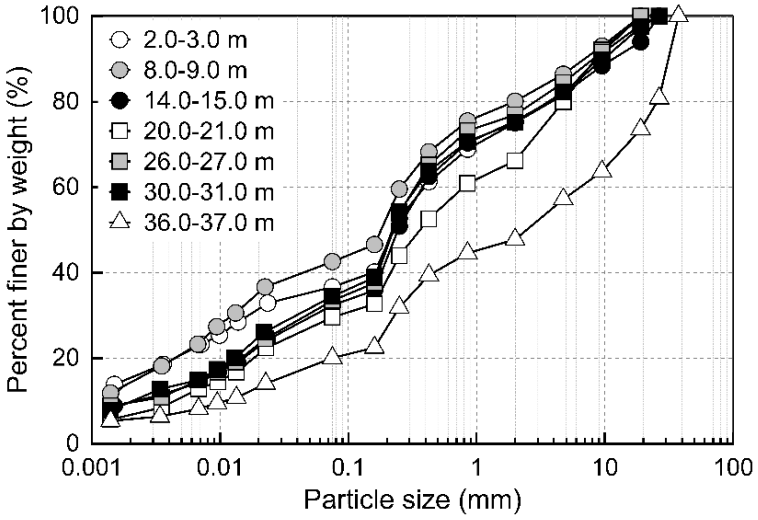

(b) SB wall

Figure 3.15. Particle size distribution curves of the core samples from Site B.

Figure 3.16 shows the gravel, sand and fines contents in different depths of the core samples. The gravels concentrated in the upper layer in native soil have been moved to each layer uniformly in SB. A gravel layer exists in the depth of 39.35–40.25 m, as reported in the boring log (Fig. 3.4), and the gravels might have been lifted during mixing. The fines content in SB was >20% in all SB depths, even though in native soil, the fines content was much scattered. Therefore, the variability in native soil might only have mild effects on the gravel, sand and fines contents in the SB wall.

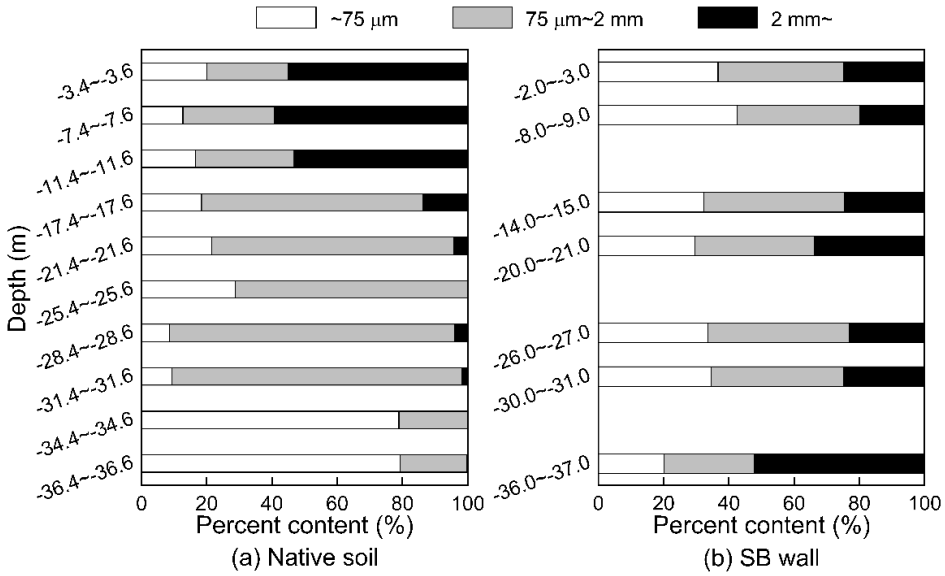

Figure 3.16. Percent of gravel, sand and fines content in the core samples from Site B.

3.5.2 Atterberg limits

Figure 3.17 shows the relationship of I_p and the w_L of the SB. The SB has an average I_p of ~20% and an average w_L of ~45%. The main components in Site B are sand, silt and gravel, while in Site A, high plastic clay exists in several depths. Therefore, I_p and the w_L of the SB in Site B is relatively low.

Figure 3.18 shows the activity of SB samples in Site B. Although the activity of SB in Site B of 2.2 is much smaller than in Site A (7.9), these values are already close to or larger than the natural sodium bentonite (Asad et al., 2013), which can be taken as a high activity soil. The I_p of the SB in Site B is ~25, close to that in Site A (~30). Therefore, the difference in activity may be caused by higher clay content in Site B than Site A.

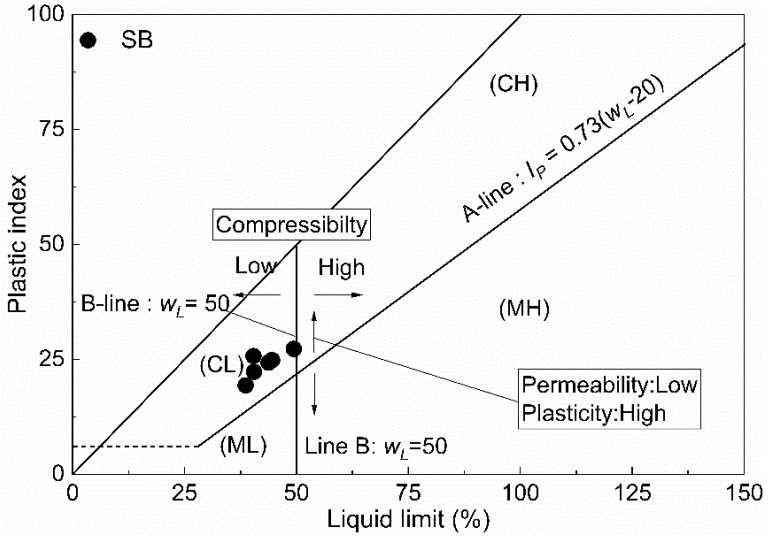

Figure 3.17. Plasticity chart for the SB of Site B.

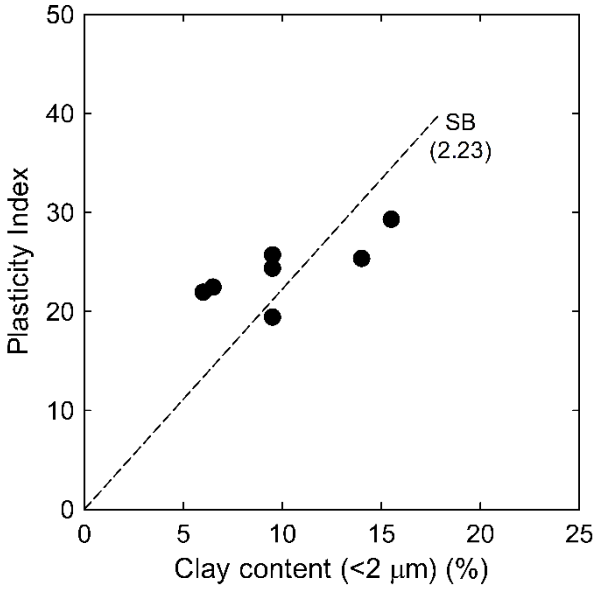

Figure 3.18. Relationship between plasticity index and clay content in the SB of Site B.

3.5.3 Consolidation behaviour

Figure 3.19 shows the *e*-log *p* curves of the SB samples. Estimation by the c_v, Taylor's method suggests that the primary consolidation of SB in Site B may take several months. The primary consolidation of the SB wall in Site B has not yet been completed at the moment of the test. The p' of the SB are mainly around 80 kPa except for the sample in the depth of 29–30 m.

Compared to Site A, the p', which should correspond to the vertical stress the SB wall has experienced, is larger in Site B. The p' distributions with depth obtained by the oedometer tests of core samples are shown in Fig. 3.20, along with the initial void ratio of the core samples. It is noted that even the p' of SB at a depth of 29.8–29.9 m is almost twice as SB at a depth of 9.7–9.8 and 19.8–19.9 m. At the same time, the difference of void ratio between the deep area and upper area is relatively low. The void ratio only decreases from around 1.0 to approximately 0.7. The p' is much lower than the overburden pressure estimated based on the averaged wet unit weight of the core samples and the groundwater level at the site (30% of overburden pressure at 8.4 m depth at Site A, and 25% of overburden pressure at 40 m depth at Site B).

Since the core samples at Site B were collected two weeks after construction, the SB had not finished primary consolidation. The previous study (Malusis et al., 2017) shows that, after the SB wall construction, both total stress and pore stress will decrease with time, while effective stress would increase slightly. It suggests the consolidation behaviour of SB in site needs a very long time for pore pressure to dissipate. Ruffing et al. (2011) and Malusis et al. (2017) reported that the total pressure and pore pressure in the SB wall would reach a peak when backfilling was completed, total stress and pore stress decrease with time, while effective stress would slightly increase. The total stress would decline because the load is transferred through shear to the sidewalls of the trench. The dissipation of excess pore water pressure may lead to the decrease of pore stress. The process usually consists of over 120 days. Also, the width of the SB wall in Site A (70 cm) is larger than Site B (55 cm). The transmittance of friction force at the centre should be lower in a wider wall. However, the p' of SB in Site B is significantly higher than samples in similar depth in Site A. This phenomenon reflects that the soil properties may have a stronger influence on consolidation behaviour than time effects.

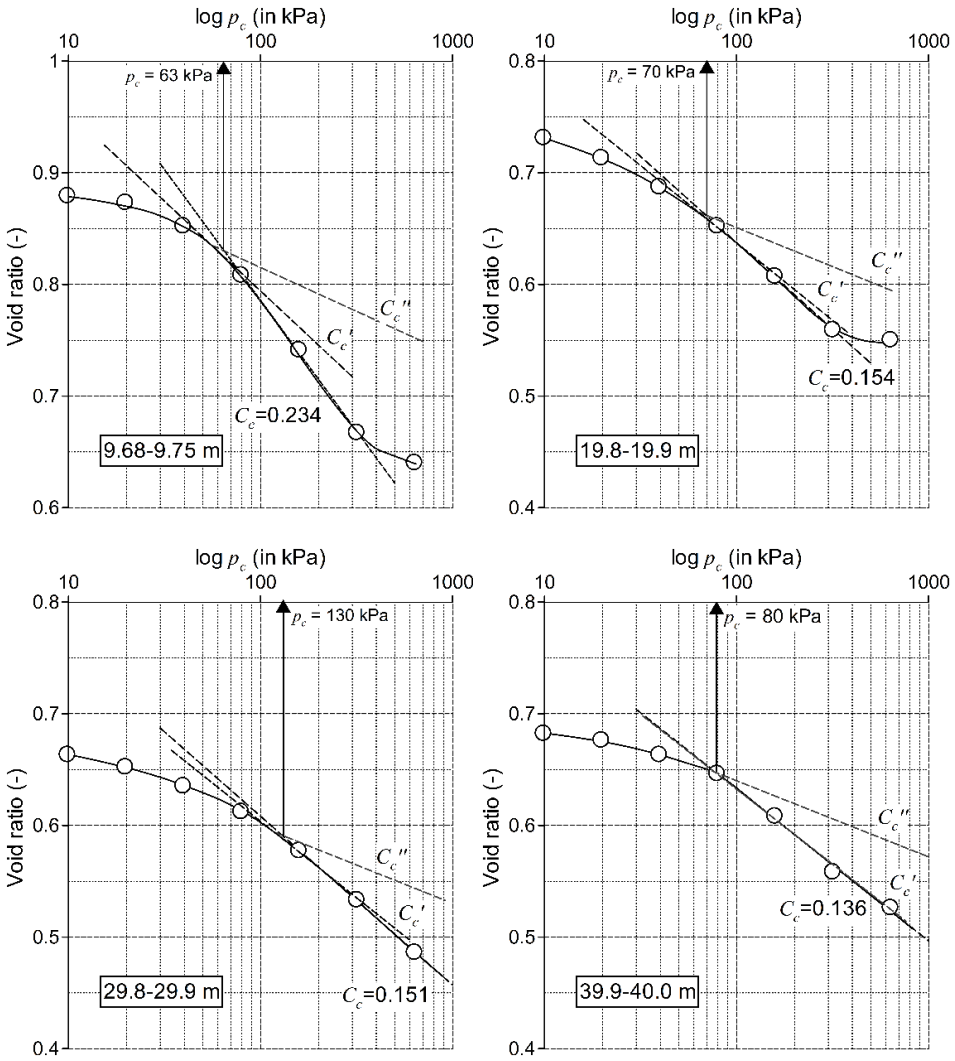

Figure 3.19. *e*-log p_c curves of the consolidation tests on the SB of Site B.

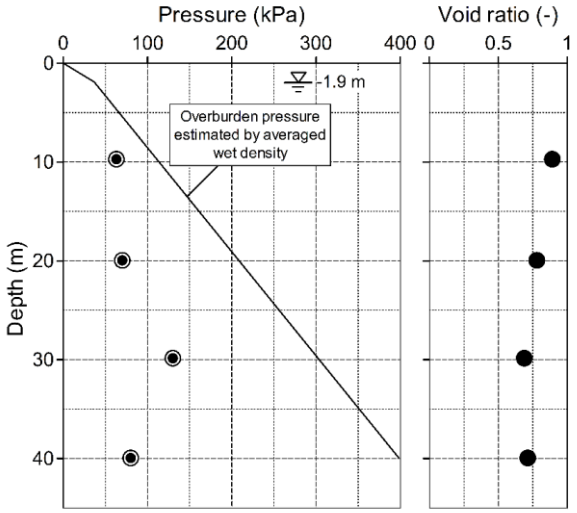

Figure 3.20. Stress and void ratio distribution in the SB wall of Site B.

3.5.4 Hydraulic conductivity

Figure 3.21(a) shows the k of the SB determined by the consolidation test. The k of SB ranged from ~1.0×10^{-10} m/s to 2.0×10^{-10} m/s under confining pressure of 55.5 kPa. The k of SB from the hydraulic conductivity tests is shown in Fig. 21(b). The maximum k of SB is ~3.0×10^{-10} m/s. This value is much lower than the design value, $k = 1.0 \times 10^{-9}$ m/s. According to the hydraulic conductivity test results, k of most specimens became steady at ~1.0×10^{-11} m/s after 60 days. Although the tests were conducted for over one year, the k values for certain specimens were still decreasing, which does not meet the termination criteria of ASTM D5084-16a (2016). The decrease of k may be explained by the creep and self-gravity consolidation of the specimen. The samples are collected from the SB wall 14 days after finishing the construction of the wall. Due to the low consolidation coefficient, the primary consolidation had not finished at that time. After finishing the hydraulic conductivity test, the void ratio of samples was measured again. The results show that the void ratio of all the samples decreases by ~5%, which also explains the low k. Results confirm that the 40-m deep wall can achieve the design hydraulic performance.

The relationship between k of SB from consolidation tests and hydraulic conductivity tests is shown in Fig. 3.22. The k from the consolidation tests is based on the value under 55.5 kPa consolidation pressure, which is most close to the confining pressure used in hydraulic conductivity tests. The k from the hydraulic conductivity tests use the last value obtained, which is considered to be most close to steady-state. The difference between k from the two tests is about 5 times. The k obtained by the consolidation tests is slightly larger than the results by the hydraulic conductivity tests and may be caused by pressure differences. The present work results suggest that the k by consolidation tests is reliable when the confining pressure is close to consolidation pressure.

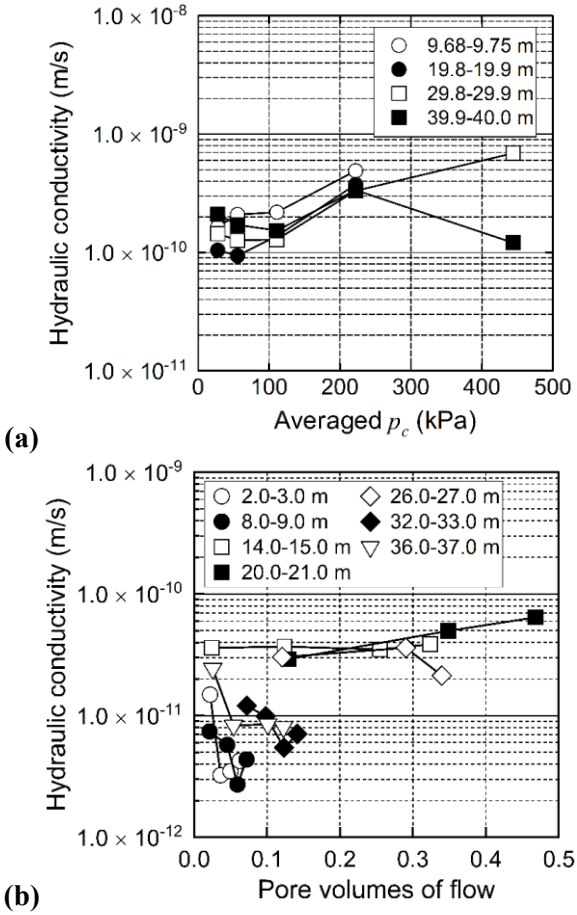

Figure 3.21. *k* values of SB from (a) consolidation tests and (b) flexible wall k tests. The results of flexible wall k tests might not necessarily meet the requirements of ASTM D5084-16a (2016).

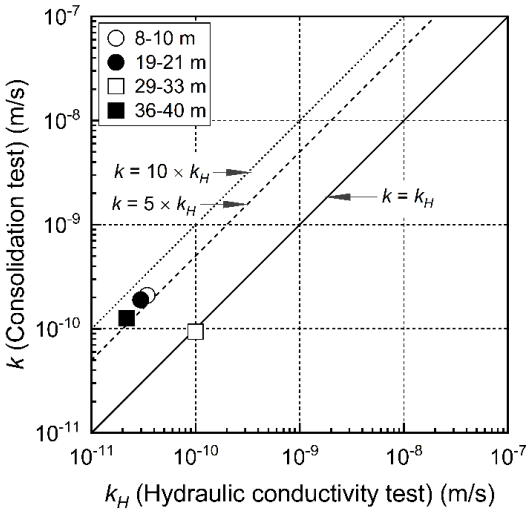

Figure 3.22. Comparison of the *k* of SB from consolidation tests and flexible wall *k* tests.

3.6 Discussion

3.6.1 Mixing effect evaluation

The homogeneity of SB will have a strong influence on the hydraulic performance of vertical cutoff walls. Geotechnical properties are discussed to evaluate whether the mixing effect could ensure the homogeneity of SB. The particle size distribution curve of SB in both sites suggests that the difference of particle size distributions of SB at different depths got relatively small compared with native soil. Since natural soil is mainly formed by weathering and sedimentation, native soil usually has multiple soil layers, while all SB samples in both sites can be classified as single-type soil—sandy gravel with fine fraction (GFS). The coefficient of uniformity for SB in both sites is larger than 10, which can be admitted as well graded. The coefficient of curvature of SB is concentrated between 0.2 and 1.5, while for native soil is up to 30. It suggests that, regardless of particle size and laminar structure of native soil, the relatively homogeneous particle size distribution of SB could be achieved. These facts also imply that the variability of the particle size distribution of native soil could be dramatically improved by installing the SB wall using the equal-thickness trench cutting machine, even if the SB wall's depth is 40 m.

Fines content may play an important role in the hydraulic conductivity of SB, which needs discussion. A previous study (Jones et al., 2007) showed that the minimum fines content of SB to consistently achieve $k < 1.0 \times 10^{-8}$ m/s was close to 20%. SB has fines content of 20–50%, which is more consistent than that of the native soil (8–80%). Moreover, standard deviations of fines content for SB in both sites are less than 10, but they are up to 20 for native soil. In Site A, the SB wall has already been constructed 15 years before. Therefore, the findings suggest that the variability of fines content with SB depth after a long service time is relatively low. The SB wall's construction quality installed using trench cutting with an equal thickness can be ensured even after 15 years. Further, even with 40 m depth, the technique mentioned above can still ensure the SB wall's construction quality.

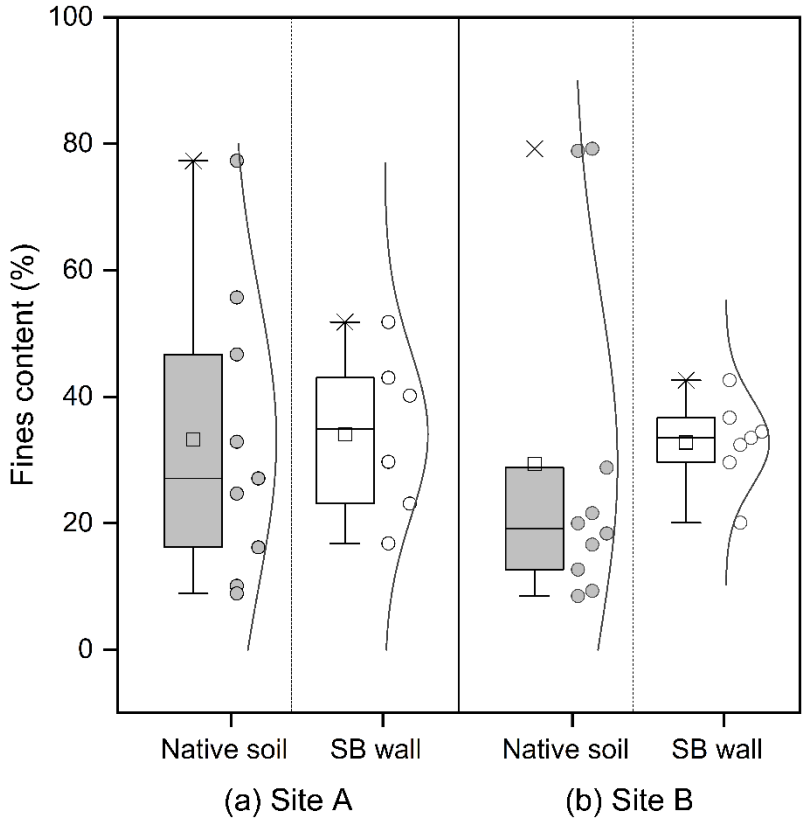

Figure 3.23. Distribution of fines content of the native soil and SB in the two sites.

Even if the fines content of >20% are assured, areas near the ground surface or close to previous gravel layers can be expected to have relatively higher gravel content (e.g., refer to '1.3–2.3 m depth' in Fig. 3.7). Firstly, considering the construction procedure, the mixing of SB by technique mentioned above relied on chain rotation in place instead of ex-situ blending and injected back to the trench (Katsumi et al., 2008). The gravels moved to the top layer would be hard to rejoin the mixing process or settle. This situation may lead to the gravel been concentrated in the top layer. Besides, the native soil layer also may influence the concertation of gravels in SB. Due to the size, gravels are harder to be mixed and easier to drop out of the mixing area. It is noted that the coefficient of variation of gravel content in SB (i.e., 0.46 in Site A and 0.38 in Site B) is higher than that of fines content (0.27 in Site A and 0.21 in Site B) or sand content (0.31 in Site A and 0.14 in Site B). During mixing, there is a possibility that gravels dropped out of the chain when lifting them with the cutting machine. Therefore, gravels may concentrate in the area slightly higher than gravel layers in native soil (e.g. '6.7–6.8 m depth'

in Fig. 3.7). How consolidation behaviour and hydraulic performance of the SB is affected by the accumulation of gravels in a certain area is discussed in the following two sub-sections.

3.6.2 Influence of arching effect on consolidation behaviour

Consolidation behaviour would influence the microstructure of SB, which may affect barrier performance. As mentioned in Sections 3.4 and 3.5, the $p^{'}$ of SB is only 30% of overburden pressure according to effective stress theory. Field and laboratory model studies of SB wall suggest that stress does not have a linearly increasing relationship with depth (McCandless and Bodocsi, 1988). The SB wall is more compressible than rigid walls, leading to lower consolidation stress (Evans et al., 2019). This phenomenon is called the arching effect, caused by friction between the SB and trench interface of adjacent ground. Therefore, it is difficult to estimate the vertical stress condition in the wall, which is important to appropriately evaluate properties of the SB, such as the hydraulic conductivity and shear strength. To determine of stress state in SB wall, a simplified model only considering overburden pressure, the pressure of soil beneath, friction, lateral pressure and weight of section is considered. The equation of stress inside SB without surcharge load based on this model is shown as follow:

$$\sigma_v = \left[\left(B/2\right)\left(\gamma - 2c/B\right)/\left(K\tan\phi'\right)\right]\times\left(1-e^{-2K\tan\phi' z/B}\right) \tag{3.4}$$

where c (kPa) is the effective cohesion of the SB and trench interface, ϕ' (ºC) is the effective angle of friction of the SB and trench interface; B (m) is the thickness of SB wall; K is the ratio of vertical stress to horizontal stress, z (m) is the depth of SB wall; γ(kN/m^3) is the unit weight of SB.

According to Eq 3.4, if other parameters do not change, with the depth of the SB wall increasing to a relatively large value, the vertical stress will become constant. The equation of maximum stress in SB wall considering arching effect (Evan et al., 1995) is shown as:

$$\sigma_{v\max} = (B/2)(\gamma' - 2c/B)/(K\tan\phi') \tag{3.5}$$

When considering the arching effect, the consolidation behaviour of SB might be more

sensitive to the percent of fines, gravel, etc., in SB, not the depth of SB. The p' of SB in both sites keeps constant with depth. At Site A, $p' \approx 30$ kPa (refer to Fig. 3.10) except at a depth of 7.5–7.6 m. On the other hand, at Site B, $p' \approx 80$ kPa. These results are harmonious with the equation above and reflect the occurrence of the arching effect. It suggests that the depth may not affect the p' of the SB as estimated by the equation, while the ground stress of native soil is usually linearly increasing. Considering that strength and stiffness of SB is usually decided by p', the consolidation properties may have a strong influence on the mechanical performance of SB.

The reason why an outlier of high p' exists at a depth of 7.5–7.6 m in the Kanagawa site is still unclear due to lacking information. There are several causes for this phenomenon, such as the bridging effect. The concentration of gravels may form a shell in this depth, leading to stress concentration. The change of friction angle of SB due to high gravel fraction may be another reason. An increase of the friction angle eventually may decrease the value of $K\tan\varphi$, given $\phi \leq 45$, which contributes to the increase of consolidation stress for SB. The consolidation results also show that the consolidation behaviour of SB will be more sensitive to material physical properties rather than the depth or thickness of SB. As mention in Eq. 3.5, an increase in thickness will increase vertical stress. Although the SB wall in Site A has a larger thickness and longer consolidation time than in Site A, which benefits the increase of vertical stress, the p' in Site B is much higher than SB in Site A in similar depth. The findings suggest the consolidation behaviour of SB is highly dependent on material properties. The estimation of vertical stress in the SB wall should rely on test results.

Hydraulic conductivity of SB may have a relationship with effective stress (Ruffing and Evans, 2010). The hydraulic conductivity of SB with 5% bentonite content is likely to reduce significantly under higher effective stress compared to SB with 2% bentonite content (or even lower) (Ruffing et al., 2010). Barrier performance and undrained shear strength of the SB under the estimated overburden pressure by considering only wet density and depth may overestimate those in the SB wall.

3.6.3 Barrier performance

Hydraulic conductivity may be the most critical parameter of barrier performance for SB walls. Especially, the large variability of *k* may cause much more outflux than a homogenous system with the same average *k* (Britton et al., 2005). As mentioned earlier, geotechnical properties also may influence hydraulic performance. The relationship between gravel contents, void ratio and hydraulic conductivity is shown in Fig. 3.24. The *k* and void ratio of SB from the consolidation tests suggests that the *k* will decrease with a reduced void ratio in the same site. A lower void ratio indicates void between soil particles needs less swollen bentonite to fill. On the other hand, a lower void ratio may lead to a narrower seepage channel between soil particles, contributing to low hydraulic conductivity. The SB with a lower void ratio should have lower hydraulic conductivity.

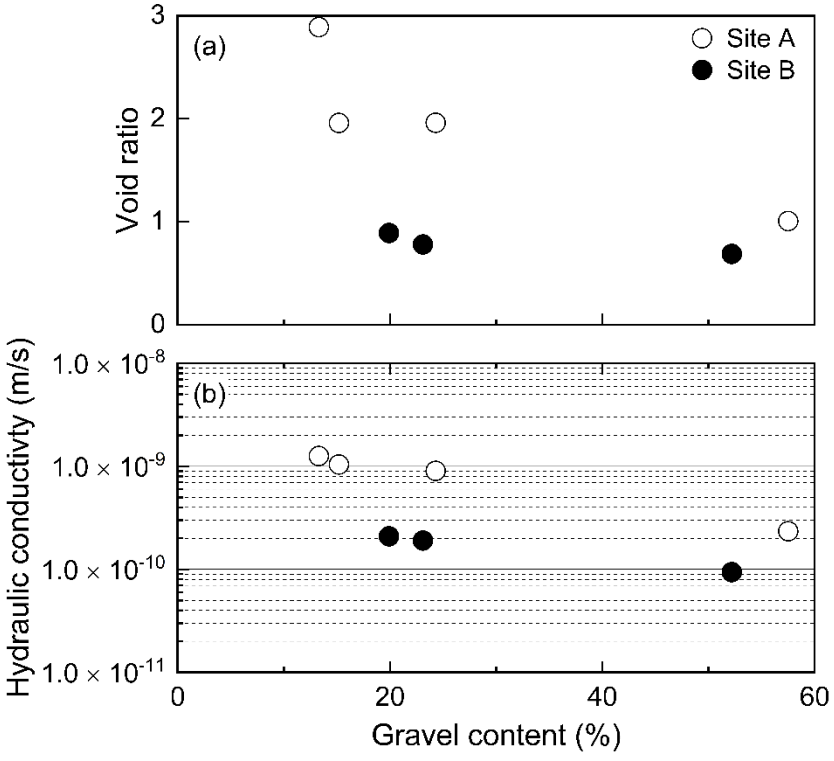

Figure 3.24. Relationship between void ratio (a) or hydraulic conductivity with gravel content (b).

Table 3.2 *k* values of SB obtained by consolidation tests.

	Number of samples	Average (m/s)	Standard deviation (m/s)	Data set
Site A in this study	5	7.4×10^{-10}	9.3×10^{-10}	k
		9.2	0.31	$-\log k$
Site B in this study	4	1.6×10^{-10}	9.3×10^{-11}	k
		9.8	0.13	$-\log k$
Barvenik and Ayres (1987)	11	5.7×10^{-9}	4.3×10^{-9}	k
		8.4	0.43	$-\log k$

Furthermore, as discussed in Sections 3.4.3 and 3.5.3, the void ratio may decrease with the increase of gravel content. Therefore, with >20% fines content, *k* of core samples from SB wall may decrease with the increase of gravel contents [Fig. 3.24(b)]. This phenomenon suggests that during the SB wall construction, the variability of gravels may not be a big issue. Even if it may concentrate in some depth due to the influence of native soil, *k* may be as low as or even lower compared to other depths. With >20% fines content, high gravel contents could even benefit the SB wall's hydraulic performance. The standard deviation of -log *k* for both sites is less than 0.35 (Table 3.2), which shows the variability of *k* is similar to other SB slurry walls tested before (Barvenik and Ayres, 1987). The *k* of SB wall in all depths is lower than 1.0×10^{-9} m/s, suggesting that barrier performance of SB wall installed using trench cutting with an equal thickness could be ensured even with 40 m depth or 15 years elapsed.

3.6.4 Void ratio change after hydraulic conductivity

After the hydraulic conductivity test, the stiffness of the core samples was found to be much high compared to the value when installed for hydraulic conductivity. Therefore, the void ratio of core samples was measured again to compare with the original state. The void ratio of core samples before and after the test is shown in Fig. 3.25.

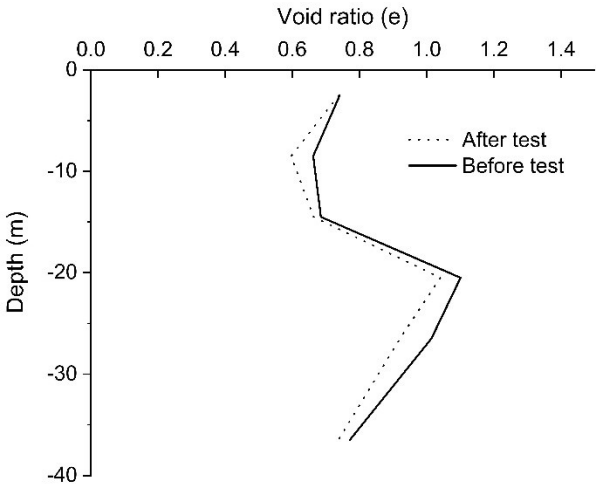

Figure 3.25. Void ratio of SB core samples before and after hydraulic conductivity test.

It can be founded that the void ratio of all samples decreased by ~5 to 10% after hydraulic conductivity. It may explain why the *k* value of some core samples experienced a significant decrease in Fig. 3.25. The reduction of the void ratio may contribute to a narrower seepage path between soil particles. The reason for the decrease in the void ratio may be caused by the consolidation. Since, in this test, the SB core samples were taken just after the SB wall was installed for 2 weeks. The primary consolidation of core samples has yet to be finished. Considering that the solution used in the hydraulic conductivity test is distilled water which is close to the water quality in situ, it suggests the hydraulic performance of the SB wall may increase significantly after installation.

3.7 Conclusion for Chapter 3

Laboratory tests were conducted to examine the physical properties, consolidation behaviour and hydraulic conductivity of core samples obtained from two sites where SB walls have been installed. One is a 40-m deep wall in Site A, 14 days prior to sampling, and another is a 10-m deep wall installed in Site B 15 years ago. These two SB walls were constructed using an equal-thickness type trench cutting machine. This construction method is now being discussed for SB wall. The results support the following conclusions:

(1) SB was classified as single soil type sandy gravel with fine fraction, while native soil constitutes multiple soil types. In addition, SB has fines content of 20−50%, which is

more consistent than that of the native soil (8−80%).

(2) Yielding stress is ~30% of estimated overburden pressure. The arching effect occurs in these walls, and p' in the walls might not be sensitive with depth. This situation may lead to an overestimated shear strength and underestimated hydraulic conductivity of the SB walls.

(3) The k values of SB ranged between 1.0×10^{-12} m/s and 1.0×10^{-9} m/s. The k of the SB can ensure a decrease in seepage velocity even if the wall is 15 years old or 40-m deep. The heterogeneity of gravel contents does not influence the hydraulic performance.

In actual application, not only the hydraulic performance but also the chemical compatibility of SB plays an essential role in contamination migration, such as attenuation performance and diffusion coefficient. As a vertical barrier, once the chemical compatibility is poor, the low hydraulic conductivity of SB can avoid advection. However, contaminants may go through the wall by diffusion. These effects, expected in the contamination migration control, were not considered. In future research, the attenuation performance, change of k due to the solution will be studied. On the other hand, native soil is estimated based on a boring hole close to the SB wall, which may have several differences between practical and results from the laboratory tests. That issue is also ignored.

References for Chapter 3

ASTM D 5084-16a, 2011. Standard Test Methods for Measurement of Hydraulic Conductivity of Saturated Porous Materials Using a Flexible Wall Permeameter. ASTM International, West Conshohocken, US.

Barvenik, M.J., Ayres, J.E., 1987. Construction Quality Control and Postconstruction Performance Verification for the Gilson Road Hazardous Waste Site Cutoff Wall. US EPA Report No. EPA/600/2-87/065, US Environmental Protection Agency (EPA).

Britton, J.P., Filz, G.M., Little, J.C., 2005. The effect of variability in hydraulic conductivity on contaminant transport through soil–bentonite cutoff walls. Journal of geotechnical and geoenvironmental engineering 131 (8), 951–957. https://doi.org/10.1061/(ASCE)1090-

0241(2005)131:8(951)

Bo, M.W., Arulrajh, A., Leong, M., Horpibulsuk, S., Disfani, M.M., 2014. Evaluating the in-situ hydraulic conductivity of soft soil under landreclamationfills with the BAT permeameter, Engineering Geology 168, pp.98–103. http://dx.doi.org/10.1016/j.enggeo.2013.11.001

Daniel, D.E., 1989. In situ hydraulic conductivity tests for compacted clay, Journal of Geotechnical Engineering 115 (9), 1205–1226. https://doi.org/10.1061/(ASCE)0733-9410(1989)115:9(1205)

Evans, J.C., Costa, M., Cooley, B.H., 1995. The state-of-stress in soil-bentonite slurry trench cutoff walls. In: Yalcin, B.A., David, E.D. (Eds.), Geoenvironment 2000: Characterization, Containment, Remediation, and Performance in Environmental Geotechnics.ASCE, US, pp. 1173–1191.

JGS 0051, 2020. Method of Classification of Geomaterials for Engineering Purposes. Japanese Geotechnical Society

JIS A 1202, 2009. Test Method for Density of Soil Particles. Japanese Standards Association

JIS A 1204, 2009. Test Methods for Particle Size Distribution of Soils. Japanese Standards Association

JIS A 1205, 2009. Test Method for Liquid Limit and Plastic Limit of Soils. Japanese Standards Association

JIS A 1217, 2009. Test Method for One-Dimensional Consolidation Properties of Soils using Incremental Loading. Japanese Standards Association

JIS A 1225, 2009. Test Method for Bulk Density of Soils. Japanese Standards Association

Jones, S., Spaulding, C., Smyth, P., 2007. Design and construction of a deep soil-bentonite groundwater barrier wall at Newcastle, Australia. In: Jay, A., Brett, T., Matthew, P. (Eds.), 10th Australian New Zealand Conference on Geomechanics Common Ground, Carillon.

Malusis, M.A., Barben, E.J., Evans, J.C., 2009. Hydraulic conductivity and compressibility of soil-bentonite backfill amended with activated carbon. Journal of Geotechnical and Geoenvironmental Engineering 135 (5), 664–672.

Malusis, M.A., Evans, J.C., Jacob, R.W., Ruffing, D., Barlow, L., Marchiori, A.M., 2017.

Construction and monitoring of an instrumented soil-bentonite cutoff wall: Field research case study. In: 29th Central Pennsylvania Geotechnical Conference, Hershey, USA, pp. 25–27. https://doi.org/10.1061/(ASCE)GT.1943-5606.0000041

Nakaya, Y.,2017. Void ratio and angle of repose for coral gravel sand mixture In: 19th International Conference on Soil Mechanics and Geotechnical Engineering, Seoul, South Korea, pp. 2313–2316

Ruffing, D.G., Evans, J.C., 2010. In situ evaluation of a shallow soil bentonite slurry trench cutoff wall. In: 6th International Congress on Environmental Geotechnics, ASCE, New Delhi, India, pp. 758–763.

Ruffing, D.G., Evans, J.C., Malusis, M.A., 2010. Prediction of earth pressures in soil-bentonite cutoff walls. In: GeoFlorida 2010, Orlando, US, pp. 2416–2425. https://doi.org/10.1061/41095(365)245

Solanki, C., Desai, M., 2008. Preconsolidation pressure from soil index and plasticity properties. In:12th International Conference of International Association for Computer Methods and Advances in Geomechanics, Goa, India. https://doi.org/10.1.1.383.7352

Chapter 4. Mechanical properties and barrier performance of SB amended with cement

4.1 General remarks

The main material of SB cutoff wall is native soil and bentonite additive, which leads to the mechanic properties of SB strongly relies on the native soil and consolidation state. While, in the construction process, the previous consolidation of native already has been broken during excavation and mixing, and the vertical stress in the trench is relatively due to the friction between the trench and surrounding soil. Considering the hydraulic conductivity of soil-bentonite is usually required to be lower than 1×10^{-9} m/s, which means that the coefficient of consolidation, C_v, is relatively low. The primary consolidation of SB may consume a large amount of time. These factors lead to the stiffness and strength of SB is very load. The low stiffness may limit the application of the SB cutoff wall in the area where previous structures have strict limitations for the deformation. Therefore, to extend the application of SB, it is necessary to enhance the mechanical properties. In this chapter, the influence of adding cement on strength and barrier performance was evaluated through a series of laboratory experiments. The contents of cement powder, C_{CP}, considered were 50, 75 and 100 kg/m^3. Unconfined compression tests were conducted to evaluate the strength and stiffness of amended SB. Hydraulic conductivity, k, of basic and amended SB was studied by using flexible-wall permeameters with the falling head system and distilled water as permeant. Batch tests were used to discuss the attenuation performance of basic and amended SB against arsenic, which is a major contaminant of geogenic and artificial contamination in Japan. By using the results of the hydraulic conductivity and batch tests, one-dimensional advection-dispersion analysis by the finite element method was conducted to simulate arsenic transport through a 0.5-m thick amended SB wall.

4.2 Materials

Decomposed granite soil was taken as host soil because it is widely distributed in Japan. Figure 4.1 shows the particle size distribution of the decomposed granite soil used in the tests. Na-bentonite with a particle density of 2.60 g/cm^3 and a free swelling index of ~20 mL/2g was used as an additive. Residue on a 75-μm sieve was ~10%. Table 4.1 summarises the chemical composition of bentonite, which is based on the data provided by the manufacturer. Portland Blast-Furnace Slag Cement was taken as the cement additive. Table 4.2 summarises the physical and chemical properties of the cement.

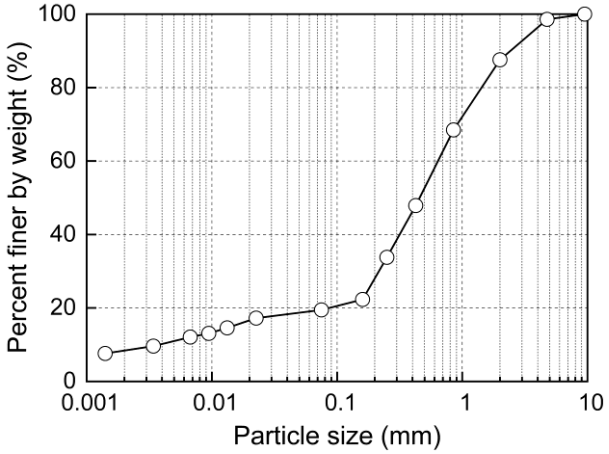

Figure 4.1. Particle size distribution of decomposed granite soil.

Table 4.1. Chemical composition of sodium-bentonite.

Parameter	Value (%)
Ig. loss	5.3
SiO_2	69.4
Al_2O_3	15.6
Fe_2O_3	2
TiO_2	0.1
MgO	2.2
CaO	2.1
Na_2O	2
K_2O	0.3

Data provided manufacturer
(Kunimine Industries Co., Ltd)

The preparation method for SB specimen considers the on-site construction process of the SB wall installed by a trench cutting machine with an equal thickness (refer to Fig. 2.6). The preparation of SB specimen involved four steps, as shown in Fig. 4.2. Firstly, dry soil was mixed with water to obtain wet soil with a water content of 22% and a wet density of 1.98 g/cm^3. These values were determined from the pre-consolidation test with 40 kPa under saturated conditions to simulate the original ground. Secondly, bentonite slurry with a concentration of 5 kg/m^3 was mixed with the wet soil. The soil-bentonite slurry mixture has a flow value of 150

Table 4.2. Properties of cement used in the test (Kameshima et al., 2012).

Parameter	Value
Density	3.04 g/cm^3
Specific surface area	3950 cm^2/g
Chemical composition	
Ignition Loss	1.3%
SiO_2	25.4%
CaO	54.9%
MgO	3.4%
SO_3	1.9%
Cl	0.012%

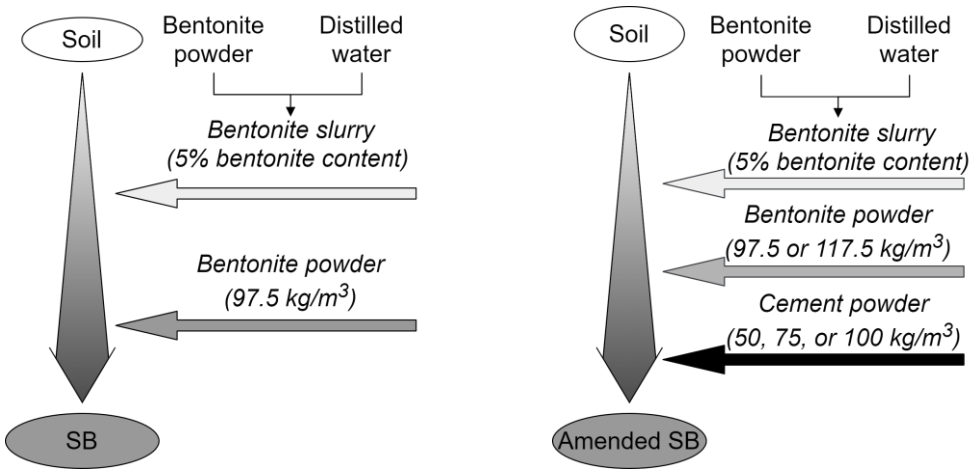

(a) Preparation of SB (b) Preparation of amended SB

Figure 4.2. The procedure of preparing SB and amended SB, respectively.

mm or more, according to JIS R 5201 (2015), which should provide better workability and mixability. Thirdly, the appropriate content of bentonite powder, C_{BP} = 97.5 or 117.5 kg/m^3, was added and mixed with SB slurry mixture for about 10 minutes to prepare basic SB. Lastly, cement powder was added in basic SB to prepare amended SB. Three different contents of cement powder, C_{CP} = 50, 75 or 100 kg/m^3, were used for the amendment.

4.3 Test methods

4.3.1 Unconfined compressive strength test

Unconfined compressive strength (UCS) tests were done following JIS A 1216 (2009) with specimen cured for 60, 90 and 180 days. The test specimens were poured into the paper mould(ϕ 5.0 cm × h 10.0 cm), allowing consolidation by self-gravity. The mould was sealed using a plastic membrane and was cured at 100% humidity. The deformation rate was 1 mm/min, equivalent to 1% of the specimen height.

4.3.2 Hydraulic conductivity test

A flexible-wall permeameter with a falling head system was used to evaluate the hydraulic conductivity, k, of the amended SB. For bentonite-cement-soil mixture, the permeability is around 10^{-9} to 10^{-10} m/s, and the falling-head method provides a more accurate alternative. Because of the relative low hydraulic conductivity of the mixture, tests were conducted corresponded to ASTM D5084-16a (2016). A schematic view of a flexible-wall permeameter is shown in Figure 4.3. The equation to calculate the hydraulic conductivity is shown as follow:

$$k = 2.3\frac{al}{A(t_2 - t_1)}\log\frac{H_1}{H_2} \tag{4.1}$$

where k is hydraulic conductivity (m/s), a is cross-section area of the standpipe (m^2), l is the height of soil sample (m), A is the cross-section area of soil sample (m^2), t_2-t_1 is a measurement time (s), and H_1 and H_2 is a water level at $t = t_1$ and t_2, respectively (m).

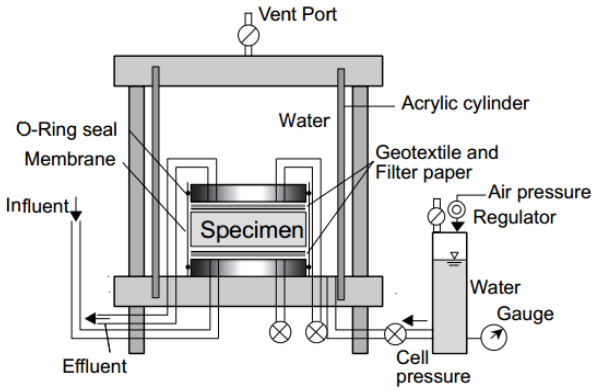

Figure 4.3. Schematic view of a flexible-wall permeameter.

Table 4.3. Mixing proportions of basic and amended SB.

Case	Bentonite slurry (L/m^3)	Bentonite powder (kg/m^3)	Cement powder (kg/m^3)	Void ratio
1	350	97.5	0	0.85
2			50	0.77
3			75	0.66
4			100	0.69
5		117.5	100	0.65

Specimens were consolidated in an oedometer cell (ϕ 6 cm × h 2 cm) under 39.2 kPa for 2 days to minimize the volume change during permeation. Table 4.3 summarises the properties of specimens. The void ratio, e, of the specimens after the consolidation decreases as cement content increases. After consolidation, the specimen was submerged in distilled water and saturated in a vacuum deaerator for 1 day with preventing swelling. Then, the specimen was removed from the cell and set on the flexible wall permeameter. The hydraulic gradient was set to ~50, and distilled water was used as the permeant. Cell pressure of 40 kPa was applied to minimise the volume change during permeation.

4.3.3 Free swelling test

Free swell tests were conducted to evaluate the effect of cement on the swelling of bentonite. The free swell test corresponds to ASTM D5890-19 (2019). The solution used in the test was distilled water and cement solution. The cement solution was used to discuss the

swelling behaviour of bentonite under relatively high electric conductivity (EC) and alkaline conditions. The solution had a cement concentration of 115, 192 or 254 kg/m^3, which is the same as the cement to pore water considering void ratio in amended SB (C_{CP} = 50, 75 or 100 kg/m^3). After mixing the cement and water for 1 day of curing, the solution was filtered by a 0.45-μm membrane filter before use in the free swelling tests.

4.3.4 Batch sorption test

Batch tests using arsenic solutions were used to discuss the attenuation performance of amended SB. $NaAsO_2$ was used to prepare the solutions with different concentrations, namely, 0.1, 0.5, 1, 5 and 10 mg/L. Arsenic concentrations of 0.1 mg/L and 0.5 mg/L are relatively low concentrations anticipated in geogenic contamination. On the other hand, arsenic concentrations of 1, 5 and 10 mg/L are relatively high concentrations anticipated in artificial contamination. The specimens were consolidated in a similar way to those used in the hydraulic conductivity tests. After consolidation and curing for 7 days or 28 days, specimens were crushed to particles smaller than 2 mm and mixed with the arsenic solutions with a liquid-to-solid (L/S) ratio of 20. L/S 20 was applied to simulate the long service duration of the SB wall. The specimens were subjected to horizontal shaking at 150 rpm for 24 hours, then left for 15 minutes. Solid-liquid separation was done by centrifugation under 3,000 rpm for 10 minutes and filtered with a 0.45-μm membrane filter. Batch tests were conducted in triplicate.

4.4 Results and discussion

4.4.1 Strength-strain relationship of amended SB

Figure 4.4 shows the stress-strain relationship of the amended SB with different C_{CP} and curing periods. The maximum stresses in the tests were used as the UCS of amended SB. Figure 4.5 shows the relationship between the UCS and C_{CP} of the amended SB cured for different periods. UCS increases as C_{CP} increases, for example, for a 60-days cured amended SB, UCS is 18, 50 and 100 kPa for C_{CP} of 50, 75 and 100 kg/m^3, respectively. UCS also increases with an increasing curing period, for example, an amended SB with C_{CP} = 100 kg/m^3, UCS is 100,

200 and 370 kPa after curing it for 60, 90 and 180 days, respectively. It should be noted that the strength of SB with higher C_{CP} will increase more significantly after a long time of curing.

Deformability in this study was evaluated by strain at maximum stress. It is noted that amended SB with $C_{CP} \leq 75$ kg/m^3 keeps a certain degree of deformability, unlike other cement bentonite materials (Alaa et al., 2015). Strains at maximum stress were ~4% for $C_{CP} = 50$ or 75 kg/m^3 with 90 days of curing. In addition, few cracks may develop in amended SB with $C_{CP} \leq$ 75 kg/m^3, even when it has a significant deformation. This is particularly important to the reliability of SB wall because when through-wall cracks develop in the wall, the wall will lose its impermeable function immediately. The seepage path of the contaminations will change to passing through cracks. Therefore, deformability greatly contributes to the safety and reliability of SB walls when experiencing large static or dynamic loads. In this study, the stress-strain relationship of the amended SB with $C_{CP} = 100$ kg/m^3 changed significantly after 180 days of curing. The amended SB had a clear elastic zone after loading, in which the strain at the maximum stress was ~1%, while the stress dropped down quickly after reaching the peak. In this situation, amended SB no longer keeps good deformability. The curing and cement additive may change the macrostructure of the clay matrix. The binding effect of hydrates might have changed the strength and had a significant influence on the strain (Kaniraj et al., 1999). However, this issue can not be clarified with the available results.

Figure 4.6 shows the tangent stiffness of amended SB. Tangent stiffness was determined by the elastic zone (0–40% deformation of strain at maximum stress). The tangent stiffness of the amended SB experienced an increase with cement mass and curing period. Stiffness of amended SB with $C_{CP} = 50$ kg/m^3 was noted to increase more significantly from 60 to 90 days (5 to 25 kPa) compared to from 90 to 180 days (25 to 32 kPa). However, for amended SB with $C_{CP} = 100$ kg/m^3, the tangent stiffness increased most significantly after curing it for more than 90 days. These observations demonstrate that amended SB with a higher cement content may need additional curing time to reach maximum tangent stiffness. On the other hand, lateral deformation in the SB wall is anticipated to be relatively low when construction is just finished. Lateral deformation will become more pronounced after pore pressure is dissipated, which usually takes a few weeks (e.g., 4 weeks) as reported by Tong et al. (2019) when monitoring a

6-m and 10-m deep SB wall located in a municipal solid waste landfill. These two SB walls were created by mixing native soil (mainly low plastic clay) with Na-bentonite. Considering the amended SB will have certain stiffness when pore pressure is dissipated, it can reduce lateral deformation of the SB wall.

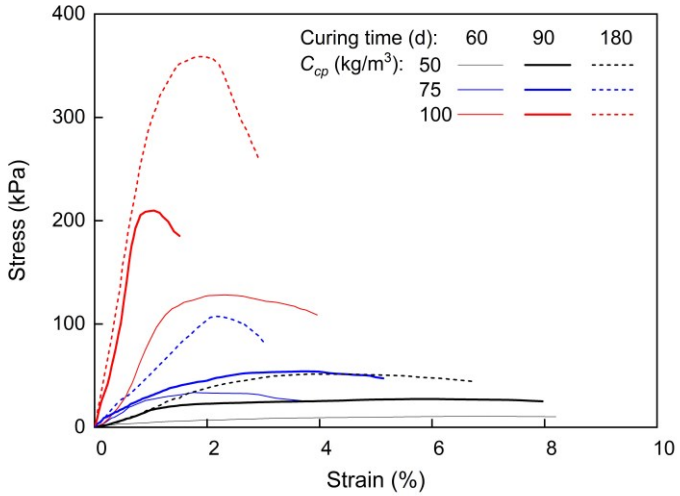

Figure 4.4. Strength-strain relationship of amended SB.

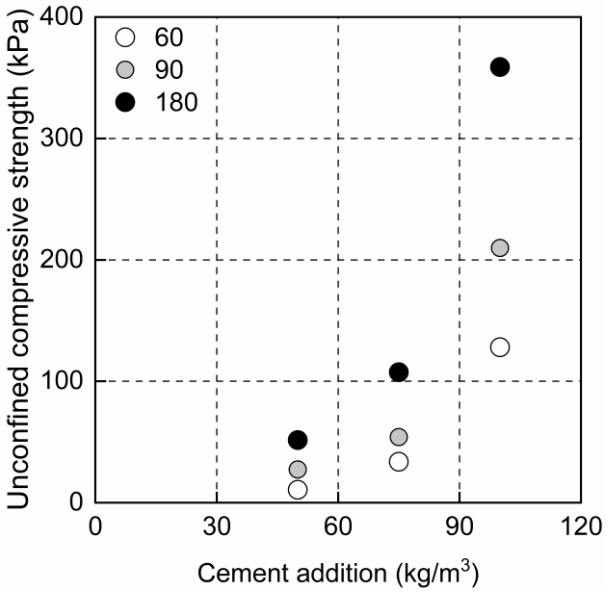

Figure 4.5. UCS strength of amended SB (C_{BP} = 97.5 kg/m^3).

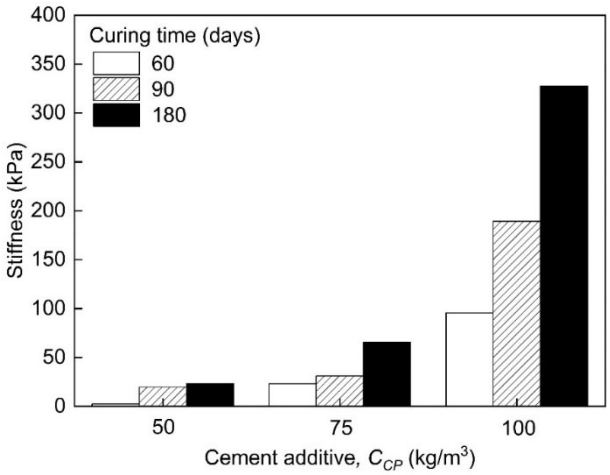

Figure 4.6. Stiffness of amended SB (C_{BP} = 97.5 kg/m^3).

4.4.2 Hydraulic conductivity

The *k* of the amended SB decreases with time or pore volumes flow (PVF), as shown in Fig. 4.7. The time starts from the day when the hydraulic conductivity test begins, which is 7 days after the preparation of the SB specimen. PVF can be calculated as the ratio of the cumulative volume of the effluent and volume of voids in the specimens. Since PVF of basic SB is too small, it was plotted as a dotted line to compare with amended SB. The results show that, by adding cement, the *k* of the amended SB increased significantly from 2.7×10^{-11} m/s to 1.0×10^{-9} m/s. The *k* of amended SB still satisfies the typical design *k* for SB wall (1.0×10^{-9} m/s), which can assure the SB wall has a certain function to control seepage. The negative effect of cement can be suppressed by increasing bentonite content. As mentioned earlier, after bentonite contacts with water, montmorillonite will swell and fill the void between the soil particles. This phenomenon may decrease the distance between the montmorillonite mineral layers. The seepage path between soil particles will become narrow, hence improving the hydraulic performance of the amended SB. The results show that initial *k* of amended SB with C_{CP} = 100 kg/m^3 is 8.0×10^{-10} and 2.8×10^{-10} m/s when C_{BP} = 97.5 and 117.5 kg/m^3, respectively. Therefore, if very low hydraulic conductivity is required immediately after construction, adding more bentonite to the amended SB could be a possible way.

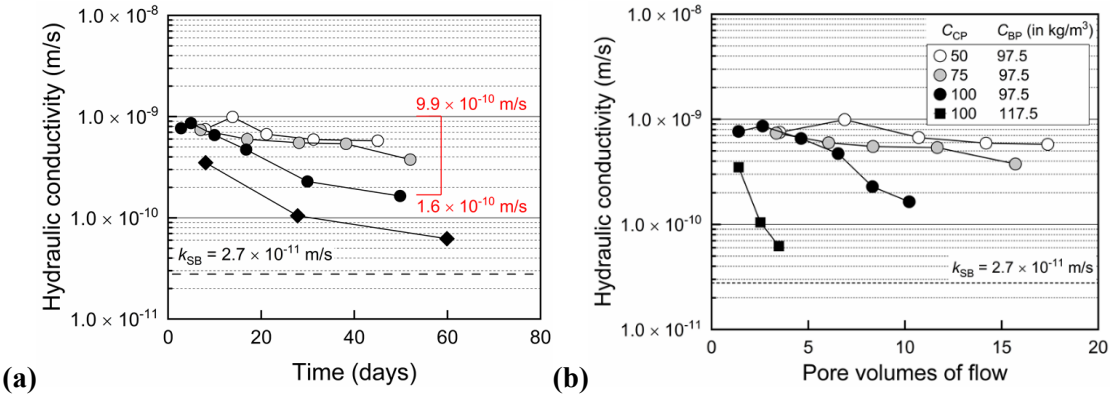

Figure 4.7. Change of hydraulic conductivity of SB with time and pore volume of flow.

The k of amended SBs with C_{CP} = 50, 75 or 100 kg/m^3 and C_{BP} = 97.5 kg/m^3 was almost the same at the beginning stage, as shown in Fig. 4.7. Although the influence of cement on k of amended SB is not clear at the beginning stage, it becomes noticeable after several weeks. Curing may benefit the hydraulic performance of amended SB. Figure .4.7 shows that, after 60 days of permeation, the k of amended SB with C_{CP} = 100 kg/m^3 decreased to 1.6 × 10^{-10} m/s. Formation of $CaCO_3$ from $Ca(OH)_2$ is anticipated to have reduced the void ratio, hence the decrease in hydraulic conductivity.

4.4.3 Effect of cement in amended SB on free swelling index and void ratio

According to Takai et al. (2016), an increase in electrical conductivity (EC) may restrict swelling performance as cations in the solution can be tightly adsorbed and held onto the surface of negatively charged clay particles. The adsorbed cations are highly concentrated near the surfaces of particles, hence could diffuse away to equalise concentrations throughout the pore fluid. Therefore, when the cation concentration is too high, those cations are preferentially adsorbed onto the clay particles, and the diffuse double layer becomes thin. This phenomenon will reduce the swelling performance of bentonite, and as a consequence, reduce hydraulic performance.

The swelling index, EC and pH values in the free swelling test are shown in Table 4.4. Solutions with relatively high cement concentration may reduce the swelling performance of bentonite. When the cement amount is 115 g/L, the free swell index slightly decreases. These results are similar to Anh et al. (2017). Solution with low $Ca(OH)_2$ concentration would benefit

the swelling performance of bentonite. However, by increasing the concentration, the free swell index would reduce.

Table 4.4. EC, pH and swelling index in free swelling test.

Cement amount in solution (g/L)	0	115	192	254
EC (mS/m)	0.1	234	290	322
pH	7.1	11.4	11.5	11.7
Swelling index (mL/2g)	20	19	18	18

Figure 4.8 shows using more cement content in amended results in high effluent EC. The EC will drop with an increase in the number of PVFs. High EC at the beginning stage indicates a high cation concentration in pore fluid. As mentioned earlier, high cation concentration in the fluid could limit the swelling of bentonite. Therefore, one possible reason for a relatively high hydraulic conductivity at the beginning stage is high EC. A decrease in EC levels implies a decrease in cation concentration. Lower cation concentration favours swelling of bentonite. Therefore, not only cement hydration but also improved swelling of bentonite contributes to the decrease of hydraulic conductivity.

Meanwhile, the generation of C-S-H may restrict the swelling performance of bentonite. The free swelling index of amended SB would be less compared to basic SB. It also contributes to the increase in k of amended SB. Moreover, the change in hydraulic conductivity may also have a relationship with the physical property of the amended SB. The void ratio is shown in Fig. 4.9, in which the void ratio was noted to decrease with a rise in cement content. This occurrence may be explained by that C-S-H may bond with bentonite and host soil. The bonding particles may change the particle size of basic SB and form a skeleton in consolidation, which may contribute to the change of consolidation behaviour, leading to a lower void ratio in amended SB. Basic SB was found to have the largest void ratio, while cement addition may significantly reduce the void ratio. When C_{CP} >75 kg/m^3, the void ratio was stable at around 0.66. The low void ratio of amended SB signified that there was less space requiring bentonite to fill.

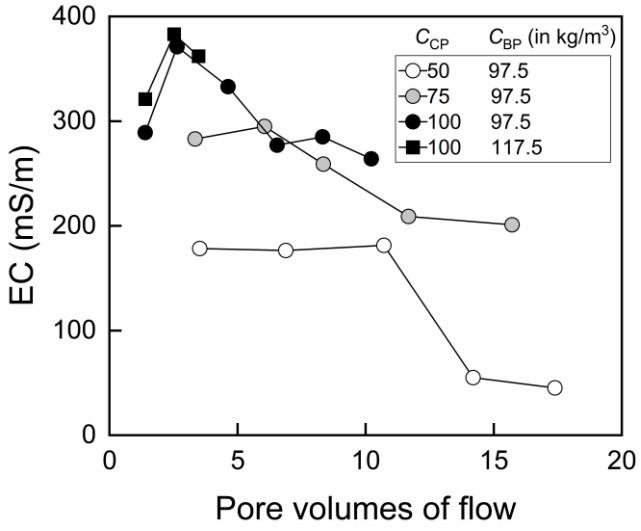

Figure 4.8. Variation of EC during the hydraulic conductivity tests.

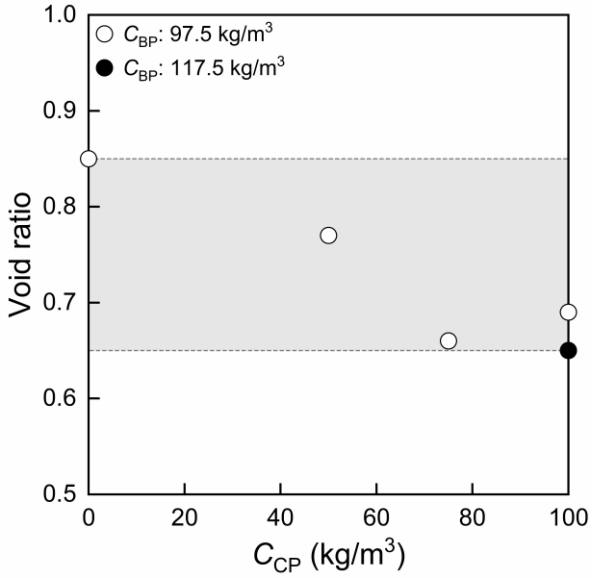

Figure 4.9. Void ratio of SB specimens used in the hydraulic conductivity tests.

Among cases with a similar void ratio and cement content, amended SB with C_{CP} = 100 kg/m^3 and C_{BP} = 117.5 kg/m^3 were found to have the lowest *k*. This suggests that the influence of cement content (C_{CP} <100 kg/m^3) on restricting swelling may be similar. The bentonite additive may have a stronger influence on the *k* at the beginning stage. After curing, the cement material acts as the main role, which may be caused by C-S-H and $CaCO_3$, filling the void between the soil particles.

4.4.4 Attenuation performance

Figure 4.10 shows the sorption isotherms of SB with different C_{CP} and cured for 7 and 28 days. The following Freundlich model best describes the relationship between the sorbed mass, S (mg/g), and equilibrium concentration, C (mg/L), in solution:

$$S = KC^N \tag{4.2}$$

where K and N are Freundlich parameters.

Freundlich parameters for basic and amended SB were used to evaluate the attenuation performance (Table 4.5). Since N was similar (0.27–0.35), N was fixed to 0.3 to compare K. Basic SB has a certain capacity to attenuate arsenic ($K \approx 3$ cm^3/g). Cement addition generally

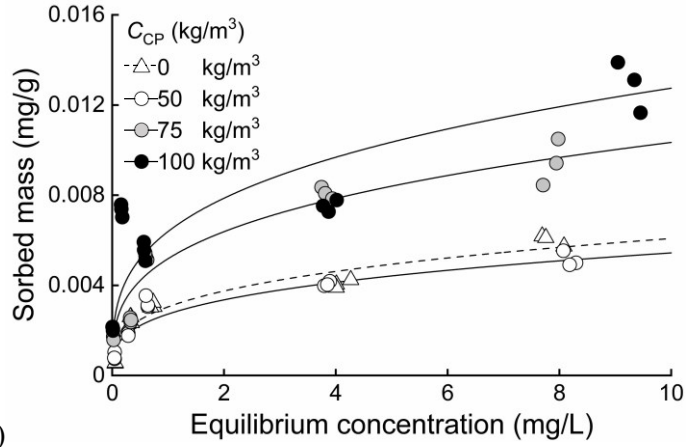

(a)

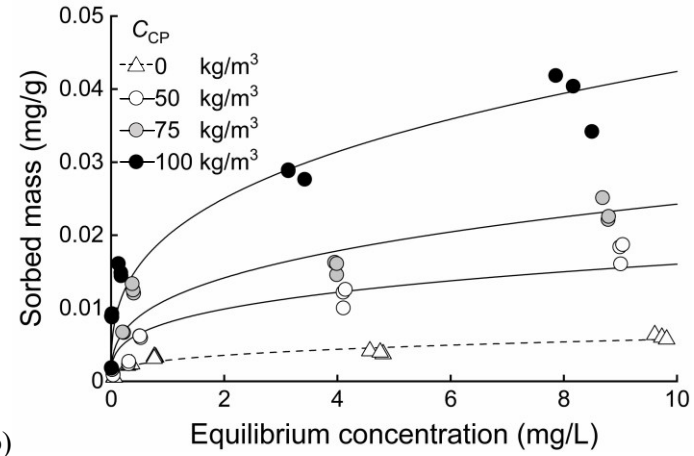

(b)

Figure 4.10. Arsenic sorption isotherm of SB cured for (a) 7 days and (b) 28 days.

Table 4.5. Summary of the Freundlich isotherm parameters.

C_{CP}	7			28		
(kg/m^3)	K (cm^3/g)	N	R^2	K (cm^3/g)	N	R^2
0	3.1	0.3	0.92	2.9	0.3	0.92
50	2.7		0.87	8.0		0.89
75	5.2		0.70	11.2		0.90
100	6.4		0.93	20.0		0.94

increases the attenuation performance of the SB. The highest attenuation performance was noted for amended SB with C_{CP} = 100 kg/m^3 and cured for 28 days, in this case, K = 20 cm^3/g. There was no obvious change in K of basic SB after curing it for different days, as shown in Table 4.5. In contrast, curing time was a critical factor in the attenuation performance for amended SB. For example, amended SB with C_{CP} = 100 kg/m^3, K = 6.4 and 20 cm^3/g for 7 and 28 days curing.

The chemistry of the solution after batch tests is shown in Fig. 4.11. Compared to amended SB, the EC of the solution for basic SB is much lower. After mixing with basic SB, the EC increased from 0.2 to 15 mS/m. The increase of EC for basic SB mainly relies on the increase of Na^+ concentration in the solution introduced by bentonite.

After batch tests for amended SB, the concentration of Ca^{2+} in the solution increased to approximately 65−85 mg/L, which may have been caused by the hydration reaction. The high EC of the solution for amended SB is due to cement releasing metal cations such as Ca^{2+}. According to a previous study (Dixit et al. 2003), the Ca^{2+} may form $CaHAsO_3$ on the surface of the soil, which greatly improves attenuation performance against As. Since $Ca(OH)_2$ was released during the hydration process, the pH of the solution after batch tests for amended SB reached ~12, as shown in Fig. 4.11. Therefore, the formation of Ca-As precipitation may be anticipated as one of the reasons for the higher attenuation performance of amended SB. In the alkaline condition caused by the released $Ca(OH)_2$ during cement hydration, the precipitation reaction can be written as

$$As_2O_3 + 2Ca(OH)_2 \xrightarrow{pH=12-13} 2CaHAsO_3 \downarrow + H_2O \quad (4.3)$$

$$As_2O_5 + 3Ca(OH)_2 \xrightarrow{pH=12-13} Ca_3(AsO_4)_2 \downarrow + 2H_2O \quad (4.4)$$

The increase in Ca cation concentration may explain why the attenuation capacity of As increased with a rise in C_{CP}.

The attenuation performance of amended SB was found to be much higher after curing for 28 days compared to 7 days. With longer curing times, additional C-S-H may be generated, which may increase the surface area. On the other term, according to Ismail et al. (2012), the microstructure of SB amended with Portland cement will significantly change after curing. The cement additive would generate needle-like crystals on its surfaces. Such crystals may significantly increase the specific surface area of the SB mixture and contribute to the improvement of attenuation performance.

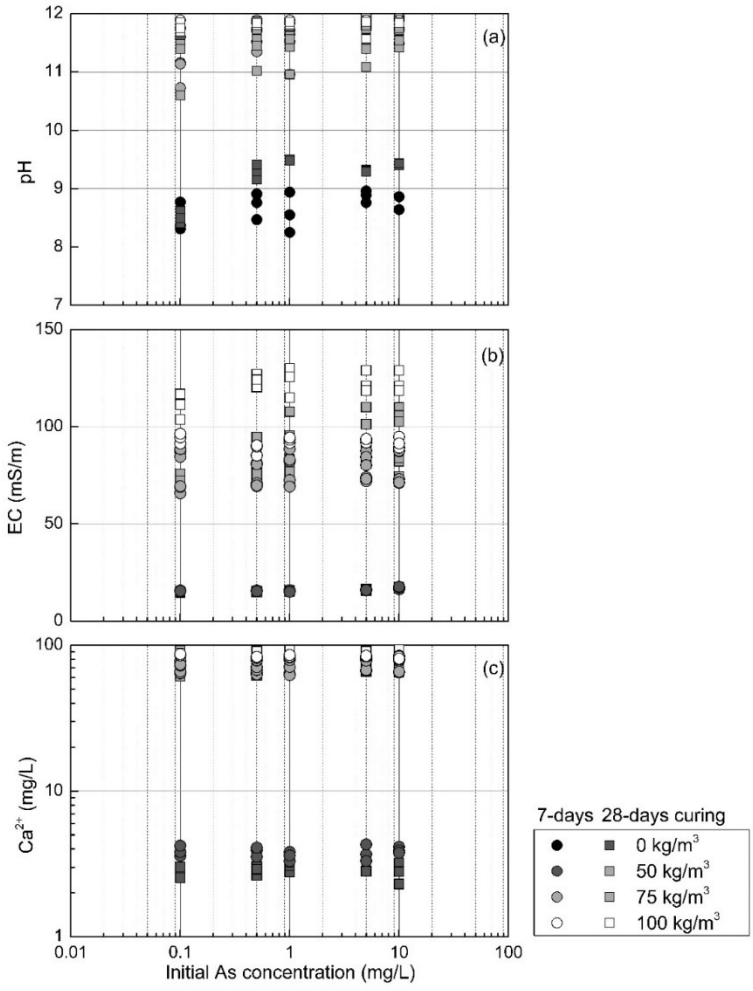

Figure 4.11. pH (a), EC (b) and Ca^{2+} (c) of solution after batch test.

The improved attenuation performance of amended SB may be due to the formation of zeolite in strong alkaline conditions. According to De La Villa et al. (2001), zeolite crystals are formed from bentonite in a strong alkaline solution of pH >11.6. Compared to bentonite, zeolite would have a stronger attenuation performance against As (Shevade et al. 2004). In this study, the pH for amended SB cases was ~12.5. Consequently, the zeolite may have been formed during curing. SEM conducted in this study for specimens with C_{CP} = 100 kg/m^3 cured for 28 days demonstrated the existence of crystal material, as shown in Fig. 4.12. The zeolite formation process was time-consuming, which may explain why the attenuation performance of amended SB increased with curing time.

4.4.5 Influence of host soil on attenuation performance

This section aims to evaluate if the host soil may have a strong influence on amended SB's attenuation performance or not. This study tested two kinds of decomposed granite soil, which came from the same company but were from different production batches, as shown in Table 4.6. The attenuation performance of the amended SB with different host soil is shown in Fig. 4.13. As shown in Fig. 4.13, with the addition of 75 kg/m^3 of cement and curing for 28 days, the attenuation performances were noted to be similar with different host soils. Consider the As removal ratio of cement 100 kg/m^3, bentonite was 115 kg/ m^3 when using two host soil. The currently used soil gave the material better removal ability. However, the disparity between the two types of soil was less than 5%. In summary, sorption is influenced by soil types at certain scales, but in our experiment, the influence of host soil was found to be relatively minimal.

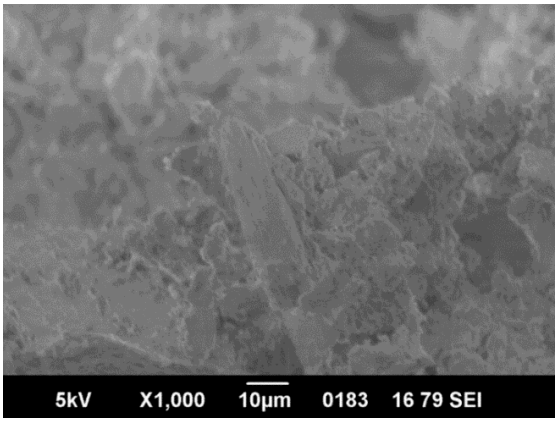

Figure 4.12. SEM micro-graph of the crystal material in amened SB.

Table 4.6. Types of soil and addition of each material with different curing days.

Host soil (kg/m^3)	Water (L/m^3)	Bentonite Slurry (L/m^3)	Bentonite Powder (kg/m^3)	Cement powder (g/L)	Curing period (days)
Masado I (Produced in 2017) Masado II (produced in 2019)	420	350	97.5	75	28

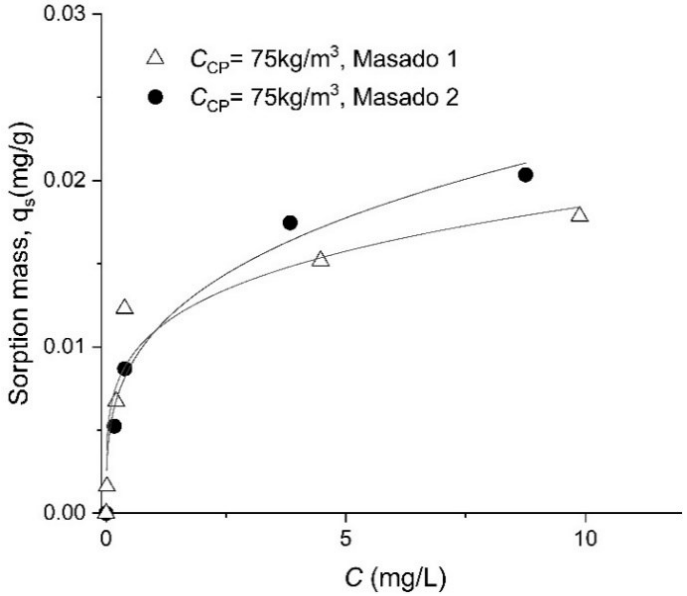

Figure 4.13. Sorption performance of amended SB with different host soil.

4.4.6 Influence of pre-hydration on attenuation performance

By comparing our test results to other studies, the attenuation performance of SB in this present work was found to be relatively poor considering that the host soils were Masado, which itself has a certain attenuation performance. The test condition of this and others studies is shown in Table 4.7. Predicted by the Freundlich model, in this present work, attenuation performance of SB is ~ 1/10 of Masado based on Mo et al. (2015), even with same the *L*/*S* ratio. The major difference between specimens was that the specimens used in this study were pre-hydrated prior to conducting the batch tests. The water content of the specimens was measured before the batch test in order to control the dry weight of the consolidated SB specimens.

This process made the experimental conditions closer to those of in-situ as the working conditions of SB are usually saturated. As the attenuation performance of SB is changed due to dry or wet conditions, it is better to consider the attenuation performance in more critical conditions. Evaluating the influence of pre-hydration for four samples with different wet/dry conditions with or without bentonite were tested as shown in Table 4.8.

Specimen 1 actually was actually dry Masado; specimen 2 was dry Masado mixed dry bentonite powder; specimen 3 was SB consolidated but dry under 100℃. Meanwhile, specimen 4 come from the wet SB, which consolidated before without drying. All these specimens were roughly crushed until their maximum diameters were under 2 mm. Photos of specimens 1, 2 and 3 are shown in Fig. 4.14.

Table 4.7. Material condition and sorption performances comparing.

References	Host soil	Soil condition	L/S	Model
Mo et al. (2020)	Masado	**Dry** soil after compaction	20	$S = 0.019C^{0.59}$
Present work	Masado with 115kg/m^3 bentonite	Crush **wet** consolidated SB	20	$S = 0.003C^{0.33}$

Table 4.8. Materials condition of specimens.

	Soil	Bentonite	Consolidation	100℃ dry	Material condition
1	Masado	×	×	√	Dry and unconsolidated soil
2		115 kg/m^3	×	√	Dry and unconsolidated soil mix with bentonite powder
3			√	√	Dry soil-bentonite block
4			√	×	Wet soil-bentonite block

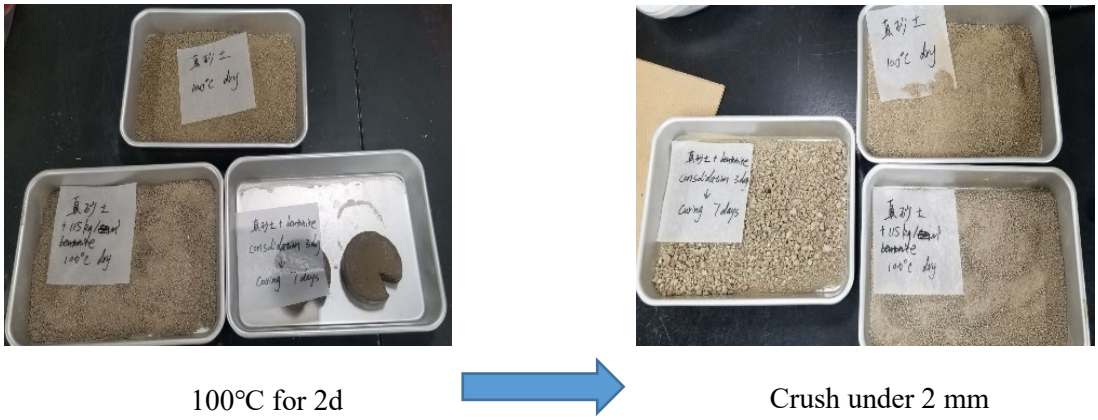

Figure 4.14. Samples 1, 2 and 3 before and after be dried.

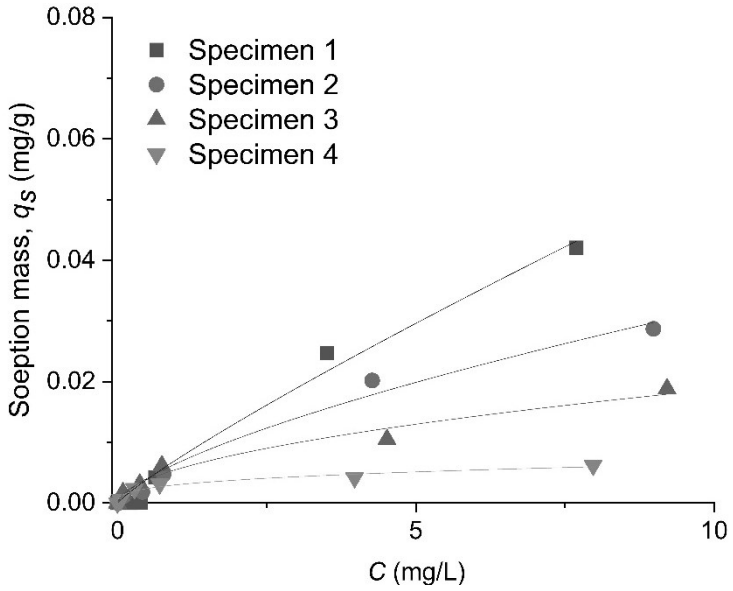

Figure 4.15. Freundlich adsorption isotherm of different soil dry/wet condition samples.

Sorption performances of each specimen are shown in Fig. 4.15. Comparing the result of specimen 1 (only containing dry soil) with that of specimen 2 (dry soil mixed with bentonite powder), the addition of bentonite was found to reduce sorption performance, which is a completely different finding from other studies, in which bentonite was always shown to enhance sorption capacity. Besides, compared to the sorption performance of specimens 2, 3 (dry consolidated SB mixture) with 4 (wet consolidated SB mixture), the consolidation process was noted to weaken sorption performance. Furthermore, wet conditions also had negative

effects on sorption performance. The sorption performance of the wet consolidated specimen 4 is 10 times weaker than that of specimen 2, which was a mixture of soil and bentonite powder.

To determine the results of the tests, the sorption performance in this test was relatively low compared to that of previous studies (Mo et al., 2020), which might be due to the soil-bentonite mixture of all samples in wet conditions being in contact with the contamination solution in this experiment. In the previous study, the SB was always in dry conditions, making it easy to control the accuracy of the dry mass. However, in natural and site conditions, SB cutoff wall mostly makes contact with contamination in wet conditions. Here, SB has less hydration during sorption, signifying that it may absorb less solution. Furthermore, the consolidated process that attempts to simulate the underground condition also weakens the sorption performance of the SB mixture. During consolidation, the actual volume of the mixture was compressed; hence, bentonite swells in order to occupy the space between the soil particles. The specific surface area further decreased with consolidation.

4.4.7 Effect of Initial pH value

Considering the enhancement of amended SB being dependent on cement material, different conditions may have an influence on attenuation performance and mechanical properties. According to Kamon et al. (2005), the mechanical properties of cement amended soil could be ensured with an environmental pH> 4. However, the influence of pH on attenuation performance has yet to be elucidated. Therefore, the material working range of pH must be identified. Moreover, the adjusting ability of soil-cement-bentonite mixture on pH requires further evaluation.

The steps to prepare an As 0.5 and 10 mg/L solution at pH = 2, 4, 6 and 12 were as follows. First, pH = 0 HCL acid and pH = 14 NaOH alkali were diluted with distilled water to prepare a solution of pH = 2, 4, 6 and 12. Then, different pH value solutions were used to dilute the high As concentration solution to make the As 0.5 or 10mg/L solution to around pH = 2, 4, 6 and 12. Finally, as the pH value will be influenced by As ions, HCl or NaOH solutions were used to neutralize the solution to target pH=2, 4, 6 and 12.

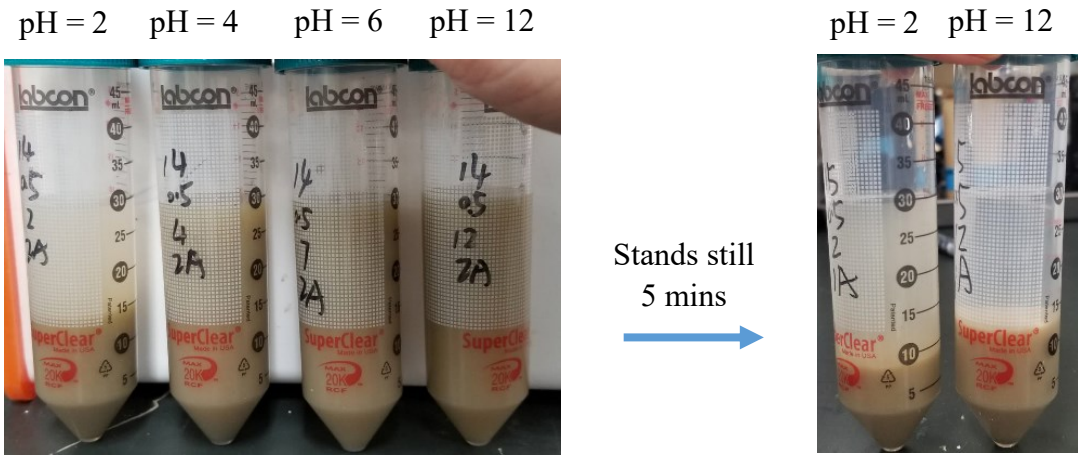

Figure 4.16. The solution stands still for 5 mins after batch tests.

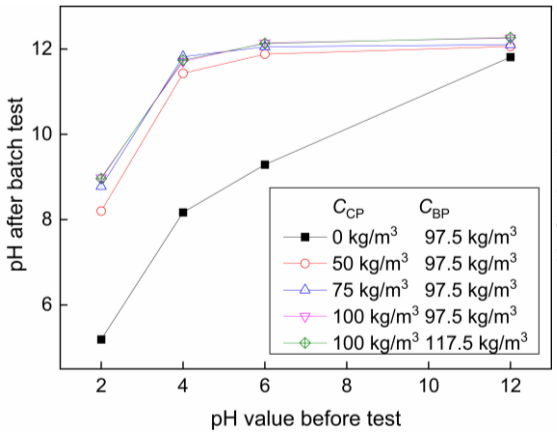

Figure 4.17. pH changes when initial As concentration is 0.5 mg/L

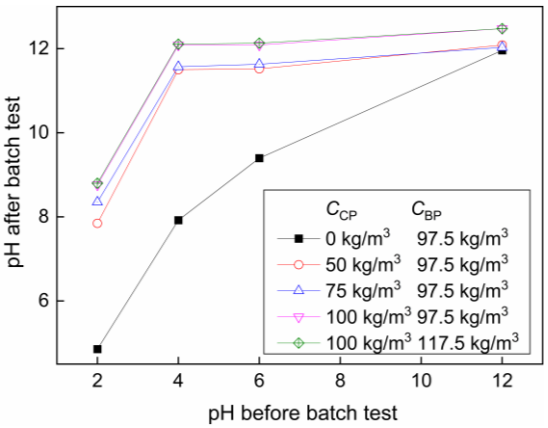

Figure 4.18. pH changes when initial As concentration is 10 mg/L

After batch tests, the solution was set for 5 mins, and the picture of the solution after setting is shown in Fig. 4.16. When the initial pH = 2, the after-test solution was noted to be relatively transparent when just finishing the batch test. After setting for 5 mins, the other solution had a transparent supernatant. However, the pH = 2 solution was still as turbid as before. This is because that the SB mixture is partly dissolved in acid conditions at the initial pH=2, in which the cations following acidolysis can only be suspended in a supernatant. However, the soil particles and Ca-As complex compound have a better precipitation capacity under alkaline conditions.

The pH of the solution after the test at different initial pH (2, 4, 6, 12) and initial As concentrations (0.5 and 10 mg/L) are shown in Figs. 4.17 and 4.18. The pH change tendencies

were little influence by As initial concentration from 0.5 to 10 mg/L, and the most obviously pH increasing occur in initial pH = 4. Both the initial As 0.5 or 10mg/L cases may be obtained, where the pH was found to increase along with the reaction. Such a rise occurred in samples with or without the addition of cement since the pH of sodium bentonite was 8.5-10.2. Meanwhile, the Al_2O_3, Fe_2O_3, MgO, and CaO contained in sodium bentonite partly underwent acidolysis in a strong acid solution in order to neutralize the pH. By comparing the red, blue and purple lines, the pH increased rapidly with the addition of more cement. This can be explained by the release of alkali during hydration as well as the setting of Portland cement. In strongly acidic conditions, such as in the initial pH = 2 solution, cement can neutralize the strong acid by partly dissolving. In the initial pH = 4 to 12 cases, the solution's pH finally reached around 12 with the addition of cement, after which a strong alkaline condition was created in the solution.

4.5 Conclusion for Chapter 4

In the study, UCS, hydraulic conductivity, free swell, and batch sorption tests were carried out to evaluate the influence of Portland blast-furnace slag cement as the addition in SB mixture on its mechanical, hydraulic and attenuation properties. Advection-dispersion analysis based on FEM was carried out to discuss the influence of changed hydraulic and attenuation performances on contaminant migration. The main findings are summarised as follow:

UCS and tangent stiffness significantly increased with cement mass. Amended SB with C_{CP} = 100 kg/m^3 cured for 90 days has strength and tangent stiffness of 200 kPa and 180 kPa. Curing time plays an essential role in mechanical properties. The strength of the amended SB increased to 350 kPa with 180 days of curing. The strain of amended SB with $C_{CP} \leqslant$ 75 kg/m^3 is >4% before it was not able to carry the load anymore, which means amended SB may still keep its barrier performance with large deformation.

The k of amended SB is higher compared to the basic SB (k = 2.7 $\times 10^{-11}$ m/s). The k of amended SB at the beginning stage is similar (k = 1.0 $\times$ 10^{-9} m/s). The k of amended SB with C_{BP} = 97.5 kg/m^3 will decrease with time to 1.6 $\times$ 10^{-10} m/s depending on C_{CP}. By increasing C_{BP} to 117.5 kg/m^3, k of amended SB significantly decreased to 5.0 $\times$ 10^{-11} m/s after 60 days.

Amended SB has higher attenuation performance than basic SB. The attenuation performance of the amended SB was noted to improve with the increase of C_{CP} and curing time. Amended SB with C_{CP} = 100 kg/m^3 and cured for 28 days exhibited the highest attenuation performance. Using Freundlich parameter K as the index, attenuation performance of 28 days cured amended SB with C_{CP} =100 kg/m^3 was 20 cm^3/g which is ~8 times than basic SB.

References for Chapter 4

ASTM D 5084-16a, 2011. Standard Test Methods for Measurement of Hydraulic Conductivity of Saturated Porous Materials Using a Flexible Wall Permeameter. ASTM International, West Conshohocken, US.

ASTM D 5890–19, 2011. Standard Test Method for Swell Index of Clay Mineral Component of Geosynthetic Clay Liners. ASTM International, West Conshohocken, US.

Anh, H.N., Ahn, H., Jo, H.Y., Kim, G.Y., 2017. Effect of alkaline solutions on bentonite properties. Environmental Earth Sciences 76(10), 374. 10.1007/s12665-017-6704-8

Daraei, A., Herki, B.M.A., Sherwani, A.F.H., Zare, S., 2018. Slope stability in swelling soils using cement grout: A case study. International Journal of Geosynthetics and Ground Engineering, 4 (1), 10. https://doi.org/10.1007/s40891-018-0127-9

De La Villa, R.V., Cuevas, J., Ramírez, S., Leguey, S., 2001. Zeolite formation during the alkaline reaction of bentonite. European Journal of Mineralogy, 13 (3), 635−644. https//doi.org/10.1127/0935-1221/2001/0013-0635

Dixit, S., Hering, J.G., 2003. Comparison of arsenic (V) and arsenic (III) sorption onto iron oxide minerals: implications for arsenic mobility. Environmental science and technology, 37(18), 4182−4189. https://doi.org/10.1021/es030309t

Ismail, M.A., Joer, H.A., Sim, W.H., Randolph, M.F., 2002. Effect of cement type on shear behavior of cemented calcareous soil. Journal of Geotechnical and Geoenvironmental Engineering, 128 (6), 520–529. https://doi.org/10.1061/(ASCE)1090-0241(2002)128:6(520)

JIS A 1216, 2009. Method for Unconfined Compression Test of Soils. Japanese Standards Association

JIS A 5201, 2015. Physical testing methods for cement, Japanese Standards Association. Japanese Standards Association

Kameshima, H., Nakamura, S., Suzuki, H., and Okamoto, H., 2012. Effect of cement admixture on characteristics of concrete. Cement Science and Concrete Technology, 66(1), 346–352

Kamon, M., Inui, T., Shoji, Y., 2005. Experimental study on the long-term environmental impact caused by the cement stabilization/solidification of soft ground. Annuals of Disaster Prevention Research Institute, Kyoto University, 48, 1-9.

Kaniraj, S.R., Havanagi, V.G., 1999. Compressive strength of cement stabilized fly ash-soil mixtures. Cement and Concrete Research, 29 (5), 673–677. https://doi.org/10.1016/S0008-8846(99)00018-6

Katsumi, T., Kamon, M., Inui, T., Araki, S., 2008. Hydraulic barrier performance of SBM cutoff wall constructed by the trench cutting and re-mixing deep wall method. In: Krishna, R.R., Milind V.K., Akram, N.A. (Eds.), GeoCongress 2008: Geotechnics of Waste Management and Remediation, ASCE. New Orleans, US, pp. 628–635. https://doi.org/10.1061/40970(309)79

Mo, J., Inui, T., Katsumi, T., Kuninishi, K., Shintaro, H., 2015. Effectiveness of immobilizing agent used as a sorption layer against natural contamination. Japanese Geotechnical Society Special Publication, 1(4), 19-24.

Mueller, B., Hug, S.J., 2018. Climatic variations and de-coupling between arsenic and iron in arsenic contaminated ground water in the lowlands of nepal. Chemosphere, 210, 347–358. https://doi.org/10.1016/j.chemosphere.2018.07.024

Opdyke, S.M., Evans, J.C., 2005. Slag-cement-bentonite slurry walls. Journal of Geotechnical and Geoenvironmental Engineering, 131 (6), 673–681. https://doi.org/10.1061/(ASCE)1090-0241(2005)131:6(673)

Shevade, S., Ford, R.G., 2004. Use of synthetic zeolites for arsenate removal from pollutant water. Water Research, 38 (14-15), 3197–3204. https//doi.org/10.1016/j.watres.2004.04.026

Tremblay, H., Duchesne, J., Locat, J., Leroueil, S., 2002. Influence of the nature of organic compounds on fine soil stabilization with cement. Canadian geotechnical journal, 39 (3), 535−546. https://doi.org/10.1139/t02-002

Tong, X., Li, Y. C., Ke, H., Li, Y., and Pan, Q., 2019. In situ stress states and lateral deformations of soil–bentonite cutoff walls during consolidation process. Canadian Geotechnical Journal, 57(1), 139-148.

Wijayawardhana, H.M.J.T., Silva, L. I. N. De., 2017. Strength, deformation and permeability characteristics of soil-cement-bentonite slurry cut off materials. In:19th International Conference on Soil Mechanics and Geotechnical Engineering, Seoul, Korea, pp.341–344.

Chapter 5. The practical implication of amended SB

5.1 General remarks

In the previous chapter, hydraulic performance and attenuation performance of enhanced SB with cement were evaluated individually by the hydraulic conductivity test and batch sorption tests. However, the barrier performance is comprehensive performance considering multiple influences at the same time (Fratalocchi et al., 2018). In this Chapter, the FEM method was used to simulation the contamination migration based on the advection-dispersion equation in amended SB wall with different C_{CP}. COMSOL Multiphysics is widely applied in contamination migration since it allows multi-field coupling (Al-Mansori et al., 2020). As concentration in the aquifer is used to evaluate the barrier performance of the SB wall.

5.2 Solute transport simulation for amended SB wall

According to the results from hydraulic conductivity tests and batch tests, cement addition may increase the hydraulic conductivity and attenuation performance. Barrier performance has a relationship with both hydraulic conductivity and attenuation performance (Tian et al., 2020). Therefore, it is necessary to evaluate the barrier performance rather than only focusing on the experimental results individually. In this study, the FEM is used to simulate the arsenic migration through the basic and amended SB wall. The simulation is based on COMSOL and uses the following advection-dispersion equation, which considers seepage, dispersion and sorption at the same time:

$$D\frac{\partial^2 C}{\partial x^2} - v_s\frac{\partial C}{\partial x} = \frac{\partial C}{\partial t}R \tag{5.1}$$

$$v_s = k \cdot i \tag{5.2}$$

where R is the retardation factor, D (m^2/s) is the dispersion coefficient, v_s (m/s) is the seepage, and i is the hydraulic gradient.

R represents the attenuation behaviour of the material without individual reactions, for instance, precipitation reactions. In this analysis, attenuation behaviour was assumed to be modelled as a non-linear behaviour. Therefore, R was calculated as, $R = (1 + \rho_d KNC^{N-1})/N$ by considering the Freundlich isotherm. A simplified model that represents a typical configuration for the SB wall is shown in Fig. 5.1. Left to the SB wall is the contaminated ground. The bottom of SB wall reaches the impermeable layer. The contaminants move through the SB wall to the aquifer (located on the right side of SB wall). Contaminant transport through SB wall includes both advection and dispersion. The following are the initial and boundary conditions of the model:

$$C\big|_{x=0,t\geq 0} = C_0,\ C\big|_{x\geq 0,t=0} = 0,\ C\big|_{x=L,t=0} = 0 \tag{5.3}$$

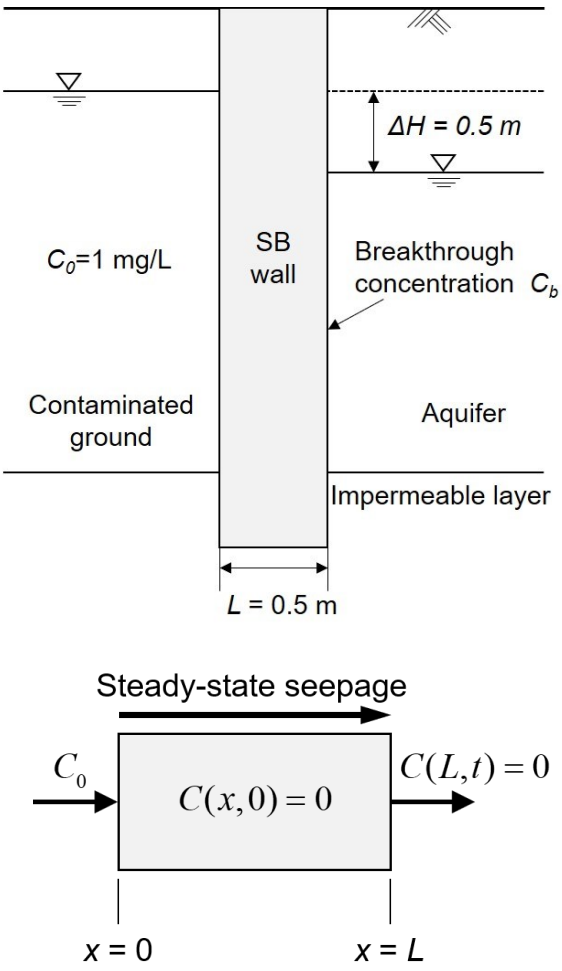

Figure 5.1. Schematic view and boundary condition of the simulation model.

The sorption isotherm parameters and k of SB are directly utilised data from the batch tests and hydraulic conductivity tests. The parameters used in this simulation are shown in Table 5.1. The model applies a 125-cm mesh size and 80 elements. The thickness of the SB wall is 50 cm. The arsenic concentration of contaminated ground, C_0, is assumed to be 10 mg/L and constant throughout. C_e and J are the effluent arsenic concentration and flux at x = 50 cm, which was used to evaluate the barrier performance (Takai et al., 2017). J was calculated using the following equation based on Fick's law:

$$J = C_e \cdot n \cdot k \cdot i \tag{5.4}$$

where n is the porosity.

Besides the left and right boundary, the top and bottom of the model were set to be impermeable boundaries. In addition, i = 1 and $D = 1 \times 10^{-12}$ m^2/s for all cases. The D is estimated by a previous study about cement amended soil (Kundu et al., 2008) . The time step was 50 days, and the whole duration was 100 years.

5.3 Results and discussion

Figure 5.2 shows changes in effluent to influent arsenic concentration ratio (concentration ratio, C_e/C_0) with time, at x= 50 cm. The barrier performance of amended SB increases with an increase of cement contents. Amended SB with C_{CP} = 100 kg/m^3 exhibits the best barrier performance when only considering effluent concentration due to its low hydraulic conductivity and highest K. The effluent concentration of amended SB with 100 kg/m^3 is 0.33 mg/L after 100 years. Basic SB has a higher effluent concentration effluent concentration compared to amended SB with C_{CP} = 100 kg/m^3 but lower than other amended SB (i.e., C_{CP} = 50 or 75 kg/m^3). After 50 years, effluent concentration of Basic SB is 0.61 mg/L which is slightly higher than for amended SB with C_{CP} = 100 kg/m^3 (C_e = 0.17 mg/L). Figure 5.2 shows changes in flux with time, at x = 50 cm. When hydraulic conductivity is considered, basic SB had the best barrier performance due to its extremely low hydraulic conductivity. Basic SB has the lowest J after 100 years (J = 0.11 mg/m^2/year). J of amended SB is 0.65 mg/m^2/year, although it has the lowest concentration and n.

Table 5.1. Hydraulic conductivity and diffusion coefficent used in FEM simulation.

C_{CP} (kg/m^3)	0	50	75	100
k (m/s)	2.8×10^{-11}	5.8×10^{-11}	3.8×10^{-10}	1.6×10^{-10}
D (m^2/s)	1.0×10^{-12}			

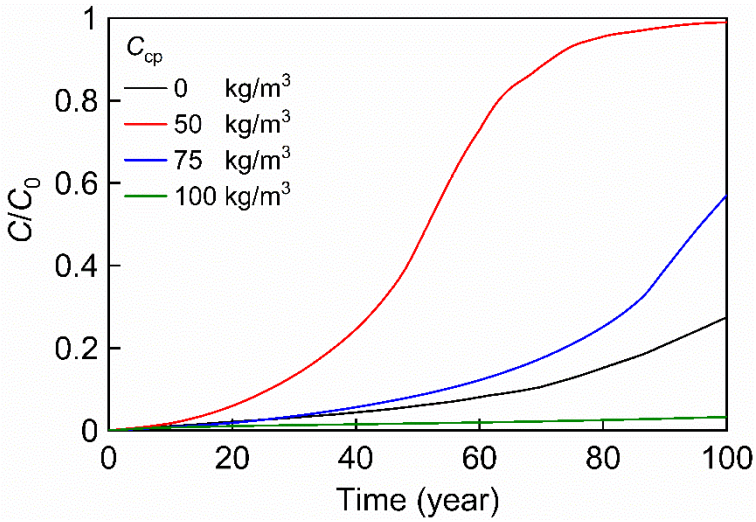

Figure 5.2. Changes in effluent arsenic concentrations with time. The breakthrough curves were obtained using one-dimensional advection-dispersion analysis for a 0.5 m thick SB wall with i = 1.

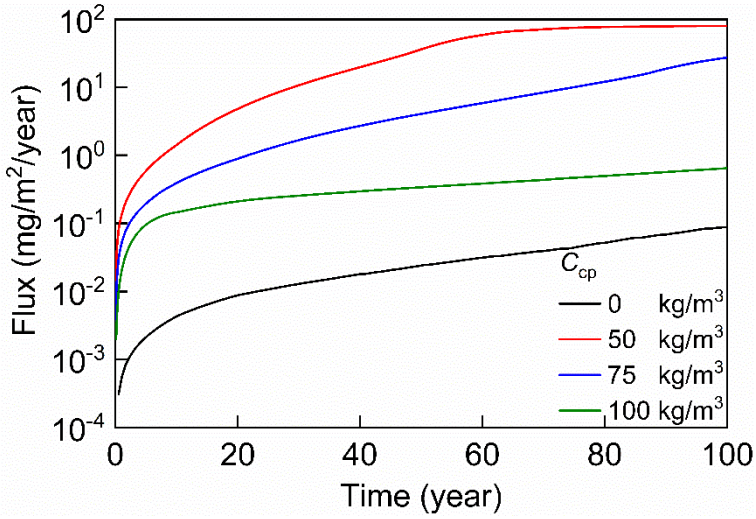

Figure 5.3. Changes in the mass flux with time.

The barrier performance of the amended SB was noted to be underestimated in this simulation. Although basic SB had the lowest attenuation performance, it continued to have the

best barrier performance, which may be explained by the much lower hydraulic conductivity compared to the amended SB. The sorbed mass of basic SB was about 25% of the amended SB. However, after adding cement, the hydraulic conductivity increased over 20 times. $D = 1.0 \times 10^{-12}$ m^2/s, while the k of amended SB with C_{CP} = 50 or 75 kg/m^3 was around 5.0×10^{-10} m/s. When the difference between attenuation performance was less than 10 times, the hydraulic conductivity may have played a more critical role when both advection and dispersion were considered. It is anticipated that chemical reactions in amended SB will contribute to lower hydraulic conductivity, which may reduce effluent concentration and flux. However, in certain conditions, SB wall may have no advection or even a negative advection due to hydraulic conditions. As such, amended SB may have better performance because dispersion dominates the contamination migration. Attenuation performance contributes more to migration control rather than hydraulic performance at that time.

Considering the mechanical properties of SB, it is noted that the strength and tangent stiffness of amended SB will increase with C_{CP} while deformability decreases. Higher strength and tangent stiffness benefit the lateral deformation control of amended SB. However, it also leads to lower deformability of amended SB, which increase the risk of cracking. By comparing the stress-strain relationship, it could be found that amended SB with C_{CP} = 75 kg/m^3 reaches its maximum stress with around 5% strain after 90 days curing, while for SB with C_{CP} = 100 kg/m^3 it is about 2%. It shows that the amended with C_{CP} = 75 kg/m^3 still keeps certain deformability. Based on the simulation results, barrier performance of SB wall is dominated by hydraulic performance, and hydraulic conductivity of amended SB can be adjusted by changing C_{BP}. Therefore, the barrier performance of amended with C_{CP} = 75 kg/m^3 could be improved by adding more bentonite if better barrier performance is required. It is recommended to use the amended SB with C_{CP} = 75 kg/m^3 when there is moderate strength requirement for SB walls.

5.4 Conclusion for Chapter 5

Advection-dispersion analysis was done considering a simple model. Although basic SB had the lowest attenuation performance, it continued to have the best barrier performance,

which may be explained by the much lower hydraulic conductivity compared to the amended SB. Amended SB with C_{CP} = 100 kg/m^3 had the closest barrier performance to basic SB. In this case, after 100 years, J = 0.65 mg/m^2/year which is still in the same magnitude as basic SB (J = 0.11 mg/m^2/year). The barrier performance of the amended SB was noted to be underestimated in this simulation since the attenuation and hydraulic performance of amended will increase with time.

References for Chapter 5

Al-Mansori, N. J., Al-Kizwini, R. S., and Al-Husseini, F. K., 2020. Modelling and simulation of pollutants dispersion in natural rivers using COMSOL Multiphysics. Journal of Engineering Science and Technology, 15(2), 1167−1185.

Fratalocchi, E., Domizi, J., Mazzieri, F., 2018, Hydraulic conductivity and sorption capacity of special barrier materials in inorganic solutions. In: The International Congress on Environmental Geotechnics, Springer, Singapore. pp. 461−469

Kundu, S., Gupta, A. K., 2008. Immobilization and leaching characteristics of arsenic from cement and/or lime solidified/stabilized spent adsorbent containing arsenic. Journal of hazardous materials, 153(1-2), 434–443.

Takai, A., Katsumi, T., Inui, T., and Kamon, M., 2017. Solute transport in soil-bentonite cutoff walls considering chemical diffusion. In: Nineteenth International Conference on Soil Mechanics and Geotechnical Engineering.

Tian, Y., He, F., Takai, A., Katsumi, T., and Araki, G., 2020. Influence of cement addition on barrier performance of soil-bentonite cut-off wall. Japanese Geotechnical Society Special Publication, 8(4), 96−101.

Chapter 6. Conclusions and Future Directions

6.1 Conclusions

In this study, in-situ samples from actual walls were used to discuss the post-construction quality of SB cutoff walls, including their physical properties, hydraulic performance and vertical homogeneity. The enhancement of cement addition on SB was mainly targeted in regard to its improvement of mechanic performance with adequate barrier performance. The mechanic and barrier performance of laboratory amended SB specimens with cement were then tested in order to evaluate the influence of cement on the strength-strain relationship, hydraulic conductivity and attenuation performance against arsenic. As a result, this study may provide insight into the reference for the following research and designs. The main achievement of each chapter can be described as follows:

In Chapter 1, the background, research objective and main contents of this study were introduced. The general information comprised of an overview of soil and underground water contamination, vertical barrier, and main experiments was introduced in this study.

In Chapter 2, the previous studies regarding SB wall were introduced, including the mechanism of bentonite in reducing the hydraulic conductivity of SB, chemical compatibility of SB, the construction process of SB installed via trench cutting with an equal thickness, and strength enhancement of SB.

In Chapter 3, in-situ samples from a 15-year-old SB cutoff wall and a 40 m-depth SB cutoff wall were tested to evaluate their physical properties and hydraulic conductivity. The result of the particle size distribution test of native soil and SB cutoff wall demonstrated that after the construction of the SB wall, the distribution of each fraction contents became much more uniformed. The coefficient of variation of each fraction contents decreased to less than 0.35, while the indexes of physical properties suggested that the viability between SB samples from different depths was relatively small. Hydraulic conductivity of the in-situ samples from SB cutoff wall constructed 15 years ago was noted to continue to maintain $< 1\times 10^{-9}$ m/s, thus

verifying the post-construction quality of SB wall can still be ensured. The hydraulic conductivity of all SB core samples from Site B was < 1×10^{-10} m/s. The post-construction quality of SB cutoff wall could be ensured using the trench cutting with an equal thickness even for the installation of a 40 m depth wall. Compared to the particle size distribution and hydraulic conductivity of the core samples, it can be found with over 20% fine contents, the hydraulic conductivity of SB installed via the technique mentioned above may decrease with a rise in gravel contents. The concentration of gravel may not have a negative influence on the hydraulic performance of the SB wall.

In Chapter 4, the UCS test was performed in order to evaluate the mechanic properties of SB amended with cement. At C_{CP} = 100 kg/m^3, the strength of the amended SB increased to ~350 kPa after 180 days of curing, while stiffness also increased to 300 kPa. However, the strain reduced to approximately 1% when reaching maximum stress after 180 days of curing. With $C_{CP} \leqslant 75$ kg/m^3, the samples continued to have certain deformability, while the strain at maximum stress remained over 4%. When C_{CP} = 100 kg/m^3, amended SB still keeps certain deformability with 60 days curing, while after 90 days of curing, the strain at maximum stress is reduced to 1%. The specimens were also unable to hold load anymore after reaching maximum stress. Accordingly, the breaking model of amended SB changed from plastic to brittle. Hydraulic conductivity tests were done in order to evaluate the k of amended SB and basic SB. Batch sorption tests were conducted to discuss the effect of cement mass, curing time, host soil and pH condition on attenuation performance. Cement addition in amended SB may decrease the void ratio of amended SB, increase EC, and restrict the swelling. Generally, cement increased the k at the beginning stage from 2.7×10^{-11} m/s for basic SB to 1×10^{-9} m/s for amended SB. The increase in k of amended SB can be controlled by adjusting the bentonite mass. The k of amended SB decreased to ~1.0×10^{-10} m/s as C_{BP} increased for 20 kg/m^3. At C_{CP} = 100 kg/m^3, k reduced to ~1.0×10^{-10} m/s, which was less than 1/5 compared to k at the beginning stage. Amended SB has higher attenuation performance than basic SB. The attenuation performance of the amended SB was noted to improve with the increase of C_{CP} and curing time. Amended SB with C_{CP} = 100 kg/m^3 and cured for 28 days exhibited the highest

attenuation performance. Using Freundlich parameter K as the index, attenuation performance of 28 days cured amended SB with C_{CP} =100 kg/m^3 was 20 cm^3/g which is ~8 times than basic SB.

In Chapter 5, the transportation of As contamination in amended and basic SB cutoff wall was simulated using the FEM method. The parameters used in the simulation were based on the test results from Chapter 5, except for the diffusion coefficient. The results suggest that when the hydraulic gradient equals 1, although basic SB had the lowest attenuation performance, it continued to have the best barrier performance, which may be explained by the much lower hydraulic conductivity compared to the amended SB. Amended SB with C_{CP} = 100 kg/m^3 had the closest barrier performance to basic SB. In this case, after 100 years, J = 0.65 mg/m^2/year which is still in the same magnitude as basic SB (J = 0.11 mg/m^2/year). The barrier performance of the amended SB was noted to be underestimated in this simulation since the attenuation, and hydraulic performance of amended will increase with time.

6.2 Future work

Due to restrictions in time and sampling, there were several limitations in this study, for which further and experiments should be done. In Chapter 3, the physical properties and hydraulic conductivity of the in-situ samples from actual SB walls were tested to evaluate the post-construction quality and vertical homogeneity of the SB cutoff wall. However, in the consolidation tests of samples from SB cutoff walls, samples from some depths had unique consolidation yield stress compared to other depths. This may have been due to the concentration of gravel contents, while some samples with irregular high consolidation yield stress did not have a relatively high gravel content ratio. The particle size distribution test results suggested that, besides particle size, other unclear issues may have influenced the consolidation state. In order to ascertain more accurate and intricate explanations for this phenomenon, further studies and experiments may be necessary. Considering that the consolidation state may have a strong influence on the barrier performance of SB, the investigation is necessary

In Chapter 4, laboratory tests were conducted in order to evaluate the influence of cement

additives on the mechanical properties and barrier performance of amended SB. In this study, the strength and stiffness properties of SB were evaluated by the UCS test. Considering its actual state, the SB cutoff wall was confined by its surrounding soil, and the deformation behaviour may have several differences between the UCS test results. Therefore, it is necessary to conduct further experiments such as tri-axial compression tests or direct shear tests, to gain more accurate and suitable data for deformation prediction or safety analysis. This is particularly crucial as deformability of SB was one of the most important advantages as a vertical barrier against other rigid walls. The large deformability ensures that the SB cutoff wall may still keep continuity, thus allowing the SB wall to keep its retain barrier performance. Therefore, in order to verify whether the amended SB still keeps this advantage, a tri-axial compressive stress test and cycling load experiments may be necessary. With the data of deformation behaviour, the behaviour of the amended SB wall during an earthquake can be predicted

In the barrier performance test, arsenic was used as a contaminant target for the batch test. However, in practice, multiple kinds of contaminants may exist simultaneously. Therefore, it is also necessary to carry out further tests pertaining to discuss the attenuation performance of amended SB against other contaminants such as fluoride or caesium. In this study, only advection and dispersion were considered in the solute transport simulation. When the hydraulic conductivity was relatively low, diffusion would also play an important role in contaminant transportation. Hence, it is important to investigate the influence of cement addition on the diffusion coefficient of the amended SB so as to provide novel design and research insight for further studies.

Acknowledgements

The research in this thesis was done during the author's academic career at Kyoto University. I wish to acknowledge all of the supervision, guidance, support and assistance that I have received from many others.

I would like to express my deep and sincere gratitude to my supervisor, Professor Takeshi Katsumi, from the Graduate school of Global Environmental Studies (GSGES), Kyoto University, for providing me with the opportunity to do research and giving invaluable guidance throughout this study. Katsumi-sensei not only taught me knowledge but also helped me build a systematic method to learn new things and engage in independent thinking.

I like to express my heartfelt thanks to my vice supervisor, Associate Professor Atsushi Takai, from the Graduate school of Global Environmental Studies (GSGES), Kyoto University, for his invaluable advice and kindness not only in the research but also in my daily life. Takai-sensei helped me get used to life in Japan.

Special thanks are due to Professor Toru Inui from the Graduate School of Engineering, Osaka University, for his suggestion and guidance of my research and manuscript. His studies about consolidation behaviour contributed a lot to this thesis.

I would like to extend my thanks to Dr Lincoln W. Gathuka, Postdoctoral researcher from the Graduate School of Global Environmental Studies (GSGES), Kyoto University, for his advice and proofreading for my manuscript.

I wish to thank Dr Jialin Mo, a previous student in Katsumi Laboratory, Kyoto University, not only for his kindly guidance in experiment teaching and research plan but also in my daily life. Mo-san helped me a lot to settle down in my doctoral student life in Japan.

I also wish to acknowledge Mr Go Arakai, Manager of Research and Development Center, Raito Kogyo, Co. Ltd and Mr Noburu Ukaji, Manager of Urban Technology Design Department, Raito Kogyo, Co. Ltd., for their great contribution and guidance in this research. Without the core samples provided by Mr Arakai and Mr Ukaji, this research would not be

possible.

I would like to express my thanks to Mr Kazuki Nishimura, Master student in Katsumi Laboratory, Kyoto University, Ms Fangxin He, Previous master student in Katsumi Laboratory, Kyoto University and Mr Guangsen Wei, previous bachelor student in Katsumi Laboratory, Ms Kyoka Yokogawa, previous master student in Inui Laboratory, Osaka University, for their help in experiments, without their help, the author has no chance to collect such large amount of data. Their unique ideas also inspired the author a lot in the research and manuscript.

I would like to express my thanks to all the members of Katsumi Laboratory, especially to Ms Miho Yasumoto, previous secretary in Katsumi Laboratory, for her help in the document work, including visa application, visa extenuation and scholarship application.

Lastly, I would like to express my gratefulness to my family, especially to my father, Songya Tian and mother Lihua Chen, for their understanding and support. Without them, I would not be able to continue my studies at Kyoto University.